

Copyright Warning & Restrictions

The copyright law of the United States (Title 17, United States Code) governs the making of photocopies or other reproductions of copyrighted material.

Under certain conditions specified in the law, libraries and archives are authorized to furnish a photocopy or other reproduction. One of these specified conditions is that the photocopy or reproduction is not to be “used for any purpose other than private study, scholarship, or research.” If a user makes a request for, or later uses, a photocopy or reproduction for purposes in excess of “fair use” that user may be liable for copyright infringement,

This institution reserves the right to refuse to accept a copying order if, in its judgment, fulfillment of the order would involve violation of copyright law.

Please Note: The author retains the copyright while the New Jersey Institute of Technology reserves the right to distribute this thesis or dissertation

Printing note: If you do not wish to print this page, then select “Pages from: first page # to: last page #” on the print dialog screen

The Van Houten library has removed some of the personal information and all signatures from the approval page and biographical sketches of theses and dissertations in order to protect the identity of NJIT graduates and faculty.

INFORMATION TO USERS

This dissertation was produced from a microfilm copy of the original document. While the most advanced technological means to photograph and reproduce this document have been used, the quality is heavily dependent upon the quality of the original submitted.

The following explanation of techniques is provided to help you understand markings or patterns which may appear on this reproduction.

1. The sign or "target" for pages apparently lacking from the document photographed is "Missing Page(s)". If it was possible to obtain the missing page(s) or section, they are spliced into the film along with adjacent pages. This may have necessitated cutting thru an image and duplicating adjacent pages to insure you complete continuity.
2. When an image on the film is obliterated with a large round black mark, it is an indication that the photographer suspected that the copy may have moved during exposure and thus cause a blurred image. You will find a good image of the page in the adjacent frame.
3. When a map, drawing or chart, etc., was part of the material being photographed the photographer followed a definite method in "sectioning" the material. It is customary to begin photoing at the upper left hand corner of a large sheet and to continue photoing from left to right in equal sections with a small overlap. If necessary, sectioning is continued again — beginning below the first row and continuing on until complete.
4. The majority of users indicate that the textual content is of greatest value, however, a somewhat higher quality reproduction could be made from "photographs" if essential to the understanding of the dissertation. Silver prints of "photographs" may be ordered at additional charge by writing the Order Department, giving the catalog number, title, author and specific pages you wish reproduced.

University Microfilms

300 North Zeeb Road
Ann Arbor, Michigan 48106

A Xerox Education Company

72-26,336

SHARE, Irwin, 1936-

ELECTROMAGNETIC WAVE PROPAGATION IN NONUNIFORM
WAVEGUIDES WITH PERFECT CONDUCTING WALLS.

Newark College of Engineering, D.Eng.Sc., 1972
Engineering, electrical

University Microfilms, A XEROX Company, Ann Arbor, Michigan

PLEASE NOTE:

Some pages may have
indistinct print.

Filmed as received.

University Microfilms, A Xerox Education Company

ELECTROMAGNETIC WAVE PROPAGATION IN NONUNIFORM
WAVEGUIDES WITH PERFECT CONDUCTING WALLS

by

IRWIN SHARE

A DISSERTATION
PRESENTED IN PARTIAL FULFILLMENT OF THE REQUIREMENTS
FOR THE DEGREE
OF
DOCTOR OF ENGINEERING SCIENCE IN ELECTRICAL ENGINEERING
AT
NEWARK COLLEGE OF ENGINEERING

This thesis is to be used only with due regard to the rights of the author(s). Bibliographical references may be noted, but passages must not be copied without permission of the College and without credit being given in subsequent written or published work.

Newark, New Jersey

1972

ABSTRACT

The analysis of nonuniform waveguides is formulated in terms of non-orthogonal generalized coordinates by utilizing the Hertz vector potentials and the Riemann metric tensor.

When the Hertz potential is expressible as a function of the propagation coordinate times a function of the transverse coordinates, then the nonuniform waveguide may be represented by transverse equations and a set of uncoupled nonuniform transmission lines. This decomposition facilitates studying propagation along the propagation coordinate. Sufficient conditions to achieve this decomposition are investigated. It is demonstrated that these constraints may provide guidelines for selecting a useful coordinate system to describe the nonuniform waveguide. In terms of this coordinate system the nonuniform waveguide analysis may be reduced to solving uncoupled nonuniform transmission lines if the eigenvalues of the transverse equations can be determined. This allows nonuniform transmission line theory to be applied to the study of certain nonuniform waveguides. It is also shown that when the diagonal element of the metric tensor (the element associated with the propagation coordinate) is unity, terms in the nonuniform transmission line differential equation and nonuniform transmission line parameters (such as characteristic impedance, and the per

length admittance and impedance) are related to the logarithmic derivative of the transverse surface area.

For more general waveguides it is suggested that the nonuniform waveguide may sometimes be approximated by a cascade of solvable nonuniform waveguides. In this cascade approximation, the study of the junction between nonuniform waveguides is important because the nature of the coupling between the various waveguide modes lies in an understanding of the waveguide junction analysis. A junction, as defined in this dissertation, is the joining of two different coordinate systems. It may (or may not) have an associated edge in the waveguide wall. A junction analysis formulation is undertaken with approximations that allow the modal field expansions on both sides of the junction to be equated. As a convenient artifice, the modes on the load side of the junction are subdivided into a constituent that is related to the totality of E-modes on the source side of the junction and a constituent that is related to the totality of H-modes on the source side of the junction. The resulting formulation considers multimode propagation and cross-coupling between E- and H-modes. The special case in which one can choose the Hertz vector potential to be in the same direction on both sides of the junction and there is no cross-coupling between E-modes and H-modes is also considered and illustrated.

A method for obtaining the scatter parameters for the propagating modes relative to surfaces sufficiently far from the junction is also indicated.

APPROVAL OF DISSERTATION

ELECTROMAGNETIC WAVE PROPAGATION IN NONUNIFORM
WAVEGUIDES WITH PERFECT CONDUCTING WALLS

BY

IRWIN SHARE

FOR

DEPARTMENT OF ELECTRICAL ENGINEERING
NEWARK COLLEGE OF ENGINEERING

BY

FACULTY COMMITTEE

APPROVED _____ Chairman
_____ Co-chairman

NEWARK, NEW JERSEY

JUNE, 1972

DEDICATION

To my family, Joan, David, Jessica and
Mathew for their patience and under-
standing during this research.

ACKNOWLEDGMENTS

The author is indebted to Dr. G. E. Ching,
Dr. F. A. Russell, Dr. G. Peyser and Dr. J. J. Padalino
for their helpful suggestions and encouragement.

The author is also indebted to Newark College of
Engineering for the grant and to the National Science
Foundation for the Fellowship which helped to make this
work possible.

TABLE OF CONTENTS

CHAPTER	PAGE
1. Introduction	1
1.1 Background	1
1.2 Approach and Organization	4
2. Review of Uniform Waveguide Theory	6
2.1 Uniform Waveguide Formulation	6
3. The Nonuniform Waveguide	19
3.1 Introduction	19
3.2 Formulation	25
3.3 Boundary Conditions	52
3.4 Engineering Application and Significance	56
3.5 Summary	86
4. Cascaded Nonuniform Waveguides	89
4.1 Introduction	89
4.2 General Junction Formulation	97
4.3 Specialized Junction Theory	123
4.4 Sectorial Wedge to Multimode Uniform Waveguide Junction	129
4.5 Summary of Results	148
5. Conclusions	153
6. Suggestions for Further Investigation	158

CHAPTER	PAGE
Appendix A: Analysis of Nonuniform Transmission Lines	160
A1 Introduction	160
A2 Exact Solution Techniques	160
A3 Approximate Solution Techniques	168
References	173

List of Illustrations

<u>Figure</u>	<u>Title</u>	<u>Page</u>
2.1-1	Uniform Waveguide Classification	7
3.1-1	Nonuniform Waveguide Classification.	21
3.4-1	Sectorial Wedge Nonuniform Waveguide	66
3.4-2	Ratio of Imaginary to Real Parts of Hankel Functions, $H_n(k_r r) = J_n(k_r r) \pm jY_n(k_r r)$	85
4.1-1	Junctions Without Wall Edges	91
4.3-1	Smooth Junction with Coinciding Constant u^3 Junction Surfaces	124
4.4-1	Sectorial Wedge to Multimode Uniform Waveguide Junction	130

List of Tables

3.4-1	Sufficient Conditions to Factor Out the u^3 Dependence	63
5-1	Sufficient Conditions to Factor Out the u^3 Dependence	154

CHAPTER 1

INTRODUCTION

1.1 Background

This dissertation is concerned with analyzing electromagnetic wave propagation in nonuniform waveguides. For this analysis, a nonuniform waveguide is considered to be a perfectly conducting hollow tube with cross sectional dimensions that vary as a function of axial position.¹ The purpose of this nonuniform waveguide is to guide the flow of energy from one end of the tube to the other end of the tube. This dissertation develops procedures for analyzing the energy flow in a nonuniform waveguide. Uniform waveguides, waveguide bends, waveguide twists and nonuniform T.E.M. lines will then be special cases to which the theory can be applied.

Nonuniform waveguides have application in the design of horn antennas [3, 37, 47, 52], broadband impedance matching structures [6, 10, 12, 13, 50], specialized filters [9, 13, 48, 49, 50, 58], directional couplers [51, 58], mode trans-

¹Only nonuniform waveguides composed of smooth surfaces will be considered. A surface is considered to be "smooth" if the surface is continuous and the normal direction to every point on the surface is uniquely defined. Both single-surface and two-set-of-surface nonuniform waveguides are considered. Examples of such nonuniform waveguides are shown in Figure 3.1-1.

ducers [25, 46], periodic slow wave structures and electron beam couplers [45], and other devices. They have even found application in modeling ionospheric propagation [2, 7].

The mathematical formulation of this problem is based upon Maxwell's equations for sinusoidal excitation which may be reduced to the form

$$\nabla^2 \bar{E} + K_0^2 \bar{E} = 0$$

and

$$\nabla^2 \bar{H} + K_0^2 \bar{H} = 0$$

where \bar{E} and \bar{H} are the electric and magnetic field intensities respectively, K_0 is the propagation constant for free space, and ∇^2 is the Laplacian operator. The ultimate goal is to solve the equations with solutions that satisfy the boundary conditions that the tangential component of the electric field intensity and the normal component of the magnetic field intensity both vanish at the perfectly conducting waveguide walls.

Most of the previous theoretical investigations of the nonuniform waveguide employed a coupled transmission line representation of the nonuniform waveguide [43, 44, 46, 47, 50]. The coupling between the modes appearing in these

representations were due to describing the nonuniform waveguide in terms of the modes of the corresponding uniform waveguide and the fact that each of the uniform waveguide modes do not satisfy the boundary conditions. As a result of the complications connected with a coupled model, only solutions for restricted situations (such as boundaries with abrupt discontinuities [27, 55, 56] and small and slow variations) were obtained. The problem was solved in a few specific geometries by describing the geometry in terms of curvilinear coordinates in which the variables could be simply separated [3, 14, 20, 27, 31, 41, 53]. General conditions needed to completely separate the Helmholtz equation into three independent equations of one variable were investigated by Moorse and Fishbach [35] and by Moon and Spencer [32, 33, 34]. However, for the nonuniform waveguide, complete separation of variables is not always required. In fact, it will be shown later that it is usually sufficient to separate out only one variable. R. C. Johnson has analyzed a nonuniform waveguide by approximating it by a cascade of uniform waveguides [18]. These results, however, neglected higher order interactions which limited its applicability. More recently, Bahar has approximated some nonuniform waveguides by a cascade of conical sections [1]. This reduced the magnitude of higher order interactions, but still did not take these interactions into account.

1.2 Approach and Organization

The next chapter presents a review of the theory of the uniform waveguide. The nature of the critical assumptions will provide a better understanding of the difficulties to be encountered in the analysis of the nonuniform waveguide.

The contribution of the research of this dissertation starts in Chapter 3, where the nonuniform waveguide is analyzed in terms of generalized Hertz vector potentials and formulated in terms of the Riemann metric tensor. It is shown that it often is possible to determine a coordinate system which allows the nonuniform waveguide to be represented by a set of uncoupled nonuniform transmission lines. A review of the methodology for analyzing nonuniform transmission lines is presented in Appendix A.

Chapter 4 is devoted to presenting a method for analyzing nonuniform waveguides that cannot be solved by the methods in Chapter 3. The basic approach is to approximate the overall nonuniform waveguide by a cascade of solvable nonuniform waveguides that are analyzable by the methods in Chapter 3. The major portion of Chapter 4 is therefore devoted to the study of the junction between nonuniform waveguides.

The relationship between Chapter 3 and Chapter 4 may also be considered from a different point of view. In both Chapter 3 and Chapter 4, the initial formulation is based on the concepts of differential geometry. In Chapter 3, however, sufficient conditions to extend the results globally throughout the entire waveguide region are required. On the other hand, Chapter 4 considers the case in which it is not possible to extend the local properties over the entire waveguide length. In the latter case, the locally correct solutions are pieced together in order to approximate the global solution.

Finally, Chapters 5 and 6 present a critical evaluation and summary of the major contributions of this dissertation and recommendations for future investigations.

CHAPTER 2

REVIEW OF UNIFORM WAVEGUIDE THEORY

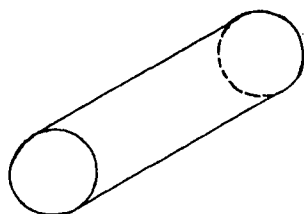
2.1 Uniform Waveguide Formulation

In order to gain a better insight into the difficulties associated with the nonuniform waveguide, the general formulation of the uniform waveguide will now be reviewed.

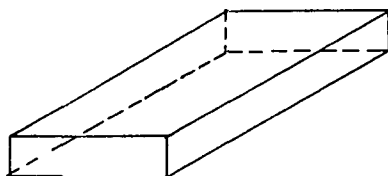
A uniform waveguide is a hollow perfectly conducting tube with a constant closed cross sectional shape. In Figure 2.1-1 are shown two general types of uniform waveguides of the type being considered. The first waveguide boundary is smooth and can therefore be conveniently described by one smooth surface. The second type requires two sets of surfaces to describe the waveguide boundary.¹

The goal of the uniform waveguide formulation is to solve the field equations subject only to the waveguide wall boundary conditions. Solutions of this type are referred to as modes. The solution to the problem is that particular linear combination of modes that also satisfies the conditions at the source and load (input and output of the waveguide).

¹The situation in which more than two sets of surfaces are required to describe the waveguide boundary (such as pentagon cross sections) will not be considered.



a) One Surface



b) Two Sets of Surfaces

Figure 2.1-1

Uniform Waveguide Classification

The basic method for achieving the desired goal² is to separate the problems into one that depends only upon the transverse coordinates (the coordinates in the waveguide cross-section) and one that depends only upon the longitudinal coordinate (or coordinate axis parallel to the axis of the waveguide and therefore parallel to the direction of propagation). This decomposition will allow the three dimensional waveguide propagation to be thought of as consisting of a two-dimensional transverse wave moving along the waveguide axis in accordance with the transmission line equations. One therefore selects transverse and longitudinal coordinates such that the longitudinal coordinate (z-axis) coincides with the waveguide axis. The remaining two transverse curvilinear coordinates, u^1 and u^2 , are chosen in such a manner that one of them is a constant on the perfectly conducting waveguide walls. (It is possible for u^1 to be constant on a portion of the boundary and u^2 to be constant on the remaining portion of the boundary, as illustrated by the rectangular waveguide.)

²The approach followed throughout most of the remainder of this section parallels Collin [11]. Marcuritz [27] uses a different (but equivalent) formulation, but Collin's approach is used here because this dissertation will generalize his technique when considering the nonuniform waveguide.

For convenience the electric and magnetic field intensities for sinusoidal fields, $\bar{E}(u^1, u^2, z)e^{j\omega t}$ and $\bar{H}(u^1, u^2, z)e^{j\omega t}$ are each decomposed into two components as shown in Equation 1.³

$$\begin{aligned}\bar{H} &= \bar{H}_e + \bar{H}_h \\ \bar{E} &= \bar{E}_e + \bar{E}_h\end{aligned}\tag{2.1-1}$$

These two components are referred to as the E-mode (subscript "e") and H-mode (subscript "h") components of the fields. Each of these two field components satisfies the field equations and the boundary conditions. The E-mode component of the magnetic field intensity, H_e , is related to z-directed electric Hertz vector potential, $\bar{\pi}_e(u^1, u^2, z)e^{j\omega t}$ by

$$\bar{H}_e = j\omega\epsilon\bar{\pi}_e(u^1, u^2, z)\tag{2.1-2}$$

where ω is the radian frequency and ϵ is the medium dielectric constant. The corresponding component of the electrical field is found from Maxwell's equations to be

³Unless otherwise specified equation numbers refer to equations in this section. Thus, Equation 1 is a shorter notation for Equation (2.1-1). Equations in other section are referred to by the longer notation.

$$\bar{E}_e = \frac{1}{j\omega\epsilon} \nabla \times \bar{H}_e = \nabla \times (\nabla \times \bar{\pi}_e) = \nabla (\nabla \cdot \bar{\pi}_e) - \nabla^2 \bar{\pi}_e \quad (2.1-3)$$

It is important to note that the divergence of the Hertz vector potential has not been specified (and therefore it is not uniquely defined). Since only the curl of the Hertz vector potential is related to the field quantities (as illustrated by Equations 2 and 3), restrictions on the divergence of the Hertz vector potential can be imposed later in order to simplify the analysis. Similarly, the H-mode components of the electric and magnetic fields intensities are related to a magnetic Hertz vector potential by the equations

$$\bar{E}_h = -j\omega\mu \nabla \times \bar{\pi}_h \quad (2.1-4)$$

and

$$\bar{H}_h = -\frac{1}{j\omega\mu} \nabla \times \bar{E}_h = \nabla \times (\nabla \times \bar{\pi}_h) = \nabla (\nabla \cdot \bar{\pi}_h) - \nabla^2 \bar{\pi}_h \quad (2.1-5)$$

As before, the divergence of the magnetic Hertz vector potential will be specified later to simplify the problem.

It follows from Equation 2 that, since the electric type Hertz vector potential is directed along the axis of the waveguide, the magnetic field intensity vector lies entirely in the plane that is transverse to this direction. The waves associated with this component are sometimes referred to as transverse magnetic (T.M.) waves. Since only the electric field of this component has an axial component, as seen from Equation 3, these fields are also described as E-mode waves. In a similar manner, it follows from Equations 4 and 5 that the waves, due to a magnetic Hertz vector potential directed along the waveguide axis results in transverse electric (T.E.) waves that are sometimes referred to as H-mode waves. Thus, in order to find the electric and magnetic fields, it is required to determine the Hertz vector potentials.

It will now be shown that the Hertz vector potential satisfies a homogeneous Helmholtz equation for an appropriate restriction on the divergence of the Hertz vector potential. Maxwell's equations require

$$\vec{H}_e = -\frac{1}{j\omega\mu} \nabla \times \vec{E}_e \quad (2.1-6)$$

Upon substituting Equation 2 and 3 into Equation 6, and

regrouping terms, it follows that

12

$$\nabla \times [\nabla^2 \bar{\pi}_e + K_o^2 \bar{\pi}_e - \nabla (\nabla \cdot \bar{\pi}_e)] = 0 \quad (2.1-7)$$

where

$$K_o = w \sqrt{\mu \epsilon} \quad (2.1-8)$$

is the propagation constant of free space. Since the curl of the gradient of a scalar function is zero, it follows that Equation 7 may be expressed as

$$\nabla^2 \bar{\pi}_e + K_o^2 \bar{\pi}_e - \nabla (\nabla \cdot \bar{\pi}_e) = - \nabla \theta \quad (2.1-9)$$

The divergence of the electric Hertz vector potential is now chosen such that

$$\nabla \cdot \bar{\pi}_e = \theta \quad (2.1-10)$$

It finally results from Equations 9 and 10 that

$$\nabla^2 \bar{\pi}_e + K_o^2 \bar{\pi}_e = 0 \quad (2.1-11)$$

In a similar manner it can be shown that

$$\nabla^2 \bar{\pi}_h + k_o^2 \bar{\pi}_h = 0 \quad (2.1-12)$$

Thus, it results that the electric and magnetic Hertz vector potentials satisfy homogeneous Helmholtz equations for an appropriate choice of the divergence of these vector potentials.

In accordance with the desire to separate the uniform waveguide propagation analysis into a transverse problem depending upon the transverse variables and an axial problem (depending upon z), it will be assumed that the Hertz vector potential can be written in the form.⁴

$$\bar{\pi}_e = \hat{a}_z \psi_e(u^1, u^2) I(z) \quad (2.1-13)$$

$$\bar{\pi}_h = \hat{a}_z \psi_h(u^1, u^2) V(z) \quad (2.1-14)$$

where \hat{a}_z is a unit vector in the z -direction, and ψ_e, ψ_h, I , and V are arbitrary functions of the variables denoted

⁴This form of solution is assumed and it is later observed that no conflict results for a uniform waveguide.

in parentheses (that are to be determined by the analysis). Upon substituting Equations 13 and 14 respectively into Equations 11 and 12 and also expanding the "del" operator into transverse and axial components ($\nabla = \nabla_t + \hat{a}_z \frac{\partial}{\partial z}$)⁵ where ∇_t is the transverse component of the "del" operator) one obtains

$$\frac{\nabla_t^2 \psi_e}{\psi_e} + K_o^2 + \left(\frac{\partial^2 I}{\partial z^2} \right) = 0 \quad (2.1-15)$$

$$\frac{\nabla_t^2 \psi_h}{\psi_h} + K_o^2 + \frac{\partial^2 V}{\partial z^2} = 0 \quad (2.1-16)$$

It can be shown by applying process of separation of variables to Equations 15 and 16 that

$$\nabla_t^2 \psi_e(u^1, u^2) + (K_o^2 - \gamma_{ze}^2) \psi_e(u^1, u^2) = 0 \quad (2.1-17A)$$

$$\frac{d^2 I(z)}{dz^2} + \gamma_{ze}^2 I(z) = 0 \quad (2.1-17B)$$

⁵This decomposition uses the fact that the z coordinate is orthogonal to both transverse coordinates.

$$\nabla_t^2 \psi_h(u^1, u^2) + (K_o^2 - \gamma_{zh}^2) \psi_h(u^1, u^2) = 0 \quad (2.1-18A)$$

$$\frac{d^2 V(z)}{dz^2} + \gamma_{zh}^2 V(z) = 0 \quad (2.1-18B)$$

where γ_{ze} and γ_{zh} are the separation constants (to be determined). Since solutions to Equations 17B and 18B are of the form $e^{\pm j\gamma z}$ where $\gamma = \gamma_{ze}$ or γ_{zh} it follows that the separation constants can be interpreted as propagation constants. Equations 17A and 18A are boundary eigenvalue problems. For each eigenvalue determined by these equations, the corresponding remaining equation, (Equation 17B or 18B) has a solution. The propagation characteristics in the direction of the waveguide axis are determined from a solution to Equations 17B and 18B.

It will now be shown that the appropriate boundary conditions for Equations 17A and 18A are

$$\psi_e = 0 \quad \text{on the boundary} \quad (2.1-19)$$

$$\frac{\partial \psi_h}{\partial n} = 0 \quad \text{on the boundary} \quad (2.1-20)$$

where $\frac{\partial \psi_h}{\partial n}$ represents the directional derivative of ψ_h in a direction normal to the waveguide wall boundary.

For E-modes and using Equation 2 one obtains

$$\bar{H}_e = j\omega\epsilon \nabla \times \bar{\pi}_e = j\omega\epsilon \nabla \times \hat{a}_z \psi_e I \quad (2.1-21)$$

From Maxwell's equations and the curl expansion it follows that

$$\bar{E}_e = \frac{\nabla \times \bar{H}_e}{j\omega\epsilon} = \nabla \times (\nabla \times \bar{\pi}_e) = \nabla (\nabla \cdot \bar{\pi}_e) - \nabla^2 \bar{\pi}_e \quad (2.1-22)$$

By expanding the "del" operator into axial and transverse parts $(\nabla = \nabla_t + \hat{a}_z \frac{\partial}{\partial z})$ and using Equation 11 one eventually obtains

$$\bar{E}_e = \left(\frac{dI}{dz}\right) \nabla_t \psi_e + \hat{a}_z K_o^2 |\bar{\pi}_e| \quad (2.1-23)$$

The axial (z-component) is therefore equal to

$$E_{ez} = K_o^2 |\bar{\pi}_e| = K_o^2 \psi_e (u^1, u^2) I(z) \quad (2.1-24)$$

It therefore follows that the axial component of the electric field is proportional to the magnitude of $\bar{\pi}_e$. Since E_z is tangential to the guide at the boundary and since the tangential components of \bar{E} must be zero at a perfect electric conductor, it follows that $|\bar{\pi}_e| = 0$ on the boundary. For this to hold (nontrivially) for all values of z requires that $\psi_e = 0$ on the boundary.

By following a similar argument for ψ_h one concludes that

$$H_{hz} = K_o^2 |\bar{\pi}_h| = K_o^2 \psi_h(u^1, u^2) V(z) \quad (2.1-25)$$

But H_z is the tangential component of \bar{H} and, since the normal derivative of the tangential component of the magnetic field intensity must vanish at a perfect conducting boundary, one concludes that $\frac{\partial \psi_h}{\partial n} = 0$ on the boundary. Thus, Equations 19 and 20 represent the boundary conditions for Equations 17A and 18A respectively.

In summary, a uniform waveguide analysis may be separated into two parts. The first is an eigenvalue problem in terms of the transverse coordinates. The solution of this problem yields a set of eigenfunctions and their corresponding eigenvalues. The second part is a transmission line analysis.

The eigenvalues of the first problem provide transmission line parameters for the second problem. The solution to the field theory problem is a supposition of the separate mode problems. Note, that in practice, closed waveguides of the type being considered only have a finite spectrum of propagating modes.

CHAPTER 3

THE NONUNIFORM WAVEGUIDE

3.1 Introduction

The formulation of the uniform waveguide discussed in the previous chapter contained several assumptions which are not necessarily true for nonuniform waveguides.¹ This chapter is concerned with extending the uniform waveguide formulation to nonuniform waveguides. To accomplish this, several restrictions will be imposed. It will be demonstrated that these restrictions can often serve as good guidelines for selecting the best coordinate system to solve the nonuniform waveguide problem.

As with the uniform waveguide, the desired goal of the nonuniform waveguide formulation is to solve the field equations subject only to the waveguide wall boundary conditions; namely, that the tangential component of the electric field intensity and the normal component of the magnetic field intensity² vanish at the waveguide wall. When the nonuniform waveguide medium is homogenous and source free, Maxwell's field equations can be reduced to solving

¹The term, "nonuniform waveguide", has been defined on Page 1.

²This latter condition is equivalent to a vanishing normal directional derivative of the tangential component of the magnetic field intensity.

a vector Helmholtz equation. Such solutions are referred to as modes. The solution to the problem is the particular combination of modes that satisfies the source and load conditions.

Typical illustrations of the two general classes of nonuniform waveguides being considered are shown in Figure (3.1-1). The waveguide wall of the first nonuniform waveguide can be conveniently described by one smooth surface while the second type requires two sets of surfaces to describe the waveguide wall boundary.³

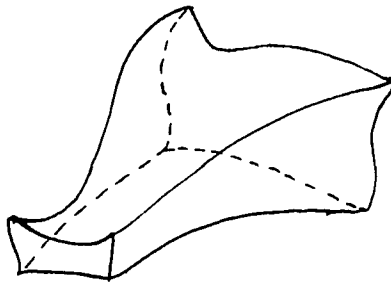
The selection of an appropriate coordinate system for solving the nonuniform waveguide problem is often a compromise between obtaining an easily solvable expression for the Helmholtz equation and getting equation solutions⁴ that satisfy the waveguide wall boundary condition (modal solutions). If one selects transverse and longitudinal coordinates, (u^1, u^2, z) , such that the longitudinal coordinate, z , is parallel to the waveguide axis and the remaining two curvilinear coordinates, u^1 and u^2 , are in the plane that is

³The situation in which more than two sets of surfaces are required to describe the nonuniform waveguide boundary will not be considered.

⁴Equation solutions are distinguished from modal solutions in that the former only satisfies the Helmholtz equation while the modal solutions satisfy both the Helmholtz equation and the waveguide wall boundary conditions.



One-Surface Nonuniform Waveguide



Two-Set-Of-Surface Nonuniform Waveguide

Figure 3.1-1

Nonuniform Waveguide Classification

transverse (orthogonal) to this axis, then equation solutions for the Helmholtz equation are facilitated. These equation solutions are similar to the corresponding uniform waveguide solution and, in general, they will not satisfy the waveguide wall boundary conditions. In this case infinite linear combinations of equation solutions are required to satisfy the waveguide wall boundary condition. The coefficients of the linear combination of solutions are referred to coupling coefficients. As indicated in Section 1.1, the evaluation of these conventional coupling coefficients for the general case is very difficult.

On the other hand, satisfying the boundary conditions is facilitated by selecting generalized coordinate surfaces that coincide with the waveguide wall boundaries. In general, however, the form of the Helmholtz equation is difficult to solve. If an equation solution to this Helmholtz equation can be found, it usually can be made to satisfy the boundary conditions. The difficulty has therefore been shifted to determining a solution. Furthermore, the factorization of the type in Equation (2.1-13) and (2.1-14) will not, in general, be possible. Nevertheless, because the generalized coordinate approach has the potential to facilitate the analysis of large and rapid boundary variations, it is this approach that will be pursued.

As with the uniform waveguide, it will be attempted to decompose the nonuniform waveguide problem into two separate problems--a problem whose solution depends only upon one coordinate, and a problem whose solution depends only upon the other two curvilinear coordinates. When such a decomposition is possible, the solution can be interpreted as consisting of a two-dimensional transverse field that is propagating in the direction of the separated coordinate. In fact, it will be shown that the separated one-dimensional problem may be represented by transverse equations that supply parameters for a set of nonuniform transmission lines. This allows nonuniform transmission line theory to be applied to the study of nonuniform waveguides (See Appendix A for a discussion of nonuniform transmission line theory and techniques). In this chapter, therefore, it will be assumed that the dependence upon the variable in the propagating direction can be factored out and sufficient conditions for this decomposition will be determined subsequently. The case in which this decomposition cannot be achieved will be the subject of Chapter 4.

This chapter will formulate the nonuniform waveguide problem in terms of generalized curvilinear coordinates (u^1, u^2, u^3) with the aid of Hertz vector potentials for sinusoidal time variation, $\vec{\pi}(u^1, u^2, u^3)e^{j\omega t}$. For a

proper choice of coordinates, these Hertz potentials will lead to a solution that is composed of a set of so-called "generalized E-mode" (T.M.) waves (generated by an electric Hertz vector potential, $\vec{\pi}_e$) and a set of "generalized H-mode" (T.E.) waves (generated by a magnetic Hertz vector potential, $\vec{\pi}_h$). The formulation for the generalized E-mode waves is performed in Section 3.2. The results obtained with the magnetic Hertz vector potential parallel this development and are presented at the end of this section. Choosing the Hertz vector potential in other directions will also be considered. The boundary conditions for the equations of Section 3.2 are developed in Section 3.3. In Section 3.4, it is shown by illustration with the sectorial wedge that the techniques and restrictions developed in the earlier sections often serve as good guidelines for selecting an optimum coordinate system. Some techniques for studying this wave propagation are also indicated in this section. Finally, Section 3.5 concludes with a summary of the major conclusions and results of this chapter.

3.2 Formulation

The nonuniform waveguide problem will now be formulated in terms of the Hertz potentials. The electric Hertz vector potential for sinusoidal time variation, $\bar{\pi}_e$, is given by⁵

$$\nabla \times \bar{\pi}_e = \frac{1}{j\omega\epsilon} \bar{H}_e \quad \text{with} \quad \nabla \cdot \bar{\pi}_e = \theta_e \quad (3.2-1)$$

where \bar{H}_e is the component of magnetic field due to $\bar{\pi}_e$ and θ_e is a scalar function that satisfies the Helmholtz equation $\nabla^2 \theta_e + K_o^2 \theta_e = 0$ and $K_o = \omega\sqrt{\mu\epsilon}$ is the propagation constant. By use of Maxwell's equations, it can be shown that $\bar{\pi}_e$ satisfies a Helmholtz equation.

$$\nabla^2 \bar{\pi}_e + K_o^2 \bar{\pi}_e = 0 \quad (3.2-2)$$

and

$$\bar{E}_e = \nabla \times (\nabla \times \bar{\pi}_e) = K_o^2 \bar{\pi}_e + \nabla (\nabla \cdot \bar{\pi}_e) \quad (3.2-3)$$

where \bar{E}_e is the component of the electric field due to $\bar{\pi}_e$.

⁵See Section 2.1

For this formulation, generalized coordinates are selected in such a manner that they facilitate satisfying the boundary conditions. This choice will be illustrated for both the "two-set-of-surfaces" and "one-surface" shapes of the types shown in Figure 3.1-1.

For the "two-set-of-boundary-surfaces" situation, the surfaces $u^1 = \text{constant}$ and $u^2 = \text{constant}$ are chosen such that they coincide with the nonuniform waveguide wall boundaries for particular values of the constants.⁶ Such a choice is meaningful since the perfect conducting non-uniform waveguide wall guides the energy flow.⁷ The u^3 coordinate is chosen orthogonal to both u^1 and u^2 . In

⁶This can always be achieved for the situations being considered in this dissertation because the nonuniform waveguide surface(s) may be represented by functions of two parameters. The third parameter is a constant on this surface (the value of this third parameter defines the surface). Also note that the coordinate surfaces are assumed to be one-to-one, continuous, and differentiable functions of the cartesian coordinates; furthermore, it is assumed that the nonuniform waveguide boundary does not consist of more than four surfaces. The situation in which the boundary consists of more than four surfaces is not considered.

⁷This follows since the electric field, \vec{E} , is normal to the boundary surface while the magnetic field, \vec{H} , is tangent to this surface. Therefore, on the perfectly conducting waveguide surface, the power flow, given by $\text{Re}(\vec{E} \times \vec{H}^*)$, must be along the bounding surface.

general, however, the u^1 and u^2 coordinates need not be orthogonal to each other (although simplification usually results when they are orthogonal).

For the "one-surface" nonuniform waveguide, the $u^1 =$ constant coordinate surface is chosen to coincide with the nonuniform waveguide surface⁶ for a particular value of the constant (because of energy flow considerations at the surface⁷). The $u^3 =$ constant surfaces are chosen to be orthogonal to the $u^1 =$ constant coordinate surfaces with an orientation that makes the waveguide axis normal to the $u^3 =$ constant surfaces. The selection thus far is consistent with "two-set-of-surface" situations previously described. Now, however, additional freedom remains for the selection of the u^2 coordinate. For reasons that will become apparent later, the u^2 coordinate will be required to be orthogonal to the u^3 coordinate. The remaining freedom in the u^2 coordinate selection is used to simplify the analysis (usually this happens with completely orthogonal coordinates).

In both the one-surface and two-surface situations, the propagation characteristics will be studied along the u^3 direction. Note that u^1 and u^2 are not always orthogonal, but great simplification will usually result if they can be made orthogonal. On the other hand, it will be shown

that the formulation techniques of this chapter requires the u^3 coordinate to be orthogonal to both u^1 and u^2 . It will be subsequently assumed that the u^i coordinates ($i = 1, 2, 3$) can be described as continuous differentiable single valued functions of cartesian coordinates.

The assumed orthogonality of u^3 to both u^1 and u^2 implies (from $\nabla u^1 \cdot \nabla u^3 = 0$ for $i = 1, 2$) that

$$\left(\frac{\partial u^1}{\partial \alpha}\right)\left(\frac{\partial u^3}{\partial \alpha}\right) = 0 \quad \text{for } i = 1, 2 \quad (3.2-4)$$

where α runs over the cartesian coordinates x, y , and z when the u^i coordinates are expressed as a function of x, y , and z . These two relations will be useful for determining a suitable set of coordinates and for deciding whether or not the uncoupled transmission line representation is possible.

When the orthogonality of the u^3 coordinate is satisfied, it follows from Equation 1 that, if the electric Hertz vector potential, $\bar{\pi}_e$, is chosen to be in the direction of the u^3 coordinate, then \bar{H}_e lies on the transverse (u^1, u^2) surface.⁸ Hence the solution derived from $\bar{\pi}_e$ is called a generalized E-mode, or transverse magnetic

⁸This is the $u^3 = \text{constant}$ surface.

(TM), wave. This is one reason for requiring u^3 to be orthogonal to both u^1 and u^2 .

In order to separate out the u^3 propagation dependence, the electric Hertz potential, $\bar{\pi}_e$ will be assumed to be expressible in the form

$$\bar{\pi}_e = \hat{a}_3 \psi_e(u^1, u^2) I_e(u^3) \quad (3.2-5)$$

where \hat{a}_3 is a unit vector normal to the surface of constant u^3 (its direction depends upon position),⁹ and ψ_e and I_e are functions of the variables denoted in parentheses that are to be determined from the analysis. Sufficient conditions for Equation 5 to hold will be discussed subsequently. In terms of the generalized coordinates selected, Equation 2 (the Helmholtz equation for $\bar{\pi}_e$) can be written as [8,28].

$$\frac{1}{\sqrt{g}} \sum_{i,j=1}^3 \frac{\partial}{\partial \mu^i} \left(\sqrt{g} g^{ij} \frac{\partial \bar{\pi}_e}{\partial \mu^j} \right) + \kappa_o^2 \bar{\pi}_e = 0 \quad (3.2-6)$$

where g^{ij} are the contravariant components of the Riemann metric tensor which are given by

⁹Later the consequences of choosing the Hertz vector potential in a different direction will be considered.

$$g^{ij} = \sum_{\alpha} \left(\frac{\partial u^i}{\partial \alpha} \right) \left(\frac{\partial u^j}{\partial \alpha} \right) \quad (3.2-7)$$

where $\alpha = x, y, z$ and $i, j = 1, 2, 3$

and

$$g = \det g_{ij} = \frac{1}{\det g^{ij}} \quad (3.2-8)$$

where g_{ij} are the covariant components of the Riemann metric tensor. The Riemann metric tensor may be defined in terms of the invariance of distance as

$$(ds)^2 = \sum_{ij} g_{ij} du^i du^j = (\text{distance element})^2 \quad (3.2-9)$$

It is related to the contravariant components by

$$\sum_j g_{ij} g^{kj} = \delta_i^k = \begin{cases} 1 & \text{if } k=i \\ 0 & \text{if } k \neq i \end{cases} \quad (3.2-10)$$

From Equations 4, 7, and 10, it follows that

$$g^{i3} = g_{i3} = 0 \quad \text{for } i = 1, 2 \quad (3.2-11)$$

Equation 6 can, therefore, be rewritten as

$$\nabla_t^2 \bar{\pi}_e + \frac{1}{\sqrt{g}} \frac{\partial}{\partial \mu^3} \left(\sqrt{g} g^{33} \frac{\partial \bar{\pi}_e}{\partial \mu^3} \right) + K_o^2 \bar{\pi}_e = 0 \quad (3.2-12)$$

where

$$\nabla_t^2 \bar{\pi}_e = \frac{1}{\sqrt{g}} \sum_{i,j=1}^2 \frac{\partial}{\partial u^i} \left(\sqrt{g} g^{ij} \frac{\partial \bar{\pi}_e}{\partial u^j} \right) \quad (3.2-13)$$

Upon substituting the form of Equation 5 for $\bar{\pi}_e$ into Equation 12 and dividing by $\psi_e I_e$ one obtains

$$\frac{\nabla_t^2 \psi_e}{\psi_e} + \frac{\frac{1}{\sqrt{g}} \frac{\partial}{\partial u^3} \left(\sqrt{g} g^{33} \frac{\partial I_e}{\partial u^3} \right)}{I_e} + \kappa_o^2 = 0 \quad (2.2-14)$$

It is desired to separate $I_e(u^3)$ from the rest of the equation in order to be able to represent propagation in the u^3 direction by uncoupled nonuniform transmission lines. However, g , g^{33} , and ∇_t are functions of all three variables and therefore separation of $I_e(u^3)$ is not possible unless an additional restriction on the coordinate system is imposed besides the orthogonality of the u^3 coordinate with respect to both the u^1 and u^2 coordinates. It is observed, however, that if

$$\frac{1}{\sqrt{g}} \frac{\partial \sqrt{g}}{\partial u^3} = \frac{1}{2} \left(\frac{\partial \ln g}{\partial u^3} \right) = f_1(u^3) \quad (3.2-15)$$

and

$$g^{33} = f_2(u^3) \quad (3.2-16)$$

where $f_1(u^3)$ and $f_2(u^3)$ are functions of the arguments in parentheses, then

$$\begin{aligned} \frac{1}{\sqrt{g}} \frac{\partial}{\partial u^3} \left(\sqrt{g} g^{33} \frac{\partial I_e}{\partial u^3} \right) &= g^{33} \frac{d^2 I_e}{(du^3)^2} + \frac{dI_e}{du^3} \left[\frac{g^{33}}{\sqrt{g}} \frac{\partial \sqrt{g}}{\partial u^3} + \frac{\partial g^{33}}{\partial u^3} \right] \\ &= f_2(u^3) \frac{d^2 I_e}{(du^3)^2} + f_3(u^3) \frac{dI_e}{du^3} \end{aligned} \quad (3.2-17)$$

where

$$f_3(u^3) = f_1(u^3) f_2(u^3) + \frac{df_2(u^3)}{du^3} \quad (3.2-17A)$$

By substituting Equation 17 into Equation 14, it results that

$$\frac{\nabla_t^2 \psi_e}{\psi_e} + K_o^2 + \frac{f_2(u^3) \frac{d^2 I_e}{(du^3)^2} + f_3(u^3) \frac{dI_e}{du^3}}{I_e} = 0 \quad (3.2-18)$$

Since I_e is a function of u^3 , Equation 18 can be written as

$$\frac{\nabla_t^2 \psi_e}{\psi_e} + K_o^2 + K_{tn}^2(u^3) = 0 \quad (3.2-19A)$$

where

$$K_{tn}^2(u^3) = \frac{f_2(u^3) \frac{d^2 I_e(u^3)}{(du^3)^2} + f_3(u^3) \frac{dI_e(u^3)}{du^3}}{I_e(u^3)} \quad (3.2-19B)$$

In general, however, the ∇_t^2 operator contains the u^3 coordinate as a parameter. This means that u^3 can appear in the ∇_t^2 operator but that there is no differentiation with respect to u^3 . The separability of Equations 19 depends upon whether or not the specific functional structure of the ∇_t^2 operator permits determination of $K_{tn}^2(u^3)$ for all values of u^3 . This requirement is studied in greater detail at the end of this section.

For the present, the case in which Equation 18 is separable¹⁰ will be considered. In this case Equations 19A and 19B can be rewritten as

$$\nabla_t^2 \psi_e(u^1, u^2) + \kappa_{\tau k}^2(u^3) \psi_e(u^1, u^2) = 0 \quad (3.2-20A)$$

¹⁰When the set of $K_{tn}^2(u^3)$ functions cannot be determined, this implies that the assumed form in Equation 5 may not be valid.

$$\frac{d^2 I_e}{(du^3)^2} + \left[\frac{f_3(u^3)}{f_2(u^3)} \right] \frac{dI_e}{du^3} + \frac{K_{tn}^2(u^3)}{f_2(u^3)} I_e = 0 \quad (3.2-21A)$$

where

$$\kappa_{tk}^2(u^3) = K_o^2 - K_{tk}^2(u^3)$$

An important special case occurs when $g^{33} = 1$ because, for this case, the u^3 coordinate represents true length¹¹ (see Equations 9 and 10). Moreover, when u^3 is a distance coordinate, a clearer physical interpretation involving distances and velocities can result. It is observed from Equation 16 that $g^{33} = 1$ for all values of u^1 , u^2 , and u^3 when $f_2(u^3)$ is unity. In this instance, Equations 17A, 20 and 21 reduce to

$$\nabla_t^2 \psi_e + \kappa_{tk}^2(u^3) \psi_e = 0 \quad (3.2-20B)$$

and

$$\frac{d^2 I_e}{(du^3)^2} + f_1(u^3) \frac{dI_e}{du^3} + K_{tn}^2(u^3) I_e = 0 \quad (3.2-21B)$$

¹¹Such coordinates will be referred to as distance coordinates.

Second order differential Equations 21 can be represented as the equation for a nonuniform transmission line. A nonuniform transmission line can be expressed in the form¹²

$$\frac{d^2 I}{(du^3)^2} - \frac{\left(\frac{dy}{du^3}\right)}{y} \frac{dI}{du^3} - yzI = 0 \quad (3.2-22)$$

where $y(u^3)$ and $z(u^3)$ are the admittance per length and impedance per length respectively. Comparing Equations 21 and 22 motivates the following substitutions in Equation 21A:

$$y(u^3) = c_1 e^{-\int_0^{u^3} \frac{f_3(\lambda)}{f_2(\lambda)} d\lambda} \quad (3.2-23)$$

$$z(u^3) = \frac{-K_{tn}^2(u^3)}{c_1 f_2(u^3)} e^{\int_0^{u^3} \frac{f_3(\lambda)}{f_2(\lambda)} d\lambda} \quad (3.2-24)$$

$$V_e(u^3) = -\frac{1}{y(u^3)} \frac{dI_e(u^3)}{du^3} \quad (3.2-25A)$$

where C_1 is a constant.¹³

¹²See Equation (A2-4) in Appendix A. (The variables have been changed to conform to the generalized coordinates used in this section.)

¹³Later, it will be shown (see Equation 58) that $C_1 = j\omega\epsilon$.

Equation 25A can equivalently be written as

$$\frac{dI_e(u^3)}{du^3} = -y(u^3) v_e(u^3) \quad (3.2-25)$$

Equations 23, 24, and 25 will now be verified by direct substitution. By differentiating Equation 23 and 25 one obtains

$$\frac{dy(u^3)}{du^3} = \frac{-c_1 f_3(u^3)}{f_2(u^3)} e^{-\int_0^{u^3} \frac{f_3(\lambda)}{f_2(\lambda)} d\lambda} = -\frac{f_3(u^3)}{f_2(u^3)} y(u^3) \quad (3.2-26)$$

and

$$\begin{aligned} \frac{d^2 I_e(u^3)}{(du^3)^2} &= - \left[\frac{dy(u^3)}{du^3} \right] v_e(u^3) - y(u^3) \frac{dv_e(u^3)}{du^3} \\ &= \left[\frac{f_3(u^3)}{f_2(u^3)} \right] y(u^3) v_e(u^3) - y(u^3) \frac{dv_e(u^3)}{du^3} \end{aligned} \quad (3.2-27)$$

Substituting Equations 26A and 27B into 21A it results that

$$\frac{dv_e(u^3)}{du^3} = \frac{K_{tn}^2(u^3)}{f_2(u^3)y(u^3)} I_e(u^3) \quad (3.2-28)$$

From Equation 24B it follows that

$$\frac{dV_e(u^3)}{du^3} = -z(u^3)I_e(u^3) \quad (3.2-29)$$

Equations 25 and 29 are the time invariant nonuniform transmission line Equations (see Equations (A2-1) and (A2-2) in Appendix A). The representation of the nonuniform waveguide by uncoupled nonuniform transmission lines for the restriction in Equations 4, 15, 16 and 20 has thus been demonstrated. There is an uncoupled nonuniform transmission line for each $\chi_{\tau k}^2(u^3)$ that is determined in Equation 20, 21A or 21B.

At this point in the discussion, it will be useful to digress and physically interpret the assumption in Equation 15. Since¹⁴

$$\text{div } \bar{V} = \nabla \cdot \bar{V} = \frac{1}{\sqrt{g}} \frac{\partial}{\partial u^i} (\sqrt{g} g^{ij} V_j) \quad (3.2-30)$$

Where V_1 is the u^1 component of an arbitrary vector, V , it follows that when $V = \hat{a}_3$ and $g^{33} = 1$, Equation 15 can be written as

¹⁴The summation convention is understood.

$$\text{div } \hat{a}_3 = f_1(u^3) \quad (3.2-31)$$

where \hat{a}_3 is a unit vector in the u^3 direction. The relationship between the $f_1(u^3)$ function and the way in which the boundary varies will now be determined by using the divergence theorem on the differential volume that is bounded by the nonuniform waveguide walls, the surface $u^3 = C_1 = \text{constant}$, and the surface $u^3 = C_2 = C_1 + \Delta u^3 = \text{constant}$. Let $A(u^3)$ represent the surface area of the constant u^3 surfaces. It is, of course, a function of u^3 . The value of $A(u^3)$ on the surface $u^3 = C_2$ is approximated by the first two terms of the Taylor expansion about $u^3 = C_1$. One obtains

$$A_2 = A(C_1 + \Delta u^3) \approx A_1 + \left. \frac{\partial A(u^3)}{\partial u^3} \right|_{u^3=C_1} \Delta u^3 \quad (3.2-32)$$

where $A_2 = A(C_2)$ and $A_1 = A(C_1)$

Thus, from Equation 31

$$\begin{aligned} \iiint \text{div } \hat{a}_3 \, d\tau &= \iiint f_1(u^3) \, d\tau = \int_{u^3}^{u^3 + \Delta u^3} f_1(u^3) [\iint d\sigma] \, du^3 \\ &= \int_{u^3}^{u^3 + \Delta u^3} f_1(u^3) A(u^3) \, du^3 \\ &= \mathcal{F}(u^3 + \Delta u^3) - \mathcal{F}(u^3) \end{aligned} \quad (3.2-33)$$

where

$$\mathcal{J}(u^3) \equiv \int_{\text{const.}}^{u^3} f_1(\xi) A(\xi) d\xi \quad (3.2-34)$$

and $d\tau$ is a differential volume element and $d\sigma$ is a differential element of surface area on the $u^3 = \text{constant}$ surfaces. One also observes that on the waveguide surface, \hat{a}_3 is tangent to the wall because of the orthogonality condition imposed on u^3 . The surface integral, $\oint \hat{a}_3 \cdot \hat{n} d\sigma$, has no contribution on the waveguide walls. Thus using Equation 32 it follows that

$$\oint \hat{a}_3 \cdot \hat{n} d\sigma = \iint_{\substack{\text{on surface} \\ u^3 = C_2}} d\sigma - \iint_{\substack{\text{on surface} \\ u^3 = C_1}} d\sigma = A_2 - A_1 = \left. \frac{dA(u^3)}{du^3} \right|_{u^3=C_1} \Delta u^3 \quad (3.2-35)$$

By using the divergence theorem, it follows from Equations 33 and 35 that

$$\frac{dA(u^3)}{du^3} \Delta u^3 = \mathcal{J}(u^3 + \Delta u^3) - \mathcal{J}(u^3) \quad (3.2-36)$$

After dividing by Δu^3 and taking the limit as Δu^3 approaches zero, it follows from Equation 34 that

$$\frac{dA(u^3)}{du^3} = \lim_{\Delta u^3 \rightarrow 0} \left[\frac{\mathcal{J}(u^3 + \Delta u^3) - \mathcal{J}(u^3)}{\Delta u^3} \right] = \frac{d\mathcal{J}(u^3)}{du^3} = f_1(u^3) A(u^3)$$

or

$$f_1(u^3) = \frac{d[\ln A(u^3)]}{du^3} \quad (3.2-37)$$

This relates $f_1(u^3)$ to the transverse surface area. Furthermore, since the g^{33} is a distance coordinate, it follows from Equation 15 that

$$\frac{1}{\sqrt{g}} \frac{d\sqrt{g}}{du^3} = \frac{\partial(\ln\sqrt{g})}{\partial u^3} = f_1(u^3) = \frac{d[\ln A(u^3)]}{du^3} \quad (3.2-38)$$

This implies that \sqrt{g} equals the transverse surface area times a function of u^1 and u^2 . The importance of Equations 37 and 38 is that a specific term in differential equation (21B) has been related to the geometry of the nonuniform waveguide.

The characteristic impedance of a propagating wave is usually defined as the ratio of the transverse electric field intensity to transverse magnetic field intensity. An expression for this impedance when $g^{33} = 1$ will now be developed. From Equations 1 and 5 it follows that

$$|\bar{H}_e| = |j\omega\epsilon I_e (\nabla_t \times \hat{a}_3 \psi_e)| \quad (3.2-39)$$

As previously indicated, this component is on the transverse surface. The total electric field is obtained from Equation 3 to be

$$\bar{E}_e = K_o^2 \bar{\pi}_e + \nabla_t (\psi_e \nabla_3 \cdot \hat{a}_3 I_e) + \nabla_3 (\psi_e \nabla_3 \cdot \hat{a}_3 I_e) \quad (3.2-40)$$

where

$$\nabla_3 = \nabla - \nabla_t \quad (3.2-41)$$

Only the middle term of this expression for the electric field intensity is in a transverse direction. Therefore,

$$|\bar{E}_t| = |\nabla_t (\psi_e \nabla_3 \cdot \hat{a}_3 I_e)| = |(\nabla_3 \cdot \hat{a}_3 I_e) \nabla_t \psi_e + \psi_e \nabla_t (\nabla_3 \cdot \hat{a}_3 I_e)| \quad (3.2-42)$$

But

$$(\nabla_3 \cdot \hat{a}_3 I_e) = I_e (\nabla_3 \cdot \hat{a}_3) + \hat{a}_3 \cdot \nabla_3 I_e = (\text{div } \hat{a}_3) I_e + \frac{dI_e}{du^3} \quad (3.2-43)$$

from Equation 31 it follows that Equation 43 only depends upon u^3 . The last term in Equation 42 therefore vanishes. From Equations 31, 42, and 43, it follows that

$$|E_t| = |[f_1(u^3) I_e + \frac{dI_e}{du^3}] \nabla_t \psi_e| \quad (3.2-44)$$

Furthermore, since \hat{a}_3 is orthogonal to ∇_t ,

$$|\nabla_t \times \hat{a}_3 \psi_e| = |\psi_e (\nabla_t \times \hat{a}_3 - \hat{a}_3 \times \nabla_t \psi_e)| = |-\hat{a}_3 \times \nabla_t \psi_e| = |\nabla_t \psi_e| \quad (3.2-45)$$

Equation 39 therefore becomes

$$|H_t| = \omega \epsilon I_e |\nabla_t \psi_e| \quad (3.2-46)$$

From Equations 44 and 46, the characteristic impedance, Z_o , therefore becomes

$$Z_o \equiv \frac{|E_t|}{|H_t|} = \frac{f_1(u^3) I_e + \left(\frac{dI_e}{du^3} \right)}{\omega \epsilon I_e} = \frac{f_1(u^3)}{\omega \epsilon} + \frac{\left(\frac{dI_e}{du^3} \right)}{\omega \epsilon I_e} \quad (3.2-47)$$

Using Equation 37, it finally results that

$$Z_o = \frac{1}{\omega \epsilon} \left[\frac{d \ln A(u^3)}{du^3} + \frac{\left(\frac{dI_e}{du^3} \right)}{I_e} \right] \quad (3.2-48)$$

The importance of this expression is that it relates characteristic impedance to the nonuniform waveguide geometry when $g^{33} = 1$.

One may observe that for the uniform waveguide (where $u^3 = z$ and $A(u^3) = \text{constant}$)

$$I_e = I_e^+ e^{-j\kappa_n z} \quad (3.2-49)$$

where I_e^+ is the forward traveling component of the current (it is a constant) and κ_n is the propagation constant for the n^{th} mode. Upon substituting this expression into Equations

tion 48 it results that for the uniform waveguide the characteristic impedance for E-modes is given by

$$Z_o = \frac{\kappa_n}{j\omega\epsilon} \quad (3.2-50)$$

This is the same result obtained by the uniform waveguide formulation.

It will be shown that the other results obtained thus far also apply for the uniform waveguide (see Chapter 2). For a uniform waveguide, the transverse surface area is a constant. Furthermore, $u^3 = z$ and $g^{33} = 1$. It therefore follows from Equation 37 that for the uniform waveguide

$$f_1(z) = 0 \quad (3.2-51)$$

Thus, from Equations 38 and 51,

$$\frac{1}{\sqrt{g}} \frac{\partial \sqrt{g}}{\partial z} = 0 \quad (3.2-52)$$

This implies that g is independent of z . Furthermore, since the surfaces of constant u^1 and u^2 are independent of z it follows from Equation 7 that g^{1j} for $1, j = 1, 2$ is independent of z . The independence of g and g^{1j} of z implies that the ∇_t operator is now independent of z (see Equation 13). Thus, the values of $\chi_{rk}(z)$, and therefore $K_{tk}(z)$, are constants (see Equation 20B). These constants are called

$\kappa_{\tau k}$ and K_{tk} respectively. Equations 20B and 21B now become

$$\nabla_t^2 \psi_e + \kappa_{\tau k}^2 \psi_e = 0 \quad (3.2-53)$$

and

$$\frac{d^2 I_e}{(du^3)^2} + [\kappa_o^2 - \kappa_{\tau k}^2] I_e = 0 \quad (3.2-54)$$

These are the uniform waveguide results. Furthermore, it follows from Equations 16 and 17A that for the uniform waveguide $f_2(u^3) = 1$ and $f_3(u^3) = f_1(u^3) = 0$. Thus the equations for the admittance and impedance per length (Equations 23 and 24) become

$$y = C_1 \quad (3.2-55)$$

$$z = \frac{k_{tn}^2}{C_1} \quad (3.2-56)$$

For a uniform transmission line, the characteristic impedance, Z_o , is related to the per length admittance and impedance by

$$Z_o = \sqrt{\frac{z}{y}} \quad (3.2-57)$$

Upon substituting the values of y and z from Equations 55 and 56 into 57 and comparing the result with the uniform

waveguide E-mode characteristic impedance (see Equation 50), it follows that an appropriate value of C_1 is

$$C_1 = j\omega\epsilon \quad (3.2-58)$$

If one repeats the previous formulation for the H-mode solutions in terms of a magnetic Hertz potential defined by

$$\nabla \times \bar{\pi}_h = \frac{\bar{E}_h}{(-j\omega u)} \quad (3.2-59A)$$

$$\nabla \cdot \bar{\pi}_h = \theta_h \quad (3.2-59B)$$

$$\bar{\pi}_h = \hat{a}_3 \psi_h(u^1, u^2) v_h(u^3) \quad (3.2-59C)$$

it follows that

$$\bar{H}_h = K_o^2 \bar{\pi}_h + \nabla(\nabla \cdot \bar{\pi}_h) \quad (3.2-60)$$

$$\nabla_t^2 \psi_h + [K_o^2 - K_{tn}^2(u^3)] \psi_h = 0 \quad (3.2-61)$$

and

$$\frac{d^2 v_h}{(du^3)^2} + \left[\frac{f_3(u^3)}{f_2(u^3)} \right] \frac{dv_h}{du^3} + K_{tn}^2(u^3) v_h = 0 \quad (3.2-62)$$

The same interpretations as for the E-mode solution, of course, apply. Furthermore, by the substitutions

$$z(u^3) = j\omega u e^{-\int_0^u \frac{f_3(\lambda)}{f_2(\lambda)} d\lambda} \quad (3.2-63)$$

$$y(u^3) = \frac{-[K_o^2 - \kappa_{rk}^2(u^3)]}{f_2(u^3)z(u^3)} \quad (3.2-64)$$

$$I_h(u^3) = -\frac{1}{z(u^3)} \frac{dV_h(u^3)}{du^3} \quad (3.2-65)$$

it follows that the Equation 62 can be put in the form of nonuniform transmission line equations. Namely,

$$\frac{dV_h(u^3)}{du^3} = -z(u^3)I_h(u^3) \quad (3.2-66)$$

$$\frac{dI_h(u^3)}{du^3} = -y(u^3)V_h(u^3) \quad (3.2-67)$$

These H-mode equations also reduce to the uniform waveguide results as a special case.

In the previous discussion the Hertz vector potential was chosen to be in the direction of \hat{a}_3 , the propagation

direction. Sometimes, however, it is advantageous to choose the Hertz vector potential in another direction. For example, in Chapter 4 it will be shown that the analysis of the junction between two nonuniform waveguides in which at least one set of boundary surfaces are sufficiently smooth may be facilitated by choosing the Hertz vector potential to be normal to the sufficiently smooth boundary surface (because the direction of this Hertz vector is the same on both sides of the junction).

By selecting Hertz vectors in different directions, different sets of generalized modes may be derived, and by paralleling the development for the original generalized modes it is discovered that an uncoupled transmission line representation is possible for the same restrictions that were previously developed. The specific choice of the Hertz vector potential in the transverse plane results in modal solutions that will be referred to as generalized longitudinal section waves (generalized LSE waves corresponding to the electric Hertz vector potential and generalized LSM waves corresponding to the magnetic Hertz vector potential).

At this point, a few comments about the implications in Equations 20A and 20B are appropriate. As indicated, it was assumed that functions $K_{tn}^2(u^3)$, and therefore $\chi_{tn}^2(u^3) = K_0^2 - K_{tn}^2(u^3)$ may be determined for all values of u^3 . It was indicated that whether or not these functions could be determined depended upon the specific functional structure of the transverse Laplacian operator. This structure, in turn, depends upon the specific coordinate system being used. A possible procedure to follow, and its implications, will now be discussed.

First, recall that from the definition of the transverse Laplacian operator for curvilinear coordinates, ∇_t^2 , that there is no differentiation with respect to u^3 . Now consider the case in which the transverse Laplacian may be expressed in the form

$$\nabla_t^2 = \sum_{k=1}^K \xi_k(u^3) \mathcal{L}_k \left(u^1, u^2, \frac{\partial}{\partial u^1}, \frac{\partial}{\partial u^2}, \frac{\partial^2}{(\partial u^1)^2}, \frac{\partial^2}{(\partial u^2)^2} \right) \quad (3.2-68)$$

where $\xi_k(u^3)$ are independent functions of u^3 , the \mathcal{L}_k operators are independent of u^3 , and $K \leq 2$ for usual situations. This form restricts the types of situations that may be handled. (Note that one of the $\xi_k(u^3)$ functions may be a constant.) It is now assumed that $\chi_{tn}^2(u^3)$ may be

expressed in the functional form given by

$$\kappa_{\tau n}^2(u^3) = \sum_{k=1}^K \sigma_{kn}^2 \mathcal{J}_k(u^3) \quad (3.2-69)$$

One now substitutes Equations 68 and 69 into

$$\nabla_t^2 \psi_n + \kappa_{\tau n}^2(u^3) \psi_n = 0 \quad (3.2-70)$$

It results that

$$\sum_{k=1}^K \xi_k(u^3) \mathcal{I}_k \psi_n + \gamma_{kn}^2 \mathcal{J}_k(u^3) \psi_n = 0 \quad (3.2-71)$$

where ψ_n represents either ψ_{en} or ψ_{hn} . In order for this equation to be valid for all values of u^3 requires

$$\mathcal{J}_k(u^3) = \xi_k(u^3) \quad ; k = 1, \dots, K. \quad (3.2-72)$$

Since $\xi_k(u^3)$ is not identically zero, it further follows from Equations 71 and 72 that

$$\mathcal{I}_k \psi_n + \gamma_{kn}^2 \psi_n = 0 \quad ; k = 1, \dots, K \quad (3.2-73)$$

It is noted that this procedure for determining the $\kappa_{\tau n}^2(u^3)$ functions requires all of the set of Equations 73 to be satisfied by the same eigenfunction, ψ_n . This requirement,

however, cannot always be achieved. It does work when $\xi_k(u^3)$ is a constant (say K_1^2). In this case there is only one term and the $\chi_{kn}^2(u^3)$ functions become a constant (see Equations 69 and 72). Namely.

$$\kappa_{tk}^2(u^3) = K_1^2 \gamma_{1n}^2 \quad (3.2-74)$$

This, of course, is the case of separating variables in the ordinary sense that is encountered with uniform waveguides. A second situation for which the requirements in Equations 73 are satisfied occurs when there are two terms in Equation 68 and, in addition, \mathcal{I}_1 depends only upon u^1 and \mathcal{I}_2 depends only upon u^2 . Such a situation is discussed in Section 3.4. A third situation for which the requirements in Equations 73 are satisfied occurs when the sequence in Equation 68 consists of one term (and the problem of satisfying a set of equations by the same eigenfunctions are thereby avoided).

When the conditions implied by Equations 73 can be satisfied, then the ordinary eigenvalue problems¹⁵ given by these equations may be used to determine the γ_{kn}^2 eigenvalues. Then Equations 69 and 72 yield expressions for

¹⁵The boundary conditions needed to solve these eigenvalues are discussed in Section 3.3.

$\chi_n^2(u^3)$. Upon substituting these functions into any of Equations 21, it results that

$$I_n'' + \frac{f_3(u^3)}{f_2(u^3)} I_n' + \left[K_o^2 - \sum_{k=1}^K \xi_k(u^3) \gamma_{kn}^2 \right] I_n = 0 \quad (3.2-75)$$

where I_n represents $I_{en}(u^3)$ or $I_{hn}(u^3)$. This permits the propagation behavior in the u^3 direction to be studied once the eigenvalues in Equations 73 have been determined. Note that only the eigenvalues of Equation 73 are required for this purpose. It is not necessary to determine the eigenfunctions. In some instances it may be convenient to use an approximation technique (such as the variational techniques) to obtain a useful approximation to these eigenvalues. In addition, it may result that an operator expansion of the type shown in Equation 68 is such that only one or two terms dominate. As an engineering approximation, one may only consider the dominating term(s) over various sections of the waveguide. If the dominating term(s) satisfy the appropriate conditions, then that waveguide section may, to a first approximation, be analyzed by determining the eigenvalues of transverse equations(s) and solving a set of equations that are analogous to the nonuniform transmission line equations.

3.3 Boundary Conditions

For a nonuniform waveguide Equations (3.2-73) should be solved subject to the appropriate boundary conditions. The requirements that the components of the electric field vector tangent to the perfect conducting waveguide walls must vanish at these walls, and the normal derivative of the components of the magnetic field intensity tangent to the perfect conducting waveguide wall must vanish at these walls, will be the bases for determining this boundary condition.¹⁶ It will be demonstrated subsequently, that the expression for the boundary condition depends upon the direction of the Hertz vector potential. The procedure will first be illustrated with a Hertz vector potential in the u^3 direction. Later the situation in which the Hertz vector potential is in the u^1 direction will be considered.

For a u^3 directed Hertz vector potential it will be most convenient to use the boundary condition that the \hat{a}_3 component of the electric field, $(E_3 = \hat{a}_3 \cdot \bar{E})$, must vanish on the boundary. It will result that $\psi_e = 0$ on the waveguide wall.

In order to see this, let $\nabla = \nabla_t + \nabla_3$ where ∇_3 is the \hat{a}_3 component of the "del" operator. Then, using Equation (3.2-3)

¹⁶The requirement that the fields are single valued will also be useful (especially with some single surface nonuniform waveguides).

$$\begin{aligned}
\bar{E}_e &= \nabla \times (\nabla \times \bar{\pi}_e) \\
&= \nabla_t \times (\nabla_t \times \bar{\pi}_e) + \nabla_3 \times (\nabla_t \times \bar{\pi}_e) + (\nabla_t + \nabla_3) \times (\nabla_3 \times \bar{\pi}_e)
\end{aligned}
\tag{3.3-1}$$

The last term is zero since ∇_3 and $\bar{\pi}_e$ are both in the \hat{a}_3 direction. Also observe that the second term is perpendicular to \hat{a}_3 (since u^3 is orthogonal to both u^1 and u^2) and, therefore, does not contribute to the \hat{a}_3 component. The first term is now expanded noting that $\nabla_t \cdot \bar{\pi}_e = 0$ because $\bar{\pi}_e$ and ∇_t are perpendicular. It results that

$$\bar{E}_3 = \hat{a}_3 \cdot \bar{E} = \hat{a}_3 \cdot [\nabla_t (\nabla_t \cdot \bar{\pi}_e) - \nabla_t^2 \bar{\pi}_e] = -\hat{a}_3 \cdot \nabla_t^2 \bar{\pi}_e
\tag{3.3-2}$$

But, as previously noted, there is no differentiation with respect to u^3 in the ∇_t operator and therefore the ∇_t^2 operator does not operate on functions of u^3 . Thus, Equation 2 can be rewritten as

$$\begin{aligned}
E_3 &= -\hat{a}_3 \cdot \nabla_t^2 [\hat{a}_3 I_e(u^3) \psi_e(u^1, u^2)] \\
&= -\hat{a}_3 \cdot \hat{a}_3 I_e(u^3) \nabla_t^2 \psi_e(u^1, u^2) = -I_e(u^3) \nabla_t^2 \psi_e(u^1, u^2)
\end{aligned}
\tag{3.3-3}$$

Using Equation (3.2-20), it follows that

$$E_3 = I_e(u^3) [K_o^2 - K_{tn}^2(u^3)] \psi_e(u^1, u^2)
\tag{3.3-4}$$

Since $I_e(u^3)$ and the coefficient of $\psi_e(u^1, u^2)$ are not identically zero on the boundary for all values of u^3 this requires

$$\psi_e(u^1, u^2) = 0 \quad \text{on the boundary}^{17}. \quad (3.3-5)$$

The waveguide wall boundary conditions for the corresponding a_3 directed magnetic Hertz vector potential can be obtained from a parallel derivation. It results that

$$\frac{\partial \psi_h(u^1, u^2)}{\partial n} = 0 \quad \text{on the boundary.} \quad (3.3-6)$$

where the notation $\frac{\partial}{\partial n}$ denotes a directional derivative normal to the boundary.

The procedure for obtaining the waveguide wall boundary conditions when the Hertz vector potential is chosen to be

$$\bar{\pi}_e = \hat{a}_1 \psi_e(u^1, u^2) I_e(u^3) \quad (3.3-7)$$

will now be illustrated for orthogonal coordinates. This is the case corresponding to LSE modes and its results will be used in Chapter 4. The magnetic field corresponding to this Hertz vector potential is therefore

¹⁷One should observe that this proof requires u^3 to be orthogonal to the (u^1, u^2) surface (since Equation 2 is based upon \hat{a}_3 being orthogonal to the ∇_t operator). This tends to reinforce the condition of Equation (3.2-4).

$$\begin{aligned}\bar{H}_e &= j\omega\epsilon \nabla \times \hat{a}_1 \psi_e(u^1, u^2) I_e(u^3) \\ &= j\omega\epsilon I_e (\nabla_t \times \hat{a}_1 \psi_e) + j\omega\epsilon \psi_e (\nabla_3 \times \hat{a}_1 I_e)\end{aligned}\tag{3.3-8}$$

It is easily verified that the first term in Equation 8 is in the \hat{a}_3 direction and the second term in Equation 8 is in the \hat{a}_2 direction. The \hat{a}_2 component of the magnetic field intensity, H_{e2} , is therefore

$$H_{e2} = j\omega\epsilon \psi_e |\nabla_3 \times \hat{a}_1 I_e|\tag{3.3-9}$$

Since this component is normal to a perfect conducting $u^2 = \text{constant}$ nonuniform waveguide surface, it must vanish on this surface for all values of u^3 . Thus, it follows from Equation 9 that

$$\nabla_e = 0 \quad \text{on a } u^2 = \text{constant boundary} \tag{3.3-10}$$

Furthermore, for the orthogonal coordinates being considered, \bar{H}_{e2} is tangent to a $u^1 = \text{constant}$ nonuniform waveguide surface. Since the normal derivative of the tangential component of the magnetic field intensity must vanish at a perfect conducting boundary for all values of u^3 , it follows from Equation 9 that

$$\left| \frac{\partial \psi_e}{\partial u^1} \right| = |\nabla \psi_e \cdot \hat{a}_1| = 0 \quad \text{on a } u^1 = \text{constant boundary} \tag{3.3-11}$$

From the derivation of these boundary conditions one can conclude that, in general, for orthogonal coordinates $\nabla_e = 0$ on a perfect conducting surface to which the Hertz vector potential is tangent and $\nabla \psi_e \cdot \hat{n} = 0$ (where \hat{n} is a unit normal) for a perfect conducting surface that is normal to the Hertz vector potential.

3.4 Engineering Application and Significance

Earlier in this chapter it was shown that when appropriate coordinate system conditions are satisfied, a nonuniform waveguide analysis may be separated into two parts. The first part is a set of eigenvalue problems in terms of the transverse coordinates. The solution to this problem yields a set of eigenfunctions and their corresponding eigenvalues. The second part is a nonuniform transmission line analysis. The eigenvalues of the first problem provide transmission line parameters for the second problem¹⁸. The solution to the field theory problem is a superposition of the separate mode problems. (Note that, in practice, for closed nonuniform waveguides, only a finite spectrum of propagating modes need be considered.)

The major significance of this analysis decomposition is that after determination of the eigenvalues of the transverse problems (by either analytic, approximate, or numerical techniques) the analysis reduces to solving a set of uncoupled nonuniform transmission lines. Thus, the body of knowledge of nonuniform transmission line analysis may be applied directly to the study of the class of nonuniform waveguides considered in this chapter. A review of the technology of nonuniform transmission lines is presented in Appendix A.

¹⁸It is often said that the previously described process enables one to represent a nonuniform waveguide by nonuniform transmission lines (the determination of the eigenvalues is implied but often not stated).

The importance of being able to separate out the u^3 coordinate into a separate problem will be clarified by the discussion of some general properties of wave propagation that follows:

In general the solution to the Helmholtz equation that was obtained by removing the time factor $e^{j\omega t}$, is a complex function of the coordinates (u^1, u^2, u^3) . Thus, the Hertz vector, $\vec{\pi}$, has the form.

$$\vec{\pi} = \hat{i}_1 A(u^1, u^2, u^3) e^{+j\phi(u^1, u^2, u^3)} \quad (3.4-1)$$

where \hat{i}_1 is a unit vector in the direction of the Hertz vector and A and ϕ are real functions of position. When the time function is reinserted it results that

$$\vec{\pi} = \hat{i}_1 A(u^1, u^2, u^3) e^{j[\omega t + \phi(u^1, u^2, u^3)]} \quad (3.4-2)$$

Surfaces over which the phase is constant are called constant phase surfaces. These are defined by

$$\omega t + \phi(u^1, u^2, u^3) = \text{constant}. \quad (3.4-3)$$

The waves are called uniform waves when the amplitude A is a constant over the equiphase surfaces. Perpendiculars to the equiphase surfaces are called wave normals (these are in the direction of $\nabla\Phi$ and are curves along which the instantaneous phase changes most rapidly. The rate at which the phase decreases in some direction is called the phase constant in that direction. The phase constants in the u^1 coordinate direction, β_1 , is given by

$$\beta_1 = -\nabla\Phi \cdot \hat{a}_1 \quad (3.4-4)$$

These may be considered as the components of the vector phase constant defined by

$$\vec{\beta} = -\nabla\Phi \quad (3.4-5)$$

These are functions of position. To keep the instantaneous phase constant for an incremental increase in time, it is required that

$$\omega dt + \nabla\Phi \cdot ds = 0 \quad (3.4-6)$$

The phase velocity of a wave in a given direction is defined as the component of the velocity of surfaces of

constant phase in that direction. For example, the phase velocity along the normal to surfaces of constant phase is given by

$$v_p = - \frac{\omega}{|\nabla\Phi|} = \frac{\omega}{|\beta|} \quad (3.4-7)$$

The phase velocity along the u^1 coordinate direction is

$$v_{p1} = \frac{\omega}{|\nabla\Phi \cdot \hat{a}_1|} = \frac{\omega}{\beta_1} \quad (3.4-8)$$

Note that $v_{p1} \geq v_p$.

The aim of the analysis in Section 3.2 was to express the Hertz vector potential in the form

$$\bar{\pi} = \hat{i}_1 \psi(u^1, u^2) I(u^3) \quad (3.4-9)$$

where ψ and I are complex functions of position. This decomposition facilitates considering velocities along the u^3 coordinate direction since, for this case, the time dependent Hertz vector may be written as

$$\bar{\pi} = \hat{i}_1 \left[\psi_A(u^1, u^2) e^{j\psi_p(u^1, u^2)} I_A(u^3) \right] e^{j[\omega t + I_p(u^3)]} \quad (3.4-10)$$

Thus, the phase velocity along the u^3 direction is given by

$$v_{p3} = \frac{\omega}{\left| \frac{dI_p(u^3)}{du^3} \right|} \quad (3.4-11)$$

This information is directly obtainable from the solution to the nonuniform transmission line problem. In addition, $I_A(u^3)$ is a direct measure of amplitude variations with position along the waveguide. It may be written in the form

$$I_A(u^3) = e^{-\alpha(u^3)} \quad (3.4-12)$$

where α is an attenuation function. For a lossless waveguide, amplitude variations are due to distributing the modal wave energy over different transverse surfaces as a function of position along the waveguide. The group velocity along the u^3 coordinate is given by

$$v_{g3} = - \frac{d\omega}{d\beta_3} \quad (3.4-13)$$

where $\beta_3 = \frac{dI_p(u^3)}{du^3}$

Note that $I_p(u^3)$ is a function of frequency because $K_0 = \omega\sqrt{\mu\epsilon}$ depends on frequency.

The problem of analyzing electromagnetic wave propagation in a specific nonuniform waveguide will now be considered. In order to perform such an analysis, an appropriate coordinate system must be selected. This involves intuition and engineering judgment and without additional guidelines an optimum decision is usually limited to relatively simple situations.

At the present time, the body of knowledge guiding engineering judgment in the selection of an optimum coordinate system has been limited to complete separation of variables in orthogonal coordinate systems [32, 33, 34, and 35]. In fact, only orthogonal quadratic surfaces have been cataloged for their complete separability properties [35]. As indicated earlier in this dissertation, however, the representation of the nonuniform waveguide by a set of uncoupled nonuniform transmission lines requires only one coordinate to be orthogonal and separated. Complete separation of variables and complete orthogonality of coordinates are not necessary for studying the nonuniform waveguide.

Fortunately, the theory developed in this chapter provides additional guidelines for selecting an appropriate coordinate system [42]. The manner in which this is useful will be illustrated with the sectorial wedge nonuniform waveguide. Instead of following the conventional procedure of

solving this problem in terms of cylindrical coordinates, engineering judgment will be coupled with the theory developed in Sections 3.2 and 3.3 to logically evolve this choice for a coordinate system. The manner in which additional wave propagation information can be extracted will also be indicated.¹⁹

This section will show that the constraints that led to an uncoupled nonuniform transmission line representation for the nonuniform waveguide often provides useful guidelines for deducing an optimum coordinate system to describe the nonuniform waveguide. This coordinate system is optimum in the sense that it permits the nonuniform waveguide to be represented by transverse equations and a set of uncoupled nonuniform transmission lines and thereby permits the technology of nonuniform transmission lines to be used to study the propagation behavior of the nonuniform waveguide. For a simple shape, the selection of such a coordinate system may be obvious, but in general, the choice may not be obvious. The guiding conditions and requirements developed in the previous sections are summarized in Table I. The balance of this section applies these conditions to the illustrative example.

¹⁹The latter has already been done for the sectorial wedge [3, 14, 27], but it will serve as a model of how to proceed for a more difficult problem.

Table 3.4-1

Sufficient Conditions to Factor

Out the u^3 Dependence $\left[\bar{\pi}(u^1, u^2, u^3) = \psi(u^1, u^2) I(u^3) \right]$

1. u^1 or u^2 are constants on the waveguide walls.
2. Propagation coordinate, u^3 , is orthogonal to both transverse coordinates (the transverse coordinates need not be orthogonal to each other).
3. The g^{33} metric coefficient is independent of u^1 and u^2 .
For convenience, one usually tries to select $g^{33} = 1$.
4. The logarithmic derivative of the determinant of the metric coefficients depends only upon the propagation coordinate.
It is equal to the logarithmic derivative of the transverse surface area when $g^{33} = 1$.
5. The coordinate surfaces are one-to-one continuous differentiable functions of cartesian coordinates.
6. The transverse Laplacian, ∇_t^2 , may be expressed in one of two general forms.

A. $\nabla_t^2 = \xi_1(u^3) \mathcal{L}_1$ where \mathcal{L}_1 is an operator that is independent of u^3 . In this case $\psi_n(u^1, u^2)$ must satisfy the eigenvalue equation $\mathcal{L}_1 \psi_n + \gamma_{1n}^2 \psi_n = 0$ where $(-\gamma_{1n}^2)$ are the eigenvalues to be determined. The corresponding u^3 equation for $I_n(u^3)$ is

$$I_n'' + \frac{f_3(u^3)}{f_2(u^3)} I_n' + K_0^2 - \xi_1(u^3) \gamma_{1n}^2 I_n = 0$$

Table 3.4-1 continued

6. B. $\nabla_t^2 = \xi_1(u^3) \mathcal{L}_1 + \xi_2(u^3) \mathcal{L}_2$ where \mathcal{L}_1 and \mathcal{L}_2 are operators that are independent of u^3 . In this case, $\psi_n(u^1, u^2)$ must simultaneously satisfy eigenvalue equations

$$\mathcal{L}_1 \psi_n + \gamma_{1n}^2 \psi_n = 0$$

$$\mathcal{L}_2 \psi_n + \gamma_{2n}^2 \psi_n = 0$$

where $(-\gamma_{1n}^2)$ and $(-\gamma_{2n}^2)$ are the eigenvalues to be determined. When this is achieved, the corresponding u^3 equation for $I_n(u^3)$ is

$$I_n'' + \frac{f_3(u^3)}{f_2(u^3)} I_n' + \left[K_0^2 - \xi_1(u^3) \gamma_{1n}^2 - \xi_2(u^3) \gamma_{2n}^2 \right] I_n = 0$$

The basic procedure for determining an appropriate coordinate system is to start with as general a form for the coordinate equations as possible (consistent with the requirement that coordinate surfaces coincide with the boundary walls). Then the consequences of requiring the u^3 coordinate to be orthogonal to both the u^1 and u^2 coordinates will be determined. Since the main concern is to study the propagation behavior in the u^3 direction, it is convenient to try to choose $g^{33} = 1$. The constraints implied by Equations (3.2-20B), and (3.2-38) will then be used to guide the selection of a coordinate system.

The waveguide surfaces of the sectorial wedge shown in Figure (3.4-1) are described by the equations

$$\left(\frac{y}{z}\right) = m = \text{constant} \quad (3.4-14A)$$

$$y = 0 \quad (3.4-14B)$$

$$x = 0 \quad (3.4-15A)$$

and

$$x = b = \text{constant} \quad (3.4-15B)$$

In order to facilitate the fitting of the boundary conditions, the general coordinates u^1 and u^2 are expressed as²⁰

²⁰One may note that for this example Equations 16 and 17 imply that u^1 is orthogonal to u^2 (as they are in cylindrical coordinates). Complete orthogonality is therefore deduced directly from the boundary conditions and not arbitrarily imposed.

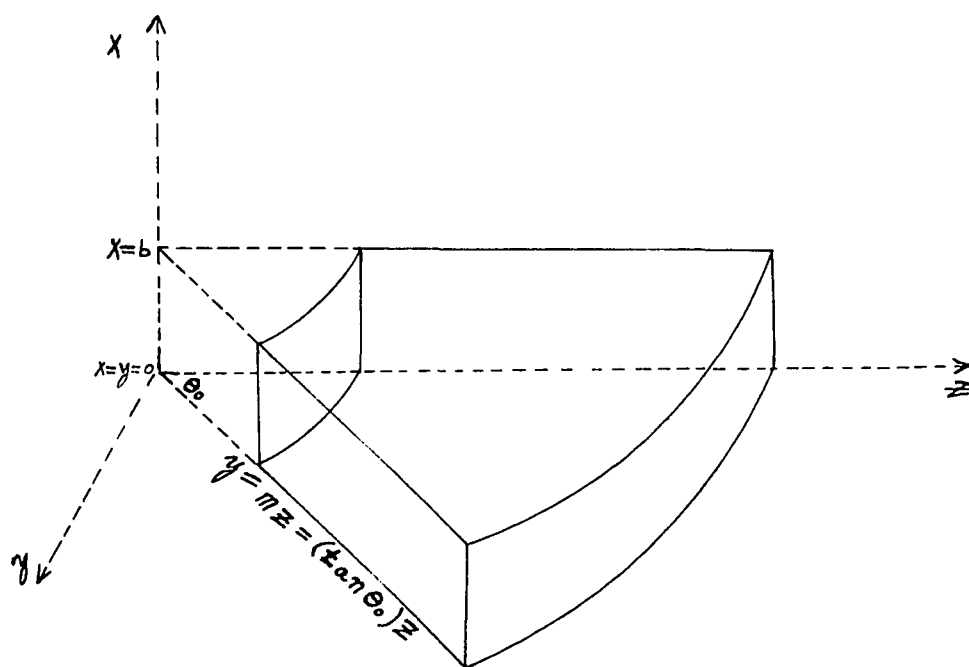


Figure 3.4-1

Sectorial Wedge Nonuniform Waveguide

$$u^1 = f\left(\frac{y}{z}\right) \quad (3.4-16)$$

and

$$u^2 = g(x) \quad (3.4-17)$$

where f and g are continuous single-value functions to be specified. For the moment, the u^3 coordinate will be completely arbitrary. Thus

$$u^3 = h(x, y, z) \quad (3.4-18)$$

where h is also a continuous single-value function.

The orthogonality of the u^3 coordinate to the u^2 coordinate (see Equation 3.2-4) requires that

$$\left(\frac{\partial g}{\partial x}\right)\left(\frac{\partial h}{\partial x}\right) = 0 \quad (3.4-19)$$

But $\frac{\partial g}{\partial x}$ cannot be equal to zero because this would imply that u^2 is a constant. Therefore Equation 19 implies that

$$\frac{\partial h}{\partial x} = 0 \quad (3.4-20)$$

or equivalently

$$u^3 = h(y, z) \quad (3.4-21)$$

In a similar manner, from Equations 16, 18, and 19 it follows that

$$\frac{1}{z} f' \left(\frac{y}{z} \right) \frac{\partial h(y, z)}{\partial y} - \left(\frac{y}{z^2} \right) f' \left(\frac{y}{z} \right) \frac{\partial h}{\partial z} = \frac{1}{z} f' \left(\frac{y}{z} \right) \left[\frac{\partial h}{\partial y} - \frac{y}{z} \frac{\partial h}{\partial z} \right] = 0$$

(3.4-22)

where $f(y/z)$ is the derivative $(df(\xi)/d\xi)$ evaluated at $\xi = y/z$. In a manner paralleling that used to obtain Equation 21 it is concluded that $f(y/z)$ cannot be zero since this would require the u^1 coordinate to be a constant. Therefore

$$\frac{\partial h}{\partial y} = \left(\frac{y}{z} \right) \frac{\partial h}{\partial z}$$

(3.4-23)

From Equation 22 the metric coefficient, g^{33} , is given by

$$g^{33} = \left(\frac{\partial u^3}{\partial x} \right)^2 + \left(\frac{\partial u^3}{\partial y} \right)^2 + \left(\frac{\partial u^3}{\partial z} \right)^2$$

(3.4-24)

By substituting Equation 20 into Equation 24, one obtains

$$g^{33} = \left(\frac{\partial h}{\partial y} \right)^2 + \left(\frac{\partial h}{\partial z} \right)^2$$

(3.4-25)

From Equations 23 and 25 it follows that

$$g^{33} = \left(\frac{y}{z} \right)^2 \left(\frac{\partial h}{\partial z} \right)^2 + \left(\frac{\partial h}{\partial z} \right)^2 = \left(\frac{\partial h}{\partial z} \right)^2 \left[\left(\frac{y}{z} \right)^2 + 1 \right] = \left(\frac{\partial h}{\partial z} \right)^2 [y^2 + z^2]$$

(3.4-26)

Similarly from Equations 16, 17, 21, and 22, the other metric coefficients are found to be

$$g^{11} = \left[\frac{f'(\frac{y}{z})}{z} \right]^2 \left[1 + \left(\frac{y}{z} \right)^2 \right] \quad (3.4-27)$$

$$g^{22} = [g'(x)]^2 \quad (3.4-28)$$

$$g^{ij} = 0 \quad \text{for } i \neq j \quad (3.4-29)$$

For g^{33} equal to one it follows from Equation 26 that

$$\frac{\partial h}{\partial z} = \frac{z}{\sqrt{y^2 + z^2}} \quad (3.4-30)$$

or

$$u^3 = h(y, z) = \sqrt{y^2 + z^2} + q(y) \quad (3.4-31)$$

Upon substituting Equation 31 into Equation 23, it is easily shown that $q(y)$ can at most be a constant. Thus

$$u^3 = \sqrt{y^2 + z^2} + r_0 \quad (3.4-31A)$$

where r_0 is a constant that can be made zero by an appropriate choice for the origin. It is observed that u^3 corresponds to the radial coordinate of a cylindrical coordinate system. This is the case that will be considered. Upon substituting the values of g^{ij} from Equations 26, 27, 28, and 29 into Equation (3.2-8) it results that

$$\sqrt{g} = \frac{\sqrt{y^2 + z^2}}{\left[1 + \left(\frac{y}{z}\right)^2\right] f'\left(\frac{y}{z}\right) g'(x)} \quad (3.4-32)$$

Equation (3.2-20B) is next expanded in terms of metric coefficients by using Equation (3.2-13). One obtains

$$\frac{1}{\sqrt{g}} \frac{\partial}{\partial u^i} \left(\sqrt{g} g^{ij} \frac{\partial \psi_e}{\partial u^j} \right) + \kappa_{\text{tn}}^2 (u^3) \psi_e = 0 \quad (3.4-33)$$

where $i, j = 1, 2$. and the summation convention is understood.

Upon substituting the values of the metric coefficients from Equations 27, 28, 29, and 32 into Equation 33, it results that

$$\begin{aligned} & \frac{\left[1 + \left(\frac{y}{z}\right)^2\right] f'\left(\frac{y}{z}\right)}{(u^3)^2} \frac{\partial}{\partial u^1} \left(\left[1 + \left(\frac{y}{z}\right)^2\right] f'\left(\frac{y}{z}\right) \frac{\partial \psi_e}{\partial u^1} \right) \\ & + g'(x) \frac{\partial}{\partial u^2} \left(g'(x) \frac{\partial \psi_e}{\partial u^2} \right) + \kappa_{\text{tn}}^2 (u^3) \psi_e = 0 \end{aligned} \quad (3.4-34)$$

By using Equations 16 and 17 this can be rewritten as

$$\begin{aligned} & \frac{[1 + (f^{-1}(u^1))^2] f'[f^{-1}(u^1)]}{(u^3)^2} \frac{\partial}{\partial u^1} [1 + (f^{-1}(u^1))^2] f'[f^{-1}(u^1)] \frac{\partial \psi_e}{\partial u^1} \\ & + g'[g^{-1}(u^2)] \frac{\partial}{\partial u^2} g'[g^{-1}(u^2)] \frac{\partial \psi_e}{\partial u^2} + \kappa_{\text{tn}}^2 (u^3) \psi_e = 0 \end{aligned} \quad (3.4-35)$$

where f^{-1} and g^{-1} are the inverse functions of f and g respectively.²¹

²¹It is assumed that the transformations are 1-1 and continuous within the region and therefore that the inverse transformation exists.

It is observed that the first term in Equation 35 is inversely proportional to $(u^3)^2$ while the second term is independent of u^3 . The transverse Laplacian, ∇_t^2 , therefore has the form

$$\nabla_t^2 = \alpha(u^3) \mathcal{L}_1 + \mathcal{L}_2 \quad (3.4-36)$$

where

$$\alpha(u^3) = \frac{1}{(u^3)^2} \quad (3.4-37)$$

and \mathcal{L}_1 and \mathcal{L}_2 are operators given by

$$\mathcal{L}_1 = \{1+[f^{-1}(u^1)]^2\} f'[f^{-1}(u^1)] \frac{\partial}{\partial u^1} \left(\{1+[f^{-1}(u^1)]^2\} f'[f^{-1}(u^1)] \frac{\partial}{\partial u^1} \right) \quad (3.4-38)$$

$$\mathcal{L}_2 = g'[g^{-1}(u^2)] \frac{\partial}{\partial u^2} \left(g'[g^{-1}(u^2)] \frac{\partial}{\partial u^2} \right) \quad (3.4-39)$$

One notes that \mathcal{L}_1 depends only on u^1 and \mathcal{L}_2 depends only on u^2 . These operators may alternately be expressed as (see Equation 34)

$$\mathcal{L}_1 = \left[1 + \left(\frac{y}{z}\right)^2\right] f' \left(\frac{y}{z}\right) \frac{\partial}{\partial u^1} \left(\left[1 + \left(\frac{y}{z}\right)^2\right] f' \left(\frac{y}{z}\right) \frac{\partial}{\partial u^1} \right) \quad (3.4-38A)$$

and

$$\mathcal{L}_2 = g'(x) \frac{\partial}{\partial u^2} \left(g'(x) \frac{\partial}{\partial u^2} \right) \quad (3.4-39A)$$

In accordance with the sixth requirement of Table 1, ψ_e must simultaneously satisfy

$$\mathcal{L}_1 \psi_{em} + \gamma_{1m}^2 \psi_{em} = 0 \quad (3.4-40)$$

and

$$\mathcal{L}_2 \psi_{em} + \gamma_{2m}^2 \psi_{em} = 0 \quad (3.4-41)$$

where n is an index that distinguishes the different modes, $-\gamma_{1n}^2$ and $-\gamma_{2n}^2$ are eigenvalues that are to be determined, and ψ_{en} are the corresponding eigenfunctions (corresponding to modes). The eigenfunctions are required to simultaneously satisfy Equations 40 and 41. This includes the appropriate boundary condition on ψ_e , namely $\psi_e = 0$ on the boundary. One therefore tries to select the functions,

$f(y/z)$ and $g(x)$, to satisfy this condition. Since \mathcal{L}_1 depends only on u^1 and \mathcal{L}_2 depends only on u^2 , one may express Ψ_{en} as the product of a function of u^1 , $U_{1i}(u^1)$, times a function of u^2 , $U_{2j}(u^2)$. For each different set of integer values of i and j there corresponds a mode number n . Equations 38A, 39A, 40 and 41 therefore become

$$\left[1 + \left(\frac{y}{z}\right)^2\right] f' \left(\frac{y}{z}\right) \frac{\partial}{\partial u^1} \left(\left[1 + \left(\frac{y}{z}\right)^2\right] f' \left(\frac{y}{z}\right) U'_{1i}(u^1) \right) + \gamma_{1i}^2 U_{1i} = 0$$

(3.4-42)

and

$$g'(x) \frac{\partial}{\partial u^2} \left(g'(x) U'_{2j}(u^2) \right) + \gamma_{2j}^2 U_{2j} = 0$$

(3.4-43)

Sinusoids are the simplest set of eigenfunctions for Equation 24 that also satisfies the boundary conditions that

Ψ_e and therefore U_2 is zero when $x = 0$ and when $x = b$. This occurs when $g'(x)$ is a constant. Since Equation 43 can be divided by the value of this constant without changing form, one may pick $g'(x) = 1$ for convenience. It therefore follows that

$$u^2 = g(x) = x + x_0 \quad (3.4-44)$$

where x_0 is a constant that can be made zero by appropriately locating the origin of the coordinate system. The values of the γ_{2j}^2 constants are determined by fitting the boundary conditions with sinusoids. It is observed that

$$\gamma_{2j}^2 = \frac{j\pi^2}{b^2} \quad j=1,2,\dots \quad (3.4-45)$$

Similarly, in order to obtain relatively simple functions (sinusoids) that are zero for $(\frac{y}{z}) = 0$ and $(\frac{y}{z}) = m$ (see Equation 14A) one chooses

$$\left[1 + \left(\frac{y}{z}\right)^2\right] f'\left(\frac{y}{z}\right) = 1 \quad (3.4-46)$$

It therefore follows that

$$u^1 = f\left(\frac{y}{z}\right) = \int \frac{d\left(\frac{y}{z}\right)}{1 + \left(\frac{y}{z}\right)^2} = \tan^{-1}\left(\frac{y}{z}\right) + \theta_k \quad (3.4-47)$$

where θ_k is a constant that can be made zero by appropriately choosing the origin of the coordinate system, and u^1 only takes on its principal values. The γ_{11}^2 constants are determined by fitting sinusoids to the

boundary conditions. It results that

$$\gamma_{1i}^2 = \frac{i\pi}{\theta_0}^2 \quad i=1,2,\dots \quad (3.4-48)$$

where

$$\theta_0 = \tan^{-1} m \quad (\text{see Equation 14A})$$

It is observed that for a coordinate origin located such that u^1 , u^2 , and u^3 are zero when x , y and z are zero that Equations 31A, 44, and 47 define the standard cylindrical coordinate system; namely.

$$u^1 = \tan^{-1} \frac{y}{z} = \theta \quad \text{for } -\frac{\pi}{2} < \theta < \frac{\pi}{2} \quad (3.4-49A)$$

$$u^2 = x \quad (3.4-49B)$$

$$u^3 = \sqrt{y^2 + z^2} = r \quad \text{for } r > 0 \quad (3.4-49C)$$

Until it is verified that Equation (3.2-38) is satisfied (recall that $g^{33} = 1$), the selection of cylindrical coordinates are not guaranteed to result in uncoupled nonuniform transmission lines. For the sectorial wedge in question the transverse surface area is proportional to the value of u^3 . Thus, Equation (3.2-38) becomes

$$\frac{1}{\sqrt{g}} \frac{\partial \sqrt{g}}{\partial u^3} = f_1(u^3) = \frac{1}{u^3} \quad (3.4-50)$$

For cylindrical coordinates, the metric coefficients reduce to

$$\begin{aligned} g^{11} &= (u^3)^2 \\ g^{22} &= 1 \\ g^{33} &= 1 \\ g^{ij} &= 0 \quad \text{for } i \neq j \end{aligned}$$

Thus,

$$\sqrt{g} = u^3 \quad (3.4-51A)$$

and Equation 50 is easily verified. One should also observe that Equation 50 would be verified if

$$\sqrt{g} = t(u^1, u^2) u^3 \quad (3.4-51B)$$

By comparing Equations 32, 51A, and 51B it follows that for this example

$$t(u^1, u^2) = \frac{1}{\left[1 + \left(\frac{y}{z}\right)^2\right] f'\left(\frac{y}{z}\right) g'(x)} = 1 \quad (3.4-52)$$

Equations 44 and 46 therefore follow directly from Equation 52. Thus, if one had assumed that $t(u^1, u^2) = 1$, the choice of cylindrical coordinates would have followed. It would then be necessary, however, to verify that condition 6 in Table 1 is satisfied.

Once the eigenvalues have been determined (see Equations 45 and 48), $\kappa_n^2(u^3)$ is given by²²

$$\kappa_{\tau n}^2(u^3) = \gamma_{2j}^2 + \frac{\gamma_{11}^2}{(u^3)^2} \quad (3.4-53)$$

Upon substituting this into Equation (3.2-21B), it is concluded that (see Equation 3.2-75)

$$I_{en}'' + \frac{1}{u^3} I_{en}' + \frac{(k_o^2 - \gamma_{2j}^2)(u^3)^2 - \gamma_{11}^2}{u^3} I_{en} = 0 \quad (3.4-54)$$

This is Bessel's equation; its solutions are well known. As previously indicated, information about propagation in the u^3 direction is contained in this equation.

Before proceeding, it should be observed that the specific choice of coordinate functions, $u^1 = f(y/z)$ and $u^2 = g(x)$ may not be unique. For example, the choice, $u^2 = g(x) = a(x + x_0)$ where a is a nonzero constant, would also work. In this case, the choice of the constant, a , may be interpreted as using a different choice of units of measurement along the u^2 coordinate; but, in general, such an interpretation may be difficult. Nevertheless, irres-

²²Recall that integer n corresponds to a set of integers i and j (this notation was used by Marcuvitz [27] in his general uniform waveguide development).

pective of which coordinates are chosen for u^1 and u^2 , Equations 42 and 43 are still eigenvalue problems. Thus, if another choice for coordinates u^1 and u^2 is possible, it is only the values of these eigenvalues that change. The general form of Equation 54 is therefore unaltered. Bessel's equation would still result, but values of the constants would change.

It should be emphasized that the technique for determining an appropriate coordinate system is not always applicable. To see this, consider the pyramidal horn²³ nonuniform waveguide whose boundaries are defined by

$$\frac{y}{z} = m_1 = \text{constant} \quad (3.4-55A)$$

$$\frac{x}{z} = m_2 = \text{constant} \quad (3.4-55B)$$

The coordinates that result are given by

$$u^1 = f(y/z) \quad (3.4-56A)$$

$$u^2 = g(x/z) \quad (3.4-56B)$$

$$u^3 = h(x, y, z) \quad (3.4-56C)$$

For $g^{33} = 1$, one can eventually conclude that

²³To date, only approximate solutions to this structure have been obtained [37].

$$u^3 = \sqrt{x^2 + y^2 + z^2} \quad (3.4-57)$$

It is interesting to observe that this is a spherical radial coordinate and note that Piefke's approximate solution [32] to this problem used spherical coordinates to approximate the shape.

Upon evaluating the metric coefficients and evaluating the expression $\frac{\partial \ln \sqrt{g}}{\partial u^3}$, one finds that this equation cannot be made to depend only upon u^3 and therefore an uncoupled nonuniform transmission line representation is not guaranteed (for $g^{33} = 1$).

A description of how one proceeds to obtain additional propagation information will now be illustrated with the sectorial wedge.²⁴ For the specific choice of cylindrical coordinates, Equations 42, 43, 45, 48, and 54 yield a solution given by

$$\bar{\pi}_e = \hat{a}_3 \sum_{n,m} A_{nm} \sin \frac{n\pi}{b} x \sin \frac{m\pi}{\theta_0} \theta \left[\begin{aligned} & H_{\frac{m\pi}{\theta_0}}^{(2)} \left(k_o^2 - \left(\frac{n\pi}{b} \right)^2 r \right) \\ & + \Gamma_{mn} H_{\frac{m\pi}{\theta_0}}^{(1)} \left(\sqrt{k_o^2 - \left(\frac{n\pi}{b} \right)^2} r \right) \end{aligned} \right] \quad (3.4-58)$$

where $H_{\frac{m\pi}{\theta_0}}^{(1)}$ and $H_{\frac{m\pi}{\theta_0}}^{(2)}$ are Hankel functions of the first and

²⁴This portion of the analysis has already been done for the sectorial wedge [3, 14, 27, 31]. It is included for illustrative purposes.

second kind of order $\frac{m\pi}{\theta_0}$, and Γ_{mn} is the reflection coefficient of the E_{nm} mode. In a similar manner the corresponding \hat{a}_3 directed magnetic Hertz vector is found

to be

$$\bar{\pi}_e = \hat{a}_3 \left\{ \sum_{n,m} B_{nm} \cos \frac{n\pi}{b} x \cos \frac{m\pi}{\theta_0} \theta \cdot \left[H_{\frac{m\pi}{\theta_0}}^{(2)} \left(\sqrt{k_0^2 - \left(\frac{n\pi}{b}\right)^2} r \right) - \Gamma_{mn} H_{\frac{m\pi}{\theta_0}}^{(1)} \left(\sqrt{k_0^2 - \left(\frac{n\pi}{b}\right)^2} r \right) \right] \right\} \quad (3.4-59)$$

For Hertz vector potentials in the \hat{a}_2 (\hat{a}_x) direction the boundary conditions in Equations (3.3-10) and (3.3-11) are used to obtain

$$\bar{\pi}_e = \hat{a}_x \sum_{p,m} A_{pm} \sin \frac{p\pi\theta}{\theta_0} \cos \frac{m\pi x}{b} \left[H_{\frac{p\pi}{\theta_0}}^{(2)}(k_{r_m} r) + \Gamma_{pm} H_{\frac{p\pi}{\theta_0}}^{(1)}(k_{r_m} r) \right] \quad (3.4-60)$$

where

$$k_{r_m} = \sqrt{k_0^2 - \left(\frac{m\pi}{b}\right)^2}$$

Similarly:

$$\bar{\pi}_h = \hat{a}_x \left[\sum_{p,m} B_{pm} \cos \frac{p\pi}{\theta_0} \sin \frac{m\pi x}{b} \left\{ H_{\frac{p\pi}{\theta_0}}^{(2)}(k_{r_m} r) + \Gamma_{pm} H_{\frac{p\pi}{\theta_0}}^{(1)}(k_{r_m} r) \right\} \right] \quad (3.4-61)$$

The radial dependence in all these equations therefore has the form

$$I_e = \sum_{n,m} A_{nm} \left[H_{\frac{m\pi}{\theta_0}}^{(2)} \left(\sqrt{K_0^2 - \left(\frac{n\pi}{b}\right)^2} r \right) + \Gamma_{mn} H_{\frac{m\pi}{\theta_0}}^{(1)} \left(\sqrt{K_0^2 - \left(\frac{n\pi}{b}\right)^2} r \right) \right] \quad (3.4-62)$$

It is noted from Equation 60 that the radial propagation constant is a real number (i.e., jk_r is real) when $\left(\frac{m\pi}{b}\right)$ is larger than K_0 . In this case, the fields are evanescent and there is no energy propagation.

The nature of radial propagation, with special attention to large and small radii, will now be considered. The first or second term have the form

$$H_{k_\theta}^{(1)}(k_r r) = J_{k_\theta}(k_r r) \pm j Y_{k_\theta}(k_r r) \quad (3.4-63)$$

where $k_\theta = \frac{n\pi}{\theta_0}$ with $n = \text{an integer}$ and J and Y are Bessel functions of the first and second kinds respectively. As previously indicated, the phase of this complex function determines the phase velocity along the u^3 direction. This phase function is proportional to the arc tangent function of the ratio of the imaginary part to real part of the Hankel functions. From the asymptotic expansion of Hankel functions

for large arguments, one notes that

$$H_{\frac{n\pi}{\theta_0}}^{(2)}(k_r r) \rightarrow \frac{2}{\sqrt{\pi k_r r}} e^{\pm j \left[k_r r \pm \frac{\pi}{2} (k_\theta + \frac{1}{2}) \right]} \quad (3.4-64)$$

From the asymptotic phase, one concludes that for large radius the phase velocity approaches a constant, $\pm (w/k_r)$. Furthermore, the term involving Hankel functions of second kind represent outward propagating waves at large radii (since the phase velocity is positive); the term involving Hankel functions of the first kind represents inward propagating waves at large radii (since the phase velocity is negative). When one considers the infinite sectorial wedge waveguide, the radiation condition dictates that there is only an outward propagating wave and therefore only Hankel functions of the second kind exist. For this case, a typical outward propagating mode is given by

$$\bar{\pi}_{e_{nm}} = \hat{a}_3 A_{nm} \sin \frac{n\pi x}{b} \sin \frac{m\pi \theta}{\theta_0} H_{\frac{m\pi}{\theta_0}}^{(2)}(k_r r) \quad (3.4-65)$$

where

$$k_r = \sqrt{k_o^2 - \left(\frac{n\pi}{b} \right)^2} \quad (3.4-66)$$

The fields for this component of Hertz vector potential are computed from Equations (3.2-1) and (3.2-3). It results that

$$\left. \begin{aligned} H_{ex_{nm}} &= -j\omega\epsilon A_{nm} \left(\frac{m\pi}{r\theta_o} \right) \sin \frac{n\pi x}{b} \cos \frac{m\pi}{\theta_o} \theta H_{\frac{m\pi}{\theta_o}}^{(2)}(k_r r) \\ H_{e\theta_{nm}} &= j\omega\epsilon A_{nm} \left(\frac{n\pi}{b} \right) \cos \frac{n\pi x}{b} \sin \frac{m\pi\theta}{\theta_o} H_{\frac{m\pi}{\theta_o}}^{(2)}(k_r r) \end{aligned} \right\} \quad (3.4-67)$$

$$\left. \begin{aligned} E_{ex_{nm}} &= A_{nm} \left(\frac{n\pi}{b} \right) \cos \frac{n\pi x}{b} \sin \frac{m\pi\theta}{\theta_o} \left[k_r H_{\frac{m\pi}{\theta_o}}^{(2)'}(k_r r) + \frac{1}{r} H_{\frac{m\pi}{\theta_o}}^{(2)}(k_r r) \right] \\ E_{e\theta_{nm}} &= A_{nm} \left(\frac{m\pi}{r\theta_o} \right) \sin \frac{n\pi x}{b} \cos \frac{m\pi\theta}{\theta_o} \left[k_r H_{\frac{m\pi}{\theta_o}}^{(2)'}(k_r r) - \frac{1}{r} H_{\frac{m\pi}{\theta_o}}^{(2)}(k_r r) \right] \\ E_{er_{nm}} &= A_{nm} k_{nm}^2 \sin \frac{n\pi x}{b} \sin \frac{m\pi}{\theta_o} \theta \left[H_{\frac{m\pi}{\theta_o}}^{(2)}(k_r r) \right] \end{aligned} \right\} \quad (3.4-68)$$

(3.4-69)

where $H_{\frac{m\pi}{\theta_o}}^{(2)'}(\xi) = \frac{d}{d\xi} H_{\frac{m\pi}{\theta_o}}^{(2)}(\xi)$

and

$$k_{nm}^2 = \left(\frac{n\pi}{b} \right)^2 + \left(\frac{m\pi}{r\theta_o} \right)^2$$

(3.4-70)

Once the fields have been determined, the nature of the energy propagation can be evaluated by computing $[1/2 \operatorname{Re} (E_x H^*)]$. Since this quantity integrated over a surface represents the power flow across the surface, one can show, after a lengthy but straight forward computation, that real energy flows only across the $r = \text{constant}$ surface.²⁵

In Figure (3.4-2)²⁶ is a plot of the ratio of the imaginary part of the Hankel function to the real part. It is observed that the Hankel function gradually becomes purely imaginary as r becomes very small. From Equations (3.2-1) and (3.2-3) it follows that \bar{E}_e becomes imaginary while \bar{H}_e becomes real. It therefore follows from the Poynting theorem that there is no real power flowing at sufficiently small radii. This radial sectorial horn nonuniform waveguide therefore approaches cutoff for small values of r . Furthermore, from the shape of Figure (3.4-2), it follows that this cutoff phenomena is gradual and therefore does not occur at a specific radius.

One may also note in Figure (3.4-2) that the ratio of the imaginary to the real part of the Hankel functions is a monotonic function that does not change sign. From

²⁵See reference [3].

²⁶This figure comes from page 211 of reference [14].

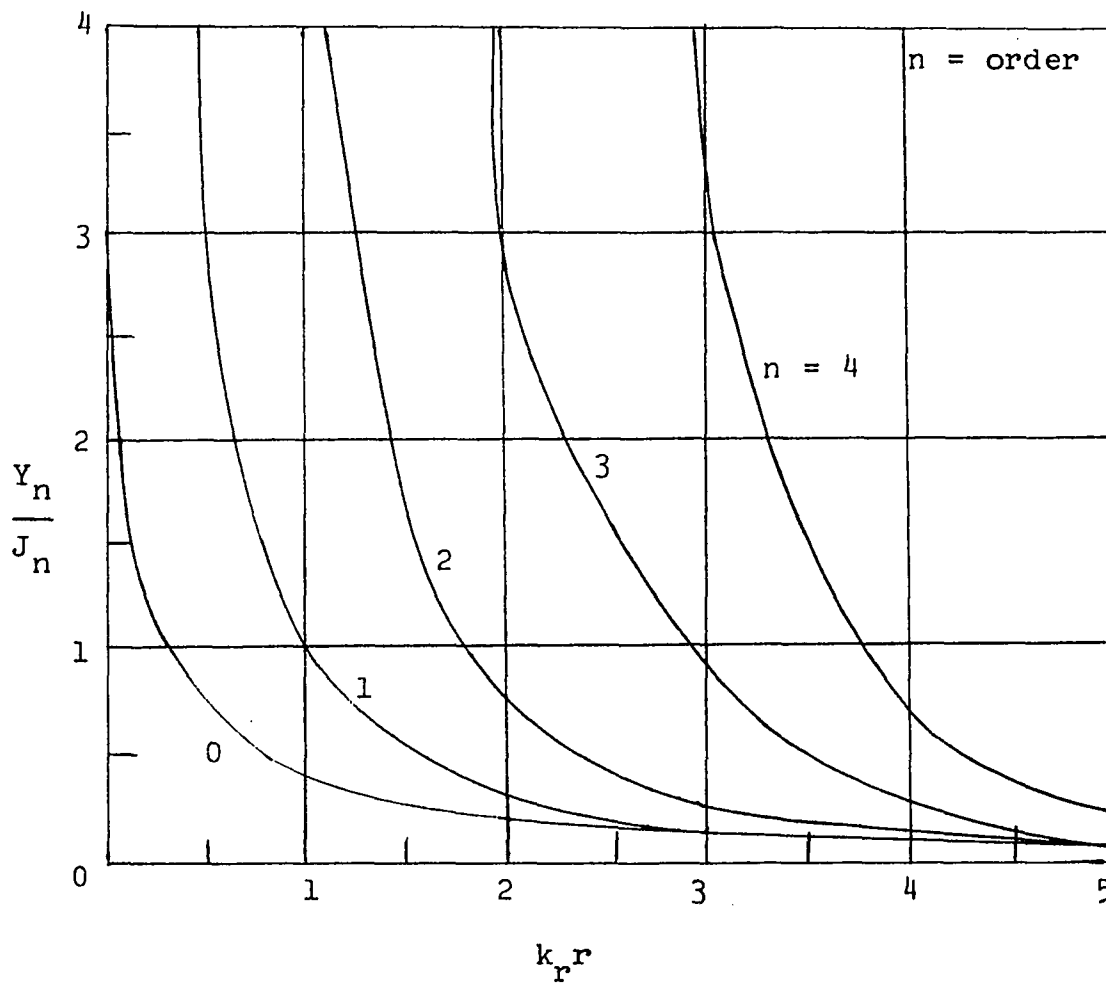


Figure 3.4-2

Ratio of Imaginary to Real Parts of
Hankel Functions, $H_n^{(2)}(k_r r) = J_n(k_r r) \pm jY_n(k_r r)$

this, one can conclude that, since $H_{k_0}^{(2)}(k_r r)$ represents its outward propagating waves for large radii, $H_{k_0}^{(2)}(k_r r)$ also represents outward propagating waves at all propagating radii. Similarly, $H_{k_0}^{(1)}(k_r r)$ represents inward propagating waves at all propagating radii.

3.5 Summary

The general formulation of the nonuniform waveguide and its consequences will now be summarized.

The first step in the formulation was to decompose the electric and magnetic fields into two portions that are associated with the electric Hertz vector potential and magnetic Hertz vector potential respectively. Generalized coordinates, (u^1, u^2, u^3) were then selected in such a manner that the waveguide wall shape coincides with the coordinate surfaces of constant u^1 and/or u^2 . This choice was motivated by a desire to obtain solutions that satisfy the boundary conditions and a realization that the waveguide walls guide the waves. It was then shown that when appropriate coordinate system conditions are satisfied, a nonuniform waveguide analysis may be separated into two parts. These are a set of eigenvalue problems in terms of the transverse coordinates and a nonuniform transmission line analysis. The eigenvalues of the first problem provide

transmission line parameters for the second problem.. The solution obtained is expressed as a function of the transverse coordinates times a function of the u^3 propagation coordinate. The physical interpretation of this solution is that the transverse electromagnetic field moves along the propagation direction. The concepts of the Riemann metric tensor were used to achieve the propagation coordinate separation when the conditions indicated in Table 3.4-1 are satisfied.

The major significance of the above analysis decomposition is that after determination of the eigenvalues of the transverse problems (by either analytic, approximate, or numerical techniques) the analysis reduces to solving a set of uncoupled nonuniform transmission lines. Thus, the body of knowledge of nonuniform transmission line analysis may be applied directly to the study of the class of nonuniform waveguides considered in this chapter. A review of the technology of nonuniform transmission lines is presented in Appendix A.

For the case in which $g^{33} = 1$, the coefficient of the first derivative term in the u^3 propagation differential equation was related to the logarithmic derivative of the transverse surface area. The per length impedance and

admittance as well as the expression for characteristic impedance also depend upon the transverse surface area of the nonuniform waveguide.

In Section 3.4, it was demonstrated that the conditions that led to separating the u^3 dependence are useful guidelines for selecting an appropriate coordinate system.

CHAPTER 4

CASCADED NONUNIFORM WAVEGUIDES

4.1 Introduction

As indicated previously, a nonuniform waveguide may be represented by transverse equations and a set of uncoupled nonuniform transmission lines when appropriate conditions are satisfied. For more general nonuniform waveguides, the overall nonuniform waveguide will be approximated by a cascade of nonuniform waveguides such that each waveguide section satisfies the conditions of Chapter 3. The propagation behavior of the entire nonuniform waveguide may be comprehended by joining these nonuniform waveguide sections. The process of joining the individual waveguide sections together can alternatively be viewed as piecing together local solutions (obtained by the methods of Chapter 3) to approximate the solution of the overall nonuniform waveguide. This approach has the advantage of dealing with large and rapid boundary variations. Some of the nonuniform waveguide analyses of previous investigators were not accurate for this case.

The region of joining two nonuniform waveguide sections is referred to as the junction region. The coordinate system on the left side of the junction is chosen in accordance with the requirements of Chapter 3 and therefore the

waveguide surface on this side of the junction is represented by constant u^1 and/or u^2 surfaces. The coordinates on the right side of the junction are chosen in a similar manner. As used in this dissertation, a junction represents a joining of two different coordinate systems. It is noted that this definition does not necessarily require an edge at the junction. Examples of junctions that do not require an edge are shown in Figure 4.1-1. The junctions considered will either have nonexistent edges or edges that have a negligible effect on the propagating modes. The junction aperture is a surface across the junction region. Usually, a constant u^3 surface is chosen as an aperture surface.

The implementation of the proposed cascaded nonuniform waveguide formulation to solve an actual problem is to start at the load (output) and work backward toward the first waveguide input (or known source). By expanding the fields (or the corresponding Hertz vector potentials) into a generalized Fourier series consisting of the natural mode functions for each region, the unknown modal constants on one side of the junction may be expressed in terms of the unknown constants on the other side of the junction. In this manner, the unknown modal constants on one side of the junction are "transferred" across the junction. The pro-

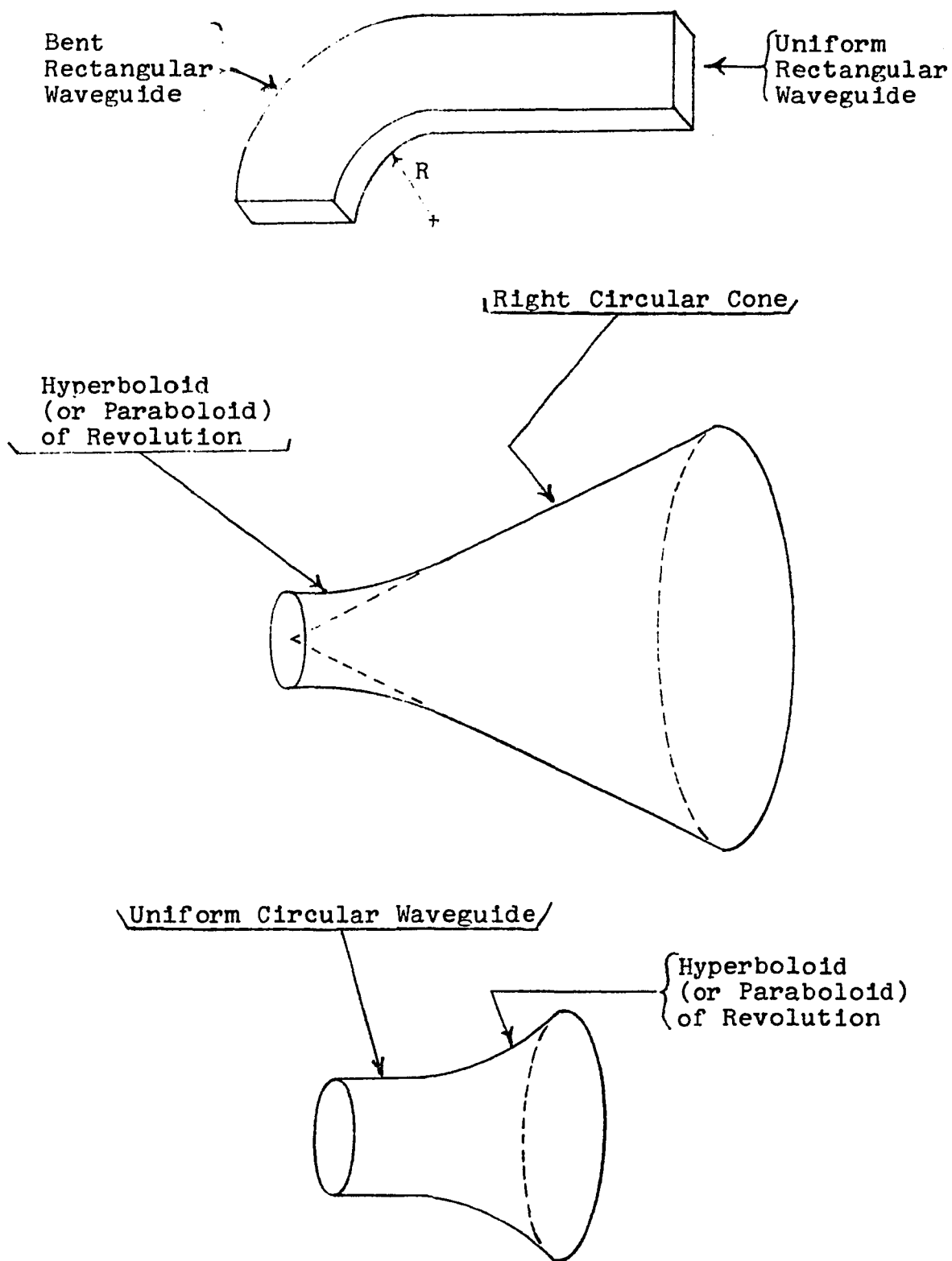


Figure 4.1-1

Junctions Without Wall Edges

cedure is to start at the load and work backward across successive junctions until one eventually reaches the known source. This source, when expressed in terms of the modes of the input waveguide (generalized Fourier series) supplies enough source conditions to, in principle, determine the modal amplitudes at the load. Thus, a source condition is available for each of the input transmission lines representing the input waveguide. The junction conditions can then be used to determine the amplitudes in the other waveguide sections.

The cascaded nonuniform waveguide approach requires a greater understanding of the junction between two nonuniform waveguides. This chapter is therefore concerned with the analysis of the junction between nonuniform waveguides and the manner in which field continuities in the junction region can be utilized as a boundary condition in terms of the parameters of the present formulation. In particular, it is desired to relate the fields (or Hertz potentials) on one side of the junction to the fields (or Hertz potentials) on the other side of the junction by expressions that facilitate the calculations. These relations equate specific modal components on one side of the junction to expressions of the modal components on the other side of the junction. The junction between a nonuniform waveguide

and a uniform waveguide is of particular importance because most waveguide measuring equipment is of the uniform waveguide variety and therefore a junction between a uniform and nonuniform waveguide will usually occur in any system incorporating nonuniform waveguides.

For the most part, the previous junction analyses were in uniform waveguides in which only one propagating mode was assumed to be present [31, 54, 55, 56]. The earlier analytical techniques were devoted to indirect procedures such as variational or quasi-static methods or other approximations. With the advent of fast computers and computational techniques it has become fashionable to obtain useful numerical results by truncating the infinite set of mode-matching equations to a finite set and solving numerically for the unknown mode amplitudes. A variation of this method is to match the field at a finite number of boundary points and select enough modes to just provide the necessary number of unknown coefficients [15, 29].

In the present analysis, it is assumed that the geometry of each side of the junction is amenable to the solution technique of Chapter 3. These techniques are therefore used to find the modal solutions on each side of the junction by an identical procedure. By definition each of these modes satisfy Maxwell's equations and the waveguide wall

boundary conditions when the junction is not present. The actual solution on each side of the junction is expressed as a linear combination of modes. To do this it is assumed that the set of modes for each region is either complete or that any missing expressions are negligible.

For the case being considered, the junction region belongs to both sides of the junction.¹ The resulting physical field quantities should be the same no matter which coordinate (and therefore which modes) are used to solve the problem. Therefore one requires the total electric and magnetic fields determined from the expansions on each side of the junction to be identical. This junction condition, however, cannot be applied to all junctions.¹ Although the fields within the aperture can be equated, it is not always possible to equate fields in the immediate vicinity of a waveguide wall edge. Since the waveguide being approximated by a cascade of nonuniform waveguides is really smooth, it is expected that these edge effects will be small and therefore that the approximation will be good. Moreover, since the true waveguide is really smooth, an

¹This requires the domains of definition of the modes on each side of the junction to overlap. Such a junction is said to be concave [23]. When the domains of definition do not overlap, the junction is called convex [23]. Nevertheless good numerical results are sometimes obtained for convex junctions [23, 24].

approximation that minimizes discontinuity effects may even be closer to the truth. Furthermore an engineering analysis is usually not interested in the fields in the immediate vicinity of an edge discontinuity. The major interest is to obtain solutions that are good approximations far from the junction where typically only one or two propagating modes are of great concern. The major effect of the non-propagating modes is to store energy in the vicinity of the junction.

The coefficients in the modal expansions for each region are determined from the junction conditions plus the source and/or load conditions of each waveguide. In practice, a finite sum will be used in the expansion.

The difficulties associated with the nonuniform waveguide junction can be visualized by expanding the fields on both sides of the nonuniform junction in terms of modes and attempting to equate the total fields on an aperture surface. This aperture surface can therefore be considered to bisect the junction analysis into two parts. Consider the constant phase surfaces of modes incident from the left side of the junction and choose an aperture surface that coincides with these surfaces. This aperture surface, however, does not, in general, coincide with the constant phase surfaces that are natural to the modes in the region

to the right of the junction. An incident mode from the left therefore creates a set of modes in the region on the right side of the junction. In general, a single incident mode on the left side of the junction transmits both E-modes and H-modes on the right side of the junction, and also reflects both E-modes and H-modes to the left side of the junction. The major complication in using the Hertz Vector Potential to analyze the junction between nonuniform waveguides is that the Hertz Vector Potential is chosen to be in a different orientation on both sides of the nonuniform waveguide junction in order to be consistent with the formulation of Chapter 3. This direction change is a consequence of the different coordinates that are used on both sides of the junction to facilitate satisfying the waveguide wall boundary conditions. Furthermore, the general multi-mode nonuniform waveguide junction is complicated by cross coupling between E-modes and H-modes.

The general formulation of a multimode nonuniform waveguide junction in which there is coupling between E-modes and H-modes is considered in more detail in Section 4.2. The major restrictions have already been discussed in this section. The equations that arise, however, are very complex and will therefore not be solved for this general case.

Since the main goal of Section 4.2 is to present a general formulation procedure for the nonuniform waveguide junction, these equations are included to specifically illustrate the procedures. An explicit solution to the general problem is not intended.

Section 4.3 considers the special case of a multimode junction in which there is no coupling between E- and H-modes. In particular, those problems that can be solved by appropriately choosing the direction of the Hertz vector are considered. The procedure is illustrated in greater detail for the sectorial wedge to uniform waveguide junction (in Section 4.4). Uniform waveguide junctions are also a special case of the formulation of Section 4.2.

Finally, Section 4.5 discusses the results and summarizes the major conclusions.

4.2 General Junction Formulation

This section considers the analysis formulation of a general nonuniform waveguide junction of the type suitable for the cascaded nonuniform waveguide approximation. It is assumed that the regions on each side of this junction may be formulated according to the procedures of Chapter 3 and the fields in each region can therefore be represented by a set of uncoupled E-modes and H-modes. These modes each

satisfy Maxwell's equations and the waveguide wall boundary conditions appropriate to that side of the junction. The space on the left side of the junction is bounded by its waveguide walls and a source and junction aperture surface; the volume on the right side of the junction is bounded by its waveguide walls and the load and junction aperture surface. This junction aperture surface therefore divides the analysis into two parts and conditions on this surface relate these two sub-problems.

The number of independent junction region equations that result from the junction condition that in the junction region the total fields described by the coordinates on both sides of the junction are the same (See Section 4.1) now will be discussed. Since \vec{E} and \vec{H} are vectors, this vector condition would be equivalent to six scalar junction region conditions. However, in accordance with Maxwell's equations, \vec{E} and \vec{H} are related by

$$\vec{E} = \frac{\nabla \times \vec{H}}{j \omega \epsilon} \quad (4.2-1)$$

$$\vec{H} = - \frac{(\nabla \times \vec{E})}{j \omega \mu} \quad (4.2-2)$$

This leaves only three scalar junction region conditions. But since the waveguide region is free from sources, the condition ($\nabla \cdot \vec{E} = 0$) or ($\nabla \cdot \vec{H} = 0$) implies that only two of these scalar conditions are independent. Furthermore, when the fields are decomposed into E-modes and H-modes, one component of the magnetic field of the E-modes and one component of the electric field of the H-modes vanishes (by definition) and therefore there is only one independent scalar junction region condition for each of the mode types (totaling the required two junction region conditions for the combined E- and H-mode combination).

It is noted that the conclusions of the preceding paragraph are for a junction region. However, when the field components are equated on a specific junction aperture surface, it does not insure that variations of these components normal to the aperture surface are also equal. This latter requirement that the directional derivatives having a component normal to the aperture surface must be the same supplies an additional set of conditions. Thus, E-modes and H-modes each require two independent junction aperture conditions and the combined field requires four junction aperture conditions. Furthermore, as indicated by Equations 1 and 2, \vec{E} and \vec{H} are related by equations such that some components involve partial derivatives with respect to variables that are not coincident with the junction aperture surface.

Therefore, as an alternate to equating outward going directional derivatives of field components one may equate both electric and magnetic transverse fields on this surface (this is in general four conditions, but when there are only E-modes or H-modes it reduces to two conditions).

The procedure will now be illustrated with an example. As previously indicated the equations that will be used in this section are intended to illustrate the procedure. In accordance with the discussion of the previous section, it is assumed that, for the case being considered, the modal expansions on both sides of the junction are either complete within the junction region or that missing terms are negligible. The totality of all H-mode electric fields on the left side of the junction, \bar{E}_{ah} , can be expressed as

$$\bar{E}_{ah} = \sum_n \left[a_{hn}^{(+)} \bar{E}_{ah}^{(+n)} + a_{hn}^{(-)} \bar{E}_{ah}^{(-n)} \right] \quad (4.2-3)$$

where $\bar{E}_{ah}^{(+n)}$ and $\bar{E}_{ah}^{(-n)}$ are respectively the electric fields of the incident n^{th} H-mode and the totality of reflections from all incident modes that couple to the n^{th} H-mode upon reflection. Alternatively, $\bar{E}_{ah}^{(+n)}$ and $\bar{E}_{ah}^{(-n)}$ are the electric fields resulting from the two solutions to the n^{th} H-mode transmission line entering the junc-

tion. In practice, infinite sums will be approximated by finite sums.

The net power flow in the positive u_a^3 direction may be obtained by integrating the Poynting vector \bar{P}^+ , given by $\bar{P}^+ = \left[\bar{E}_{ah}^{(+n)} \times \left(\bar{H}_{ah}^{(+n)} \right)^* \right]$ over a constant u_a^3 surface. For power flow in the negative u_a^3 direction $\bar{E}_{ah}^{(-n)}$ and $\bar{H}_{ah}^{(-n)}$ are used in place of $\bar{E}_{ah}^{(+n)}$ and $\bar{H}_{ah}^{(+n)}$ respectively. Subscript "a" is used to denote that the quantity is determined from the coordinates on the left side of the junction (region "a"), and "*" is used to denote a complex conjugate of the quantity involved. A similar situation to the one above exists on the right side of the junction (region "b").

For the moment, it will be assumed that the source condition is in a form such that $a_{hn}^{(+)}$ is known for all propagating modes and $a_{hn}^{(+)} = 0$ for all non-propagating modes. The $a_{hn}^{(-)}$ coefficients sum reflections from all incident modes that couple to the n^{th} H-mode upon reflection. These constants must be determined as part of the solution. In addition, it is initially assumed that the load condition is such that there are only positive power flowing terms in region "b" (i.e., there is no reflected power from the load). Other types of source and load conditions will be considered in Section 4.4.

Since the modes on the right side of the junction are assumed to form a complete set (in the sense previously indicated), \bar{E}_{ah} may also be expressed in terms of the modes on the right side of the junction. Thus,

$$\begin{aligned}\bar{E}_{ah} &= \sum_n \left[a_{hn}^{(+)} \bar{E}_{ah}^{(+n)} + a_{hn}^{(-)} \bar{E}_{ah}^{(-n)} \right] = \\ &= \sum_k \left[b_{Hhk}^{(+)} E_{bh}^{(+k)} + b_{Heh}^{(+)} E_{be}^{(+)} \right]\end{aligned}\quad (4.2-4)$$

where subscript "e" and "h" refer to E-mode and H-mode types respectively and subscript "H" indicates that the coefficients sum the contributions of waves transmitted across the junction that are due to H-modes being incident on the left side of the junction.

To facilitate the formulation using the results of Chapter 3, it is convenient to express Equation 4 in terms of Hertz vector potentials. One obtains:

$$-j\omega\mu \sum_n (\nabla \times \bar{\pi}_{ha}^n) = -j\omega\mu \sum_k (\nabla \times \bar{\pi}_{Hhb}^k) + \sum_k [\nabla \times (\nabla \times \bar{\pi}_{Heb}^k)] \quad (4.2-5)$$

or equivalently

$$\sum_n \bar{\pi}_{ha}^n = \sum_k \bar{\pi}_{Hhb}^k + \sum_k \frac{(\nabla \times \bar{\pi}_{Heb}^k)}{(-j\omega\mu)} + \nabla f_h \quad (4.2-6)$$

where, for the case being considered

$$\bar{\pi}_{ha}^n = \hat{i}_{a1} \left[a_{hn}^{(+)} I_{ha}^{(+)}(u_a^3) + a_{hn}^{(-)} I_{ha}^{(-)}(u_a^3) \right] \psi_{ha}^n(u_a^1, u_a^2) \quad (4.2-7A)$$

$$\bar{\pi}_{Hhb}^k = \hat{i}_{b1} b_{Hhk}^{(+)} I_{hb}^{(+)}(u_b^3) \psi_{hb}^k(u_b^1, u_b^2) \quad (4.2-7B)$$

$$\bar{\pi}_{Heb}^k = \hat{i}_{b1} b_{Hek}^{(+)} I_{eb}^{(+)}(u_b^3) \psi_{eb}^k(u_b^1, u_b^2) \quad (4.2-7C)$$

and f_h is a scalar function of position and \hat{i}_{a1} and \hat{i}_{b1} are unit vectors in the direction of the Hertz vectors for region "a" and region "b" respectively. For the moment, these Hertz vectors need not be in the u_a^3 direction and the u_b^3 direction.

From Equations 6 and 7 it follows that

$$\begin{aligned} \sum_n \hat{i}_{a1} [a_{hn}^{(+)} I_{ha}^{(+)}(u_a^3) + a_{hn}^{(-)} I_{ha}^{(-)}(u_a^3)] \psi_{ha}^n(u_a^1, u_a^2) = \\ = \sum_k \left[\hat{i}_{b1} b_{Hhk}^{(+)} I_{hb}^{(+)} \psi_{hb}^k + b_{Hek}^{(+)} \frac{(\nabla \times \hat{i}_{b1} I_{eb}^{(+)} \psi_{eb}^k)}{(-j\omega\mu)} \right] + \nabla f_h \end{aligned} \quad (4.2-8)$$

Later, the modes on the right side of the junction will be expressed in terms of the modes on the left side of the junction (using the assumed completeness of modes). Then, since the modes are independent, the coefficients on the

left side of the junction may be expressed in terms of the coefficients on the right side of the junction by requiring the resulting equations to hold for all values of u_a^1 and u_a^2 . (When the modes are orthogonal, the process of solving for the coefficients may be greatly facilitated.) It will be shown that for the case being considered, the junction can usually be represented by a matrix.

In a similar manner, when the magnetic fields due to E-modes, \bar{H}_{ae} , are expanded in terms of the modes on both sides of the junction the equations corresponding respectively to Equations 4, 6 and 8 for the case being considered are

$$\bar{H}_{ae} = \sum_n [a_{en}^{(+)} \bar{H}_{ae}^{(+n)} + a_{en}^{(-)} \bar{H}_{ae}^{(-n)}] = \sum_k [b_{Ehk}^{(+)} H_{be}^{(+k)} + b_{Eek}^{(+)} H_{bh}^{(+k)}] \quad (4.2-9)$$

$$\sum_n \bar{\pi}_{ea}^n = \sum_k \bar{\pi}_{Eeb}^k + \sum_k \frac{(\nabla_x \bar{\pi}_{Ehb}^k)}{j\omega\epsilon} + \nabla f_e \quad (4.2-10)$$

$$\begin{aligned} \hat{i}_{al} [a_{en}^{(+)} I_{ea}^{(+n)} + a_{en}^{(-)} I_{ea}^{(-n)}] \psi_{ea}^n = \\ = \sum_k \left[\hat{i}_{bl} b_{Eek}^{(+)} I_{eb}^{(+k)} \psi_{eb}^k + b_{Ehk}^{(+)} \frac{(\nabla_x \hat{i}_{bl} I_{hb}^{(+k)} \psi_{hb}^k)}{j\omega\epsilon} \right] + \nabla f_e \end{aligned} \quad (4.2-11)$$

where

$$\bar{\pi}_{ea}^n = \hat{i}_{a1} [a_{en}^{(+)} I_{ea}^{(+)}(u_a^3) + a_{en}^{(-)} I_{ea}^{(-)}(u_a^3)] \psi_{ea}^n(u_a^1, u_a^2) \quad (4.2-12A)$$

$$\bar{\pi}_{Eeb}^k = \hat{i}_{b1} b_{Hek}^{(+)} I_{hb}^{(+)}(u_b^3) \psi_{hb}^k(u_b^1, u_b^2) \quad (4.2-12B)$$

$$\bar{\pi}_{Ehb}^k = \hat{i}_{b1} b_{Hhk}^{(+)} I_{eb}^{(+)}(u_b^3) \psi_{eb}^k(u_b^1, u_b^2) \quad (4.2-12C)$$

and f_e is a scalar function of position.

Equations 8 and 11 (or 6 and 10) are both vector equations and are therefore each equivalent to three equations. In order to proceed with a study of these equations, orthogonal unit vectors \hat{i}_1 , \hat{i}_2 , and \hat{i}_3 , are chosen in such a manner that \hat{i}_1 is in the direction of \hat{i}_{a1}^2 , \hat{i}_2 is orthogonal to both \hat{i}_1 and \hat{i}_{b1} , and \hat{i}_3 is orthogonal to both \hat{i}_1 and \hat{i}_2 in a sense that makes \hat{i}_1 , \hat{i}_2 , \hat{i}_3 a righthand coordinate system. Observe that for the directions of the unit vectors selected

$$\hat{i}_1 \cdot \bar{\pi}_{ea} = \hat{i}_1 \cdot \hat{i}_1 \pi_{ea} = \pi_{ea} \quad (4.2-13)$$

$$\hat{i}_2 \cdot \bar{\pi}_{ea} = 0 \quad (4.2-14)$$

²When \hat{i}_{a1} is in the u_a^3 direction, then $\hat{i}_1 = \hat{a}_{3a}$. In general, \hat{i}_1 can be in a different direction. The case in which \hat{i}_{a1} and \hat{i}_{b1} are in the same direction is discussed in Section 4.3.

$$\hat{i}_2 \cdot \bar{\pi}_{eb} = 0 \quad (4.2-15)$$

$$\hat{i}_3 \cdot \bar{\pi}_{ea} = 0 \quad (4.2-16)$$

where π_{ea} is the amplitude of the $\bar{\pi}_{ea}$ Hertz vector. A corresponding set of equations hold for $\bar{\pi}_{ha}$ and $\bar{\pi}_{hb}$. From Equations 13, 14, 15, 16, and 11, one obtains

$$\begin{aligned} \sum_n [a_{en}^{(+)} I_{ea}^{(+n)} + a_{en}^{(-)} I_{ea}^{(-n)}] \psi_{ea}^n = \\ = \sum_k (\hat{i}_1 \cdot \hat{i}_{b1}) b_{Eek}^{(+)} I_{eb}^{(+k)} \psi_{eb}^k + \sum_k b_{Ehk}^{(+)} \frac{\hat{i}_1 \cdot (\nabla \times \hat{i}_{b1} I_{hb}^{(+k)} \psi_{hb}^k)}{j\omega\epsilon} + \hat{i}_1 \cdot \nabla f_e \end{aligned} \quad (4.2-17)$$

$$0 = \sum_k b_{Ehk}^{(+)} \left[\frac{\hat{i}_2 \cdot (\nabla \times \hat{i}_{b1} I_{hb}^{(+k)} \psi_{hb}^k)}{j\omega\epsilon} \right] + \hat{i}_2 \cdot \nabla f_e \quad (4.2-18)$$

$$0 = \sum_k (\hat{i}_3 \cdot \hat{i}_{b1}) b_{Eek}^{(+)} I_{eb}^{(+k)} \psi_{eb}^k + \sum_k b_{Ehk}^{(+)} \left[\frac{\hat{i}_3 \cdot (\nabla \times \hat{i}_{b1} I_{hb}^{(+k)} \psi_{hb}^k)}{j\omega\epsilon} \right] + \hat{i}_3 \cdot \nabla f_e \quad (4.2-19)$$

In a similar manner, for the selected unit vectors,

$$\hat{i}_1 \cdot \bar{\pi}_{ha} = \pi_{ha} \quad (4.2-20)$$

$$\hat{i}_2 \cdot \bar{\pi}_{ha} = 0 \quad (4.2-21)$$

$$\hat{i}_2 \cdot \bar{\pi}_{hb} = 0 \quad (4.2-22)$$

$$\hat{i}_3 \cdot \bar{\pi}_{ha} = 0 \quad (4.2-23)$$

From Equations 20, 21, 22, 23, and 8, it follows that

$$\begin{aligned} \sum_n [a_{hn}^{(+)} I_{ha}^{(+n)} + a_{hn}^{(-)} I_{ha}^{(-n)}] \psi_{ha}^n = \\ \sum_k b_{Hhk}^{(+)} (\hat{i}_1 \cdot \hat{i}_{b1}) I_{hb}^{(+k)} \psi_{hb}^k + \sum_k b_{Hek}^{(+)} \left[\frac{\hat{i}_1 \cdot (\nabla \times \hat{i}_{b1} I_{eb}^{(+k)} \psi_{eb}^k)}{-j\omega\mu} \right] + \hat{i}_1 \cdot \nabla f_h \end{aligned} \quad (4.2-24)$$

$$0 = \sum_k b_{Hek}^{(+)} \left[\frac{\hat{i}_2 \cdot (\nabla \times \hat{i}_{b1} I_{eb}^{(+k)} \psi_{eb}^k)}{-j\omega\mu} \right] + \hat{i}_2 \cdot \nabla f_h \quad (4.2-25)$$

$$0 = \sum_k b_{Hhk}^{(+)} (\hat{i}_3 \cdot \hat{i}_{b1}) I_{hb}^{(+k)} \psi_{hb}^k + \sum_k b_{Hek}^{(+)} \left[\frac{\hat{i}_3 \cdot (\nabla \times \hat{i}_{b1} I_{eb}^{(+k)} \psi_{eb}^k)}{-j\omega\mu} \right] + \hat{i}_3 \cdot \nabla f_h \quad (4.2-26)$$

A general solution to Equations 17-19 and 24-26 is complicated and depends upon the specific problem under consideration. However, the procedure will be illustrated with a more tractable special case in Section 4.4 without carrying out the detailed calculations. Towards this end, it is useful to examine the nature of the three components of ∇f_e and ∇f_h that appear in Equations 17-19 and 24-26

respectively. These equations came from vector Equations 8 and 11 which were derived by equating total fields within the junction region. These fields, however, are related to curls of Hertz potentials and since the operator "curl grad" yields a null vector, it follows that ∇f_e and ∇f_h do not contribute to the physical fields. However, they are needed to correct for changes in direction of the Hertz potential that results from using different coordinate systems on both sides of the junction and using the formulation of Chapter 3 on each side of the junction. The structure of ∇f_e (∇f_h) is dictated by the requirement that it perform direction correction such that Equations 17 and 24 have the form

$$\begin{aligned} \sum_n \left[a_{en}^{(+)} I_{ea}^{(+n)}(u_a^3) + a_{en}^{(-)} I_{ea}^{(-n)}(u_a^3) \right] \psi_{ea}^n(u_a^1, u_a^2) \\ = \sum_k \left[b_{Eek}^{(+)} q_{Ee}^k(u_b^1, u_b^2, u_b^3) + b_{Ehk}^{(+)} q_{Eh}^k(u_b^1, u_b^2, u_b^3) \right] \end{aligned} \quad (4.2-31)$$

$$\begin{aligned} \sum_n \left[a_{hn}^{(+)} I_{ha}^{(+n)}(u_a^3) + a_{hn}^{(-)} I_{ha}^{(-n)}(u_a^3) \right] \psi_{ha}^n(u_a^1, u_a^2) = \\ = \sum_k \left[b_{Hek}^{(+)} q_{He}^k(u_b^1, u_b^2, u_b^3) + b_{Hhk}^{(+)} q_{Hh}^k(u_b^1, u_b^2, u_b^3) \right] \end{aligned} \quad (4.2-32)$$

where the q_{He}^k 's, q_{Eh}^k 's, q_{He}^k 's, and q_{Hh}^k 's may be complicated, but at least in principle known, functions of the coordinates used on the right side of the junction. It is assumed, however, that the coordinates on both sides of the junction are related by a one-to-one continuous coordinate transformation and that the coordinates in region "b" are known explicitly as functions of the coordinates of region "a". Thus, every "q" function on the right side of Equations 31 and 32 may be expressed in terms of the coordinates on the left side of the junction. Let the resulting functions be referred to as "g" functions. Thus, Equations 31 and 32 now have the form

$$\begin{aligned} \sum_n \left[a_{en}^{(+)} I_{ea}^{(+n)}(u_a^3) + a_{en}^{(-)} I_{ea}^{(-n)}(u_a^3) \right] \psi_{ea}^n(u_a^1, u_a^2) = \\ = \sum_k \left[b_{Eek}^{(+)} g_{Ee}^k(u_a^1, u_a^2, u_a^3) + b_{Ehk}^{(+)} g_{Eh}^k(u_a^1, u_a^2, u_a^3) \right] \end{aligned} \quad (4.2-33)$$

$$\begin{aligned} \sum_n \left[a_{hn}^{(+)} I_{ha}^{(+n)}(u_a^3) + a_{hn}^{(-)} I_{ha}^{(-n)}(u_a^3) \right] \psi_{ha}^n(u_a^1, u_a^2) = \\ = \sum_k \left[b_{Hek}^{(+)} g_{He}^k(u_a^1, u_a^2, u_a^3) + b_{Hhk}^{(+)} g_{Hh}^k(u_a^1, u_a^2, u_a^3) \right] \end{aligned} \quad (4.2-34)$$

It should be noted that junction Equations 33 and 34 actually hold in a region. In order to utilize these equations, it is convenient to apply them on a specific junction

aperture surface. The constant u_a^3 junction aperture surface will be selected for this purpose. However, as discussed previously, when Equations 33 and 34 are applied on an aperture surface, partials of these equations with respect to u_a^3 should also be equated on the constant u_a^3 aperture surface³. The resulting junction equations on this surface become

$$\sum_n c_{en} \psi_{ea}^n(u_a^1, u_a^2) = \sum_k b_{Eek}^{(+)} G_{Ee}^k(u_a^1, u_a^2) + b_{Ehk}^{(+)} G_{Eh}^k(u_a^1, u_a^2) \quad (4.2-35)$$

$$\sum_n c'_{en} \psi_{ea}^n(u_a^1, u_a^2) = \sum_k b_{Eek}^{(+)} F_{Ee}^k(u_a^1, u_a^2) + b_{Ehk}^{(+)} F_{Eh}^k(u_a^1, u_a^2) \quad (4.2-36)$$

$$\sum_n c_{hn} \psi_{ha}^n(u_a^1, u_a^2) = \sum_k b_{Hek}^{(+)} G_{He}^k(u_a^1, u_a^2) + b_{Hhk}^{(+)} G_{Hh}^k(u_a^1, u_a^2) \quad (4.2-37)$$

$$\sum_n c'_{hn} \psi_{ha}^n(u_a^1, u_a^2) = \sum_k b_{Hek}^{(+)} F_{He}^k(u_a^1, u_a^2) + b_{Hhk}^{(+)} F_{Hh}^k(u_a^1, u_a^2) \quad (4.2-38)$$

where

$$c_{en} = [a_{en}^{(+)} I_{ea}^{(+)} + a_{en}^{(-)} I_{ea}^{(-)}] \quad \text{evaluated on the constant } u_a^3 \text{ surface} \quad (4.2-39)$$

³Alternatively, any outward going directional derivative could be used.

$$c'_{en} = a_{en}^{(+)} \frac{dI_{ea}^{(+)}n}{du_a^3} + \frac{a_{en}^{(-)} dI_{ea}^{(-)}n}{du_a^3}$$

evaluated on the constant

 u_a^3 surface (4.2-40)

$$c_{hn} = \left[a_{hn}^{+} I_{ha}^{(+)}n + a_{hn}^{(-)} I_{ha}^{(-)}n \right]$$

evaluated on the constant

 u_a^3 surface (4.2-41)

$$c'_{hn} = \left[a_{hn}^{+} \frac{dI_{ha}^{(+)}n}{du_a^3} + \frac{a_{hn}^{(-)} dI_{ha}^{(-)}n}{du_a^3} \right]$$

evaluated on the constant

 u_a^3 surface (4.2-42)

$$G(u_a^1, u_a^2) = g(u_a^1, u_a^2, u_a^3)$$

evaluated on the constant u_a^3

surface for all subscripts and

superscripts (4.2-43)

$$F(u_a^1, u_a^2) = \frac{\partial g(u_a^1, u_a^2, u_a^3)}{\partial u_a^3}$$

evaluated on the constant u_a^3

surface for all subscripts and

superscripts (4.2-44)

The only unknowns in Equations 35-38 are C_{en} , C'_{en} , $b_{Eek}^{(+)}$, $b_{Ehk}^{(+)}$, C_{hn} , C'_{hn} , $b_{Hek}^{(+)}$, and $b_{Hhk}^{(+)}$. Since the modes are independent, these equations can be used to express the C_{en} , C'_{en} , C_{hn} , and C'_{hn} constants in terms of the $b_{Eek}^{(+)}$, $b_{Ehk}^{(+)}$, $b_{Hek}^{(+)}$, and $b_{Hhk}^{(+)}$ constants and Equations 39-42 can then be used to determine $a_{en}^{(-)}$ and $a_{hn}^{(-)}$ (since, for the case being considered, $a_{en}^{(+)}$ and $a_{hn}^{(+)}$ are both assumed known). The calculation procedure illustrated expands the "G" and "F" functions in terms of the ψ_{ea}^n and ψ_{ha}^n functions (this assumes mode completeness). Because of the independence of the mode functions, the "c" constants can be expressed in terms of the "b" constants. When the modes are orthogonal, then the orthogonal expansion can be viewed as a generalized Fourier series and the orthogonality may be used to facilitate expressing the "c" constants in terms of the "b" constants. The Gram-Schmidt orthogonalization procedure may be used to obtain an orthogonal set of modes.

In accordance with the first procedure, the assumed mode completeness (in the sense indicated in Section 4.1) is now used to express the "G" and "F" functions in terms of the " ψ " functions. Thus,

$$G_{Ee}^k(u_a^1, u_a^2) = \sum_m \lambda_{Eem}^{(e)k} \psi_{ea}^m(u_a^1, u_a^2) + \sum_m \lambda_{Eem}^{(h)k} \psi_{ha}^m(u_a^1, u_a^2) \quad (4.2-45)$$

$$G_{Eh}^k(u_a^1, u_a^2) = \sum_m \lambda_{Ehm}^{(e)k} \psi_{ea}^m(u_a^1, u_a^2) + \sum_m \lambda_{Ehm}^{(h)k} \psi_{ha}^m(u_a^1, u_a^2) \quad (4.2-46)$$

$$G_{He}^k(u_a^1, u_a^2) = \sum_m \lambda_{Hem}^{(h)k} \psi_{ha}^m(u_a^1, u_a^2) + \sum_m \lambda_{Hem}^{(e)k} \psi_{ea}^m(u_a^1, u_a^2) \quad (4.2-47)$$

$$G_{Hh}^k(u_a^1, u_a^2) = \sum_m \lambda_{Hhm}^{(h)k} \psi_{ha}^m(u_a^1, u_a^2) + \sum_m \lambda_{Hhm}^{(e)k} \psi_{ea}^m(u_a^1, u_a^2) \quad (4.2-48)$$

$$F_{Ee}^k(u_a^1, u_a^2) = \sum_m \gamma_{Eem}^{(e)k} \psi_{ea}^m(u_a^1, u_a^2) + \sum_m \gamma_{Eem}^{(h)k} \psi_{ha}^m(u_a^1, u_a^2) \quad (4.2-49)$$

$$F_{Eh}^k(u_a^1, u_a^2) = \sum_m \gamma_{Ehm}^{(e)k} \psi_{ea}^m(u_a^1, u_a^2) + \sum_m \gamma_{Ehm}^{(h)k} \psi_{ha}^m(u_a^1, u_a^2) \quad (4.2-50)$$

$$F_{He}^k(u_a^1, u_a^2) = \sum_m \gamma_{Hem}^{(h)k} \psi_{ha}^m(u_a^1, u_a^2) + \sum_m \gamma_{Hem}^{(e)k} \psi_{ea}^m(u_a^1, u_a^2) \quad (4.2-51)$$

$$F_{Hh}^k(u_a^1, u_a^2) = \sum_m \gamma_{Hhm}^{(h)k} \psi_{ha}^m(u_a^1, u_a^2) + \sum_m \gamma_{Hhm}^{(e)k} \psi_{ea}^m(u_a^1, u_a^2) \quad (4.2-52)$$

where all λ and γ are determinable. When the modes in region "a" are orthogonal this determination is facilitated. For this case

$$\lambda_m^k = \frac{(\psi^m, G^k)}{(\psi^m, \psi^m)} \quad (4.2-53)$$

$$\gamma_m^k = \frac{(\psi^m, F^k)}{(\psi^m, \psi^m)} \quad (4.2-54)$$

for all E, e, H, and h subscripts and superscripts. The notation (f, g) represents the inner product of functions f and g . For the situation on hand, this inner product is an integration over the constant u_a^3 aperture surface. When these independent modes are not orthogonal, one can evaluate these constants by either first using the Gram-Schmidt orthogonalization procedure or by employing a point matching procedure and solving the linear set of equations that result for the desired coefficients.

Upon substituting Equations 45-52 into Equations 35-38 and regrouping terms, one obtains

$$\sum_n c_{en} \psi_{ea}^n = \sum_m t_{Em}^{(e)} \psi_{ea}^m + \sum_m t_{Em}^{(h)} \psi_{ha}^m \quad (4.2-55)$$

$$\sum_n c'_{en} \psi_{ea}^n = \sum_m r_{Em}^{(e)} \psi_{ea}^m + \sum_m r_{Em}^{(h)} \psi_{ha}^m \quad (4.2-56)$$

$$\sum_n c_{hn} \psi_{ha}^n = \sum_m t_{Hm}^{(h)} \psi_{ha}^m + \sum_m t_{Hm}^{(e)} \psi_{ea}^m \quad (4.2-57)$$

$$\sum_n c'_{hn} \psi_{ha}^n = \sum_m r_{Hm}^{(h)} \psi_{ha}^m + \sum_m r_{Hm}^{(e)} \psi_{ea}^m \quad (4.2-58)$$

where

$$t_m = \sum_k b_{ek}^{(+)} \lambda_{em}^k + \sum_k b_{hk}^{(+)} \lambda_{hm}^k \quad (4.2-59)$$

and

$$r_m = \sum_k b_{ek}^{(+)} \gamma_{em}^k + \sum_k b_{hk}^{(+)} \lambda_{hm}^k \quad (4.2-60)$$

for all subscripts E and H and superscripts (e) and (h).

When the fields on the right side of the junction due to incident E-modes are expressed in terms of the coordinates on the left side of the junction, it is reasonable to assume that the result is expressable in terms of the E-modes on the left side of the junction. A similar statement applies when H-modes are incident. Thus, an expansion of E-modes and H-modes on the right side of the junction that are due to E-modes on the left side of the junction are assumed to be expressable in terms of only E-modes on the left side of the junction.

In other words, $t_{Em}^{(h)}$, $t_{Hm}^{(e)}$, $r_{Em}^{(h)}$, and $r_{Hm}^{(e)}$ are zero. Furthermore since the modes are independent and Equations 55-58 hold for a continuum of values of u_a^1 and u_a^2 , it follows from these equations and Equations 39-42 and 59-60 that

$$t_{Em}^{(e)} = \sum_k \lambda_{Eem}^{(e)k} b_{Eek}^{(+)} + \sum_k \lambda_{Ehm}^{(e)k} b_{Ehk}^{(+)} = c_{em} = I_{ea}^{(+m)} a_{em}^{(+)} + I_{ea}^{(-m)} a_{em}^{(-)}$$

for $m = 1, 2, \dots$ (4.2-61)

$$r_{Em}^{(e)} = \sum_k \gamma_{Eem}^{(e)k} b_{Eek}^{(+)} + \sum_k \gamma_{Ehm}^{(e)k} b_{Ehk}^{(+)} = c'_{em} = \frac{dI_{ea}^{(+m)}}{du_a^3} a_{em}^{(+)} + \frac{dI_{ea}^{(-m)}}{du_a^3} a_{em}^{(-)}$$

for $m = 1, 2, \dots$ (4.2-62)

$$t_{Hn}^{(h)} = \sum_k \lambda_{Hen}^{(h)k} b_{Hek}^{(+)} + \sum_k \lambda_{Hhn}^{(h)k} b_{Hhk}^{(+)} = c_{hn} = I_{ha}^{(+n)} a_{hn}^{(+)} + I_{ha}^{(-n)} a_{hn}^{(-)}$$

for $n = 1, 2, \dots$ (4.2-63)

$$r_{Hn}^{(h)} = \sum_k \gamma_{Hen}^{(h)k} b_{Hek}^{(+)} + \sum_k \gamma_{Hhn}^{(h)k} b_{Hhk}^{(+)} = c'_{hn} = \frac{dI_{ha}^{(+n)}}{du_a^3} a_{hn}^{(+)} + \frac{dI_{ha}^{(-n)}}{du_a^3} a_{hn}^{(-)}$$

for $n=1, 2, \dots$ (4.2-64)

$$t_{Em}^{(h)} = \sum_k \lambda_{Eem}^{(h)k} b_{Eek}^{(+)} + \sum_k \lambda_{Ehm}^{(h)k} b_{Ehk}^{(+)} = 0 \quad ; m = 1, 2, \dots \quad (4.2-65A)$$

$$t_{Hm}^{(e)} = \sum_k \lambda_{Hem}^{(e)k} b_{Hek}^{(+)} + \sum_k \lambda_{Hhm}^{(e)k} b_{Hhk}^{(+)} = 0 \quad ; m = 1, 2, \dots \quad (4.2-65B)$$

$$r_{Em}^{(h)} = \sum_k \gamma_{Eem}^{(e)k} b_{Eek}^{(+)} + \sum_k \gamma_{Ehm}^{(h)k} b_{Ehk}^{(+)} = 0 \quad ; m = 1, 2, \dots \quad (4.2-66A)$$

$$r_{Hm}^{(e)} = \sum_k \gamma_{Hem}^{(e)k} b_{Hek}^{(+)} + \sum_k \gamma_{Hhm}^{(h)k} b_{Hhk}^{(+)} = 0 \quad ; m = 1, 2, \dots \quad 4.2-66B)$$

As previously indicated, finite summations and a finite number of equations will be used to obtain an approximate solution. This truncation, however, must be accomplished in such a manner that a good unique approximation to the true solution is obtained.⁴ Since the $a^{(+)}$ terms for the source condition being considered are assumed to be known, the appropriately truncated form of Equations 61-66 may be used to determine all unknown "b" and " $a^{(-)}$ " coefficients. Before proceeding, it should be noted that it is $(b_{Ehk}^{(+)} + b_{Hhk}^{(+)} = b_{hk}^{(+)})$

⁴Procedures for insuring this are of current interest in the literature [22, 29, 30].

and $(b_{Eek}^{(+)} + b_{Hek}^{(+)} = b_{ek}^{(+)})$ that must be determined. Thus, one can substitute $b_{Ehk}^{(+)} = b_{hk}^{(+)} - b_{Hhk}^{(+)}$ and $b_{Hek}^{(+)} = b_{ek}^{(+)} - b_{Eek}^{(+)}$ to eliminate $b_{Eek}^{(+)}$ and $b_{Hhk}^{(+)}$ and solve directly for the desired $b_{ek}^{(+)}$ and $b_{hk}^{(+)}$ quantities.

Once the coefficients have been determined, the Hertz potentials, and therefore the fields, may be determined for all values of u_a^3 to the left of the aperture from Equations 7A and 12A. For values of u_b^3 to the right of the aperture surface the Hertz potentials, and therefore the fields, may be determined by summing Equations 7B and 12C (or 7C and 12B) to respectively obtain

$$\begin{aligned}
 \overline{\pi}_{hb}^k &= \overline{\pi}_{Ehb}^k + \overline{\pi}_{Hhb}^k \\
 &= \hat{i}_{b1} [b_{Ehk}^{(+)} + b_{Hhk}^{(+)}] I_{hb}^{(+k}(u_b^3) \psi_{hb}^k(u_b^1, u_b^2) \\
 &= \hat{i}_{b1} b_{hk}^{(+)} I_{hb}^{(+k}(u_b^3) \psi_{hb}^k(u_b^1, u_b^2)
 \end{aligned} \tag{4.2-67}$$

$$\begin{aligned}
 \overline{\pi}_{eb}^k &= \overline{\pi}_{Eeb}^k + \overline{\pi}_{Heb}^k \\
 &= \hat{i}_{b1} [b_{Eek}^{(+)} + b_{Ehk}^{(+)}] I_{eb}^{(+k}(u_b^3) \psi_{eb}^k(u_b^1, u_b^2) \\
 &= \hat{i}_{b1} b_{ek}^{(+)} I_{eb}^{(+k}(u_b^3) \psi_{eb}^k(u_b^1, u_b^2)
 \end{aligned} \tag{4.2-68}$$

The previous discussion assumed a particular source and load condition. If the load were not matched, there would also be terms involving $b_{Eek}^{(-)}$, $b_{Ehk}^{(-)}$, $b_{Hek}^{(-)}$, and $b_{Hhk}^{(-)}$, and the load condition would relate the $b^{(-)}$ coefficients to the $b^{(+)}$ coefficients. Similarly, for the source condition specifying the resultant of incident and reflected fields, a set of equations relating the $a^{(+)}$ and $a^{(-)}$ coefficients would replace the source condition. If the previous procedures were followed with these new source and load conditions, enough equations to solve the problem would still result. However, the resulting equations would be more complicated algebraically. Instead of pursuing these more general source and load conditions for the general junction, the approach, in this case, will be illustrated in Section 4.4 by the case in which there is no coupling between E-modes and H-modes.

When possible, it is desirable to characterize the junction independent of the source and load conditions. Consider the case in which there is only one incident mode (say the first E-mode). Then Equations 61-66 may be divided by $a_{el}^{(+)}$. Upon noting that $a_{em}^{(+)}$ is zero for m greater than one and $a_{hm}^{(+)}$ is zero for all m , it is seen that for this case Equations 61-66 can be used to determine the ratios of $\frac{a_{em}^{(-)}}{a_{el}^{(+)}}$, $\frac{a_{hm}^{(-)}}{a_{el}^{(+)}}$, $\frac{b_{ek}^{(+)}}{a_{el}^{(+)}}$ and $\frac{b_{hk}^{(+)}}{a_{el}^{(+)}}$.

The first two ratios relate reflected to incident levels while the last two ratios relate transmitted to incident ratios.

From a practical point of view, engineers usually are interested in the effect that the junction has on propagating modes rather than the fields in the vicinity of the aperture surface. Thus, they usually consider two surfaces, one sufficiently to the right of the junction and one sufficiently to the left of the junction such that nonpropagating modes have attenuated to negligible amplitudes. Equations 7A, 12A, 67 and 68 may be used to "translate" the coefficients to the desired surfaces. For the example of one E-mode, the previous ratios evaluated on the left surface reduces to $\left[\begin{pmatrix} a_{e1}^{(-)'} \\ \frac{a_{e1}^{(-)'}}{a_{e1}^{(+)'}} \end{pmatrix} \right] \equiv S_1^1$ and the ratio on the right surface reduces to $\left[\begin{pmatrix} b_{e1}^{(+)'} \\ \frac{b_{e1}^{(+)'}}{a_{e1}^{(+)'}} \end{pmatrix} \right] \equiv S_1^2$.

where $a_{e1}^{(-)'} = a_{e1}^{(-)} I_{ea}^{(-)1}(u_a^3)$ evaluated on the left surface
(4.2-69)

$a_{e1}^{(+)'} = a_{e1}^{(+)} I_{ea}^{(+)1}(u_a^3)$ evaluated on the left surface
(4.2-70)

and $b_{e1}^{(+)*} = b_{e1}^{(+)} I_{eb}^{(+)*} (u_b^3)$ evaluated on the right surface
(4.2-71)

The process can now be repeated for an incident mode on the right side of the junction and the resulting ratios together with the previous two ratios define the scatter parameter, S_1^j , of a linear two part device. These scatter parameters define the junction properties as far as the one propagating mode is concerned. One advantage of introducing scatter parameters is that these parameters are often determinable experimentally.

When two modes can propagate on both sides of the junction, one may attempt to develop four port parameters by the previous procedures. To do this, the ratios of four problems are evaluated--one for each possible incident mode. A 4 X 4 scatter matrix would result.

In order to reduce the number of scatter parameter ratios that are computed, one may take advantage of the fact that the junction is both reciprocal and lossless. Thus, the scatter matrix is both unitary and symmetric for the case being considered [27]. This simplification can be achieved for any number of propagating modes.

4.3 Specialized Junction Theory

This section discusses the procedures for the special cases in which it is possible to choose the Hertz vector potential to be in the same direction on both sides of the junction and there is no cross-coupling between E-modes and H-modes across the junction. This situation leads to a set of simplified junction equations that apply to a large number of problems. The applicable junction geometries can therefore be analyzed more conveniently by appropriately selecting the direction of the Hertz vector potential. Direction generalizations of the Hertz potential were referred to in Sections 3.2 and 3.3.

One situation in which it is advantageous to choose a different direction for the Hertz vector potential occurs when at least one of the two sets of boundary (or coordinate) surfaces at the junction between the nonuniform waveguide is sufficiently smooth. This situation is always true for uniform waveguides and for the class of nonuniform waveguides illustrated in Figure 4.3-1.

(These junctions have smooth surfaces and in addition $u_a^3 = u_b^3 = \text{constant}$ may be selected for the aperture surface.) The sufficiently smooth condition is also often satisfied by one-surface waveguide junctions and sectorial horn junctions (because one dimension is uniform).

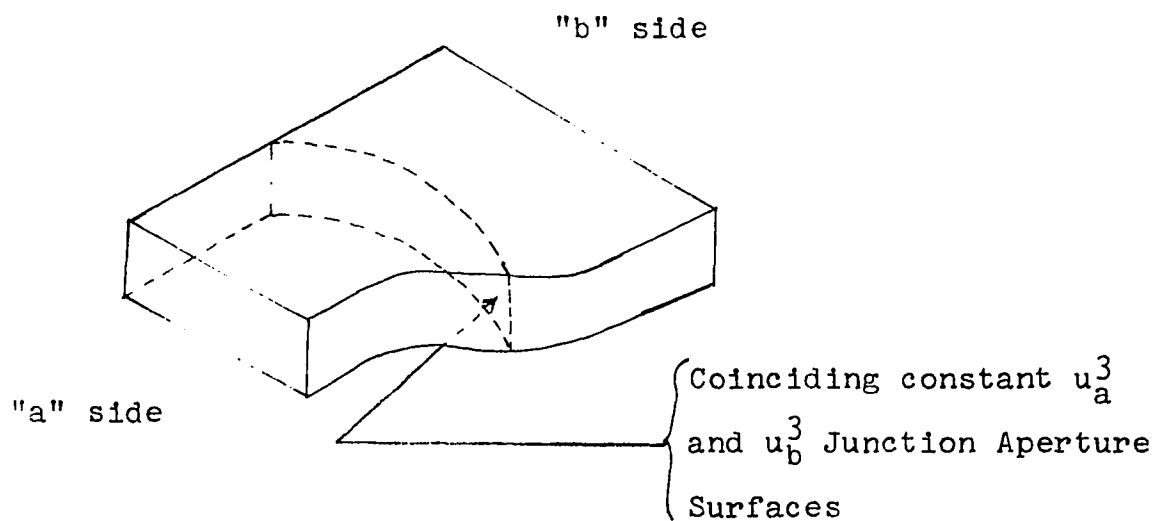


Figure 4.3-1

Smooth Junction with Coinciding Constant u^3 Junction Aperture
Surfaces

It is usually advantageous to select the Hertz vector potential to be normal to the sufficiently smooth surfaces since, for this direction, there is no Hertz vector potential direction change at the junction when the coordinates are selected consistent with the procedure of Chapter 3. This situation will not be true, however, unless one set of coordinate surfaces are sufficiently smooth. It is seen from the above discussion that the technique of appropriately choosing the direction of the Hertz vector potential is applicable to a relatively large number of junctions.

In order for the field quantities, \bar{E} and \bar{H} , to be expressible in terms of the Hertz potentials on either side of the junction for the case in which there is no coupling between generalized E and generalized H modes, the curl of the Hertz vector potentials of both regions must be the same (see Equations 2.2-2, 2.2-3, 2.2-4 and 2.2-5). Thus, in the junction region

$$\nabla \times \bar{\pi}_{ea} = \nabla \times \bar{\pi}_{eb} \quad (4.3-1)$$

$$\nabla \times \bar{\pi}_{ha} = \nabla \times \bar{\pi}_{hb} \quad (4.3-2)$$

where $\bar{\pi}_{ea}$ ($\bar{\pi}_{ha}$) is the totality of E-modes (H-modes) on the "a" side of the junction and $\bar{\pi}_{eb}$ ($\bar{\pi}_{hb}$) is the sum of E-modes (H-modes) on the "b" side of the junction. From Equations 1 and 2 it follows that

$$\bar{\pi}_{ea} = \bar{\pi}_{eb} + \nabla f_e \quad (4.3-3)$$

$$\bar{\pi}_{ha} = \bar{\pi}_{hb} + \nabla f_b \quad (4.3-4)$$

However, since the Hertz vector potentials have been selected in the same direction, it follows that either ∇f_e (∇f_h) is zero or it is in the direction of the Hertz vectors. But if ∇f_e (∇f_h) is in the direction of the Hertz vector potential, it is not needed for direction correction. Also, noting that the Hertz potential is not unique, one can set ∇f_e and ∇f_h equal to zero. The resulting equations are

$$\pi_{ea} = \pi_{eb} \quad (4.3-5)$$

and

$$\pi_{ha} = \pi_{hb} \quad (4.3-6)$$

where π_{ea} , π_{eb} , π_{ha} , and π_{hb} are the magnitudes of the corresponding Hertz vectors. As discussed in Section

4.2, this equation holds in a region. On the constant u_a^3 junction aperture surface one may also require

$$\frac{\partial \pi_{ea}}{\partial u_a^3} = \frac{\partial \pi_{eb}}{\partial u_a^3} \quad (4.3-7)$$

and

$$\frac{\partial \pi_{ha}}{\partial u_a^3} = \frac{\partial \pi_{hb}}{\partial u_a^3} \quad (4.3-8)$$

Or equivalently

$$\nabla \pi_{ea} \cdot \hat{n} = \nabla \pi_{eb} \cdot \hat{n} \quad (4.3-9)$$

and

$$\nabla \pi_{ha} \cdot \hat{n} = \nabla \pi_{hb} \cdot \hat{n} \quad (4.3-10)$$

where \hat{n} is a unit vector normal to the aperture surface ($u_a^3 = \text{constant}$). Actually, any directional derivative that has a component that is normal to the aperture surface (outward-going directional derivative) will suffice. The normal direction, however, is usually the most convenient.

Alternatively, when the Hertz vector potential can be chosen in the same direction on both sides of the junction

and there is no cross-coupling between E-modes and H-modes, then Equations 4.2-17 through 4.2-19, respectively, become:

$$\sum_n \left[a_{en}^{(+)} I_{ea}^{(+)} n + a_{en}^{(-)} I_{ea}^{(-)} n \right] \psi_{ea}^n = \sum_k b_{Eek}^{(+)} I_{eb}^{(+)} k \psi_{eb}^k + \hat{i}_1 \cdot \nabla f_e \quad (4.3-11)$$

$$\hat{i}_2 \cdot \nabla f_e = 0 \quad (4.3-12)$$

$$\hat{i}_3 \cdot \nabla f_e = 0 \quad (4.3-13)$$

As before, the \hat{i}_1 component of ∇f_e may be selected equal to zero. Equation 11 (which is also a reduction of Equation 4.2-10) is then recognized to be the same as Equation 5 when there are only "outward-going" waves on side "b" of the junction (to this extent, Equation 5 is more general). A similar discussion holds for Equations 4.2-24 through 4.2-26 and 4.2-6. Thus, the theory of Section 4.2 reduces appropriately to the equations of the specialized junction theory.

4.4 Sectorial Wedge to Multimode Uniform Waveguide Junction

As an example, the junction between the sectorial wedge and uniform waveguide shown in Figure 4.4-1 will be considered. In this example, the $y = \text{constant}$ surfaces are smooth for both regions. The Hertz vector potentials will be chosen normal to the $y = \text{constant}$ surfaces (i.e., in the y direction).⁵ This choice permits the Hertz potential to be in the same direction on both sides of the aperture and therefore satisfies the simplified equations in Section 4.3.

Let region "a" be the uniform waveguide to the right of the junction and let region "b" be the sectorial horn to the left of the junction⁶ with cartesian and cylindrical coordinates respectively being used. The junction aperture surface is at $z = z_1$ (or equivalently at $r \cos \theta = z_1$). It will be supposed that more than one

⁵This direction for the Hertz vector potential yields generalized E-modes and H-modes that are referred to as LSE-modes (Longitudinal Section E-modes) and LSH-modes (Longitudinal Section H-modes) respectively.

⁶This was intentionally chosen opposite to the preceding sections to emphasize that the choice is arbitrary.

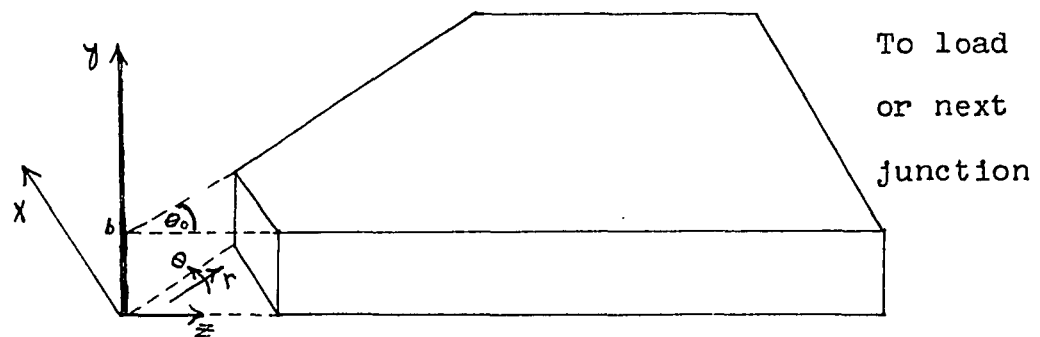


Figure 4.4-1

Sectorial Wedge to Uniform Waveguide Junction

mode is propagating and that only LSE modes are incident to the junction in region "b".⁷ As indicated subsequently, a more general load condition will be assumed. The procedures of Section 4.2 (in specialized form) will be followed. As before, equations are used to clarify procedures. An explicit detailed solution is not intended.

In a straightforward manner the methods of Chapter 3 can be used to show that the amplitude of the electric Hertz vector potential for region "b" is given by

$$\pi_{eb} = \sum_{p=1} \sum_{m=0} \left\{ A^{pm} \left[\sin \frac{p\pi\theta}{\theta_0} \cos \frac{m\pi y}{b} \left(H_{\frac{p\pi}{\theta_0}}^{(2)}(k_r r) \right) \right] + D^{pm} \left[\sin \frac{p\pi\theta}{\theta_0} \cos \frac{m\pi y}{b} \left(H_{\frac{p\pi}{\theta_0}}^{(1)}(k_r r) \right) \right] \right\} \quad (4.4-1)$$

$$\text{where} \quad k_r = \sqrt{k_0^2 - \left(\frac{m\pi}{b}\right)^2} \quad (4.4-2)$$

θ_0 is the angle of the sectorial wedge (see Figure 4.4-1)

b is the height of the waveguide (y - dimension)

$H^{(1)}$ and $H^{(2)}$ are Hankel functions⁸ of the first and second kind, respectively, both of order $\frac{p\pi}{\theta_0}$

and r and θ are cylindrical coordinates which are related to cartesian coordinates by

⁷There is no coupling between LSE and LSH modes for this geometry. Superposition can be used if both mode types are present.

⁸These functions are defined in Section 3.4.

$$\theta = \tan^{-1} \left(\frac{x}{z} \right) \quad (4.4-3)$$

and

$$r = \sqrt{x^2 + z^2} \quad (4.4-4)$$

Since region "a" is described in terms of cartesian coordinates, it is convenient to express the Hertz potential for region "b" in terms of cartesian coordinates, namely

$$\pi_{eb} = \sum_{p=1}^{\infty} \sum_{m=0}^{\infty} \left[A^{pm} \cos \frac{m\pi y}{b} G_p^{(2)}(x,z) + D^{pm} \cos \frac{m\pi y}{b} G_p^{(1)}(x,z) \right] \quad (4.4-5)$$

where

$$G_p^{(2)}(x,z) = \sin \left(\frac{p\pi}{\theta_0} \tan^{-1} \frac{x}{z} \right) H_{\frac{p\pi}{\theta_0}}^{(2)}(k_r \sqrt{x^2 + z^2}) \quad (4.4-6)$$

Note that since the Hankel functions are in general complex functions, it follows that $G_p^{(1)}(x,z)$ and $G_p^{(2)}(x,z)$ are also complex functions. Also observe that

$$\frac{\partial \pi_{eb}}{\partial z} = \sum_{p=1}^{\infty} \sum_{m=0}^{\infty} \left[A^{pm} \cos \frac{m\pi y}{b} F_p^{(2)}(x,z) + D^{pm} \cos \frac{m\pi y}{b} F_p^{(1)}(x,z) \right] \quad (4.4-7)$$

where

$$F_p^{(2)}(x,z) = \frac{\partial}{\partial z} [G_p^{(2)}(x,z)] \quad (4.4-8)$$

By using the methods of Chapter 3, the Hertz vector potential for a point in region "a" can be shown to be⁹

$$\bar{\pi}_{ea} = \hat{a}_y \sum_{n=1} \sum_{m=0} B^{nm} \left[\sin \frac{n\pi x}{a} \cos \frac{m\pi y}{b} e^{-k_{nm} z} + \sum_{r=1} \sum_{t=0} \Gamma_{nm}^{rt} \sin \frac{r\pi x}{a} \cos \frac{t\pi y}{b} e^{k_{rt} z} \right] \quad (4.4-9)$$

where n , m , r , and t are integer indices, a is the width (x-dimension) of the waveguide, and

$$k_{nm} = k_{z_{nm}} = \sqrt{\left(\frac{n}{a}\right)^2 + \left(\frac{m}{b}\right)^2 - k_o^2} \quad (4.4-10)$$

It is purely imaginary (and positive) for propagating modes and positive real for nonpropagating modes and

$$\Gamma_{nm}^{rt} \equiv \left[\frac{\text{complex amplitude returning from load in the } (r,t) \text{ mode evaluated at the position}}{\text{complex amplitude incident at the load in the } (n,m) \text{ mode evaluated at the position}} \right] \quad (4.4-11)$$

⁹ Note the more general load condition.

For the uniform output waveguide it is related to the quantities at the load (or next junction) by¹⁰

$$\Gamma_{nm}^{rt}(z) = \Gamma_{nm}^{rt}(z_L) e^{-k_{rt}d} \quad (4.4-12)$$

where $d = z_L - z$ is the distance in front of the load and z_L is the location of the load. This implies that the amplitude of this factor is a constant as a function of position for propagating modes and decays exponentially for nonpropagating modes. The quantity, Γ_{nm}^{rt} , in Equation 9 accounts for conversion between modes that may occur at the load. For example, if the load being considered is the input to another junction then cross-coupling between modes may occur. If the load is far from the junction under analysis, then only propagating modes need be considered to be reflected from the load and Γ_{nm}^{rt} can be considered to be zero for all nonpropagating reflected modes. In many loads cross-coupling terms are not generated. For this case

$$\Gamma_{nm}^{rt} = \delta_n^r \delta_m^t \Gamma_{nm} \quad (4.4-13)$$

where

$$\delta_j^i \equiv \begin{cases} 1 & \text{if } i = j \\ 0 & \text{if } i \neq j \end{cases} \quad \text{is the Kronecker delta}$$

¹⁰This equation follows directly from uniform transmission line theory.

and Γ_{nm} is the reflection coefficient of the (n, m) mode. When Γ_{nm} is zero for all modes, then there is no reflection. (This is the case in Section 4.2).

In order to satisfy the junction conditions of Section 4.3, the partial derivative of Equation 9 is taken. Thus,

$$\frac{\partial \pi_{ea}}{\partial z} = \sum_{n=1} \sum_{m=0} B^{nm} \left[-k_{nm} \sin \frac{n\pi x}{a} \cos \frac{m\pi y}{b} e^{-k_{nm} z} + \sum_{r=1} \sum_{t=0} \Gamma_{nm}^{rt} \sin \frac{r\pi x}{a} \cos \frac{t\pi y}{b} e^{k_{rt} z} \right] \quad (4.4-14)$$

As indicated in Section 4.3, the junction conditions for this example are

$$\pi_{ea} = \pi_{eb} \text{ for } z = z_1 \quad (4.4-15)$$

$$\left. \frac{\partial \pi_{ea}}{\partial z} \right|_{z=z_1} = \left. \frac{\partial \pi_{eb}}{\partial z} \right|_{z=z_1} \quad (4.4-16)$$

From Equations (15), (5), and (9), one obtains (after interchanging summation orders)

$$\begin{aligned}
& \sum_{m=0}^{\infty} \sum_{p=1}^{\infty} \left[A^{pm} \cos \frac{m\pi y}{b} G_p^{(2)}(x, z_1) + D^{pm} \cos \frac{m\pi y}{b} G_p^{(1)}(x, z_1) \right] = \\
& = \sum_{m=0}^{\infty} \sum_{n=1}^{\infty} B^{nm} \left[\sin \frac{n\pi x}{a} \cos \frac{m\pi y}{b} e^{-k_{nm} z_1} + \sum_{k=0}^{\infty} \sum_{r=1}^{\infty} \Gamma_{nm}^{rt} \sin \frac{r\pi x}{a} \cos \frac{t\pi y}{b} e^{k_{rt} z_1} \right] \\
& = \sum_{m=0}^{\infty} \sum_{n=1}^{\infty} B^{nm} \sin \frac{n\pi x}{a} \cos \frac{m\pi y}{b} e^{-k_{nm} z_1} + \sum_{t=0}^{\infty} \sum_{r=1}^{\infty} \sum_{m=0}^{\infty} \sum_{n=1}^{\infty} B^{nm} \Gamma_{nm}^{rt} \sin \frac{r\pi x}{a} \cos \frac{t\pi y}{b} e^{k_{rt} z_1} \\
& \hspace{25em} (4.4-17)
\end{aligned}$$

Interchanging dummy indices r with n and t with m in the second term and recombining, one obtains after re-writing

$$\begin{aligned}
& \sum_{m=0}^{\infty} \sum_{p=1}^{\infty} \left\{ \cos \frac{m\pi y}{b} \left[A^{pm} G_p^{(2)}(x, z_1) + D^{pm} G_p^{(1)}(x, z_1) \right] \right\} = \\
& = \sum_{m=0}^{\infty} \sum_{n=1}^{\infty} \cos \frac{m\pi y}{b} \sin \frac{n\pi x}{a} \left[B^{nm} e^{-k_{nm} z_1} + \left(\sum_{t=0}^{\infty} \sum_{r=1}^{\infty} B^{rt} \Gamma_{rt}^{nm} \right) e^{k_{nm} z_1} \right] \\
& \hspace{25em} (4.4-18)
\end{aligned}$$

By either using the orthogonality of cosine functions or simply noting that Equation 18 holds for all values of y in the interval $[0, b]$, it follows that

$$\begin{aligned}
\sum_{p=1} \left[A^{pm} G_p^{(2)}(x, z_1) + D^{pm} G_p^{(1)}(x, z_1) \right] &= \\
= \sum_{p=1} \left[B^{nm} e^{-k_{nm} z_1} + \sum_{t=0} \sum_{r=1} B^{rt} \Gamma_{rt}^{nm} e^{k_{nm} z_1} \right] \sin \frac{n\pi x}{a} &\quad (4.4-19) \\
&\text{for } m = 0, 1, 2, \dots
\end{aligned}$$

Observe that at the junction $z = z_1$, the functions $G_p^{(2)}(x, z_1)$ depend only on x and that this function is defined on the junction plane within the waveguide. These functions can be completed as a periodic function in all space whose values coincide with this function within the waveguide aperture. Because of the "sin" function dependence that resulted from the boundary conditions, $G_p^{(2)}(x, z_1)$ will be completed as odd functions of x and expanded as a Fourier series of the form

$$G_p^{(2)}(x, z_1) = \sum_{n=1} \lambda_{np}^{(2)} \sin \frac{n\pi x}{a} \quad (4.4-20)$$

where $\lambda_{np}^{(2)}$ and $\lambda_{np}^{(1)}$ are known complex Fourier sin series coefficients. after substituting Equation 20 into Equation 19 one obtains

$$\begin{aligned}
\sum_{n=1} \sum_{p=1} \left(A^{pm} \lambda_{np}^{(2)} + D^{pm} \lambda_{np}^{(1)} \right) \sin \frac{n\pi x}{a} &= \\
= \sum_{n=1} \left[B^{nm} e^{-k_{nm} z_1} + \sum_{t=0} \sum_{r=1} B^{rt} \Gamma_{rt}^{nm} e^{k_{nm} z_1} \right] \sin \frac{n\pi x}{a} &\quad (4.4-21) \\
&\text{for } m = 0, 1, 2 \dots
\end{aligned}$$

Again using orthogonality of sinusoids, it follows that

$$\begin{aligned}
 \sum_{p=1}^{\infty} \left[\lambda_{np}^{(2)} A^{pm} + \lambda_{np}^{(1)} D^{pm} \right] &= \\
 &= e^{-k_{nm} z_1} B^{nm} + \sum_{t=0}^{\infty} \sum_{r=1}^{\infty} \left(\Gamma_{rt}^{nm} e^{k_{nm} z_1} \right) B^{rt} \\
 &\quad \text{for } m = 0, 1, 2, 3, \dots \\
 &\quad n = 1, 2, 3, \dots \quad (4.4-22)
 \end{aligned}$$

The junction condition of Equation 16 is now applied to Equations 7 and 14 to obtain

$$\begin{aligned}
 \sum_{p=1}^{\infty} \sum_{m=0}^{\infty} \left[A^{pm} \cos \frac{m\pi y}{b} F_p^{(2)}(x, z_1) + D^{pm} \cos \frac{m\pi y}{b} F_p^{(1)}(x, z_1) \right] \\
 = \sum_{m=0}^{\infty} \sum_{n=1}^{\infty} B^{nm} \left\{ \begin{aligned} &-k_{nm} \sin \frac{n\pi x}{a} \cos \frac{m\pi y}{b} e^{-k_{nm} z_1} \\ &+ \sum_{t=0}^{\infty} \sum_{r=1}^{\infty} \Gamma_{rt}^{nm} k_{rt} \sin \frac{r\pi x}{a} \cos \frac{t\pi y}{b} e^{k_{rt} z_1} \end{aligned} \right\} \quad (4.4-23)
 \end{aligned}$$

Observe that the same expression can be obtained from Equation 17 by making the substitutions

$$G_p^{(2)}(x, z_1) \rightarrow F_p^{(2)}(x, z_1) \quad (4.4-24A)$$

$$e^{-k_{nm} z_1} \rightarrow -k_{nm} e^{-k_{nm} z_1} \quad (4.4-24B)$$

$$e^{k_{rt} z_1} \rightarrow k_{rt} e^{k_{rt} z_1} \quad (4.4-24C)$$

Thus, following the previous steps the equation corresponding to Equation 19 should be

$$\begin{aligned} \sum_{p=1} A_{np}^{pm} F_p^{(2)}(x, z_1) + D_{np}^{pm} F_p^{(1)} &= \\ &= \sum_{n=1} -B_{nm}^{nm} k_{nm} e^{-k_{nm} z_1} + \sum_{t=0} \sum_{r=1} k_{nm} B_{rt}^{rt} \Gamma_{rt}^{nm} e^{k_{nm} z_1} \sin \frac{n\pi x}{a} \\ &\quad \text{for } m = 0, 1, 2, \dots \end{aligned} \quad (4.4-25)$$

Similarly after making the expansion

$$F_p^{(2)}(x, z_1) = \sum_{n=1} \gamma_{np}^{(2)} \sin \frac{n\pi x}{a} \quad (4.4-26)$$

one obtains

$$\begin{aligned} \sum_{p=1} \gamma_{np}^{(2)} A_{np}^{pm} + \gamma_{np}^{(1)} D_{np}^{pm} &= \\ &= (-k_{nm} e^{-k_{nm} z_1}) B_{nm}^{nm} + \sum_{t=0} \sum_{r=1} (\Gamma_{rt}^{nm} k_{nm} e^{k_{nm} z_1}) B_{rt}^{rt} \\ &\quad \text{for } m = 0, 1, 2, \dots \\ &\quad n = 1, 2, \dots \end{aligned} \quad (4.4-27)$$

For simplicity, let

$$\alpha_{rt}^{nm} = e^{-k_{nm} z_1} \delta_r^n \delta_k^m + \Gamma_{rt}^{nm} e^{k_{nm} z_1} \quad (4.4-28)$$

and let

$$\sigma_{rt}^{nm} = -k_{nm} e^{-k_{nm} z_1} \delta_r^n \delta_k^m + k_{nm} \Gamma_{rt}^{nm} e^{k_{nm} z_1} \quad (4.4-29)$$

where δ_r^n and δ_k^m are Kronecker deltas. Then, after simplification, Equations 22 and 27 can be respectively rewritten as

$$\sum_{p=1} \lambda_{np}^{(2)} A^{pm} + \sum_{p=1} \lambda_{np}^{(1)} D^{pm} = \sum_{t=0} \sum_{r=1} \alpha_{rt}^{nm} B^{rt} \quad \begin{matrix} n=1, 2, \dots \\ m=0, 1, 2, \dots \end{matrix} \quad (4.4-30)$$

$$\sum_{p=1} \gamma_{np}^{(2)} A^{pm} + \sum_p \gamma_{np}^{(1)} D^{pm} = \sum_{t=0} \sum_{r=1} \gamma_{rt}^{nm} B^{rt} \quad (4.4-31)$$

Although, in principle, infinite sums are required to be rigorous in Equations 30 and 31, in practice a finite sum and a finite set of equations can be used. Moreover, with digital computer computation, core size, truncation errors, and round-off errors set an upper limit on the number of terms that can be carried.

At this point in the discussion it is necessary to use physical conditions in order to arrive at a meaningful truncation of the infinite sets of equations. Based

on the work presented in Harrington [14] and the curves in Figure 3.4-2, the "gradual radius of mode cutoff" occurs approximately where the sectorial horn width is the same as the corresponding uniform waveguide at cutoff. It will therefore be assumed that the number of modes that are considered on the left side of the junction is the same as the number of modes considered on the right side of the junction. Reviewing the roles of the various subscripts one further assumes that the upper values of r , p , and n should be the same (say N) and the value required for t should be the same as the upper value required for m (say M). Note that for the usual dimensions, $M \leq N$. Thus, Equations 30 and 31 can be written as

$$\sum_{p=1}^N \lambda_{np}^{(2)} A^{pm} + \sum_{p=1}^N \lambda_{np}^{(1)} D^{pm} = \sum_{t=0}^M \sum_{r=1}^N \alpha_{rt}^{nm} B^{rt} \quad (4.4-30A)$$

$$n=1,2,\dots,N$$

$$m=0,1,2,\dots,M$$

$$\sum_{p=1}^N \gamma_{np}^{(2)} A^{pm} + \sum_{p=1}^N \gamma_{np}^{(1)} D^{pm} = \sum_{t=0}^M \sum_{r=1}^N \sigma_{rt}^{nm} B^{rt} \quad (4.4-31A)$$

In principle, set of Equations 30A have $N(M+1)$ unknown B 's in $N(M+1)$ equations. One can therefore use Equations 30A to solve for the B 's in terms of the A 's and D 's.

Upon substituting these expressions for the B's into Equation 31A the resulting $N(M+1)$ set of equations can be used to solve for the A's in terms of the D's and then, after dividing each equation through by the A^{pm} 's, one can solve the resulting set of equations for the (D^{pn}/A^{qs}) ratios. These ratios are interpreted as the reflection coefficients looking at the junction. In a similar manner the junction transmission coefficient ratios can be obtained by first eliminating the D's and ultimately solving for the (B^{rt}/A^{qs}) ratios.

An alternate to the previous procedure for evaluating the transmission and reflection coefficient ratios, however, will be followed. The aim of this alternate procedure is to organize the calculations by using matrices. Toward this end, the following matrices are defined:

$$\lambda^{(1)} = \left| \lambda_{np}^{(1)} \right| \quad (4.4-32A)$$

$$\lambda^{(2)} = \left| \lambda_{np}^{(2)} \right| \quad (4.4-32B)$$

$$\alpha = \left| \alpha_{rt}^{nm} \right| \quad (4.4-32C)$$

$$\gamma^{(1)} = \left| \gamma_{np}^{(1)} \right| \quad (4.4-32D)$$

$$\gamma^{(2)} = \left| \gamma_{np}^{(2)} \right| \quad (4.4-32E)$$

$$\sigma = \left| \sigma_{rt}^{nm} \right| \quad (4.4-32F)$$

$$A = \left| A^{pm} \right| \quad (4.4-32G)$$

$$D = \left| D^{pm} \right| \quad (4.4-32H)$$

$$B = \left| B^{rt} \right| \quad (4.4-32I)$$

Note that many terms in some matrices (such as $\Lambda^{(2)}$) are identical since the element values are the same for all values of m .

After substitution of the matrices into Equations 30A and 31A, the resulting equations are

$$\lambda^{(2)} A + \lambda^{(1)} D = \alpha B \quad (4.4-33)$$

$$\gamma^{(2)} A + \gamma^{(1)} D = \sigma B \quad (4.4-34)$$

It is observed from the definition of the elements in Equations 28 and 29 that if an element in the α matrix is zero, then the corresponding element in the σ matrix cannot be zero. With multimode interaction, however, the same cannot be said about the corresponding matrices.

Upon eliminating matrix B from the above matrix equations and solving for matrix A , one obtains:

$$A = \eta D \quad (4.4-35)$$

where matrix η is given by one of the following equivalent matrix expressions.

$$\begin{aligned} \eta &= [\alpha^{-1} \lambda^{(2)} - \sigma^{-1} \delta^{(2)}]^{-1} [\sigma^{-1} \delta^{(1)} - \alpha^{-1} \lambda^{(1)}] \\ &= [\lambda^{(2)} - \alpha \sigma^{-1} \delta^{(2)}]^{-1} [\alpha \sigma^{-1} \delta^{(1)} - \lambda^{(1)}] \\ &= [\sigma \alpha^{-1} \lambda^{(2)} - \delta^{(2)}]^{-1} [\delta^{(1)} - \sigma \alpha^{-1} \lambda^{(1)}] \end{aligned} \quad (4.4-36)$$

When some of the matrices involved are singular, the choice of which expression to use in Equation 36 is not arbitrary since the inverse of a singular matrix is not defined.

The case in which matrix η cannot be determined from at

least one of the expressions in Equation 36 is not considered. It is also presumed that matrix \mathcal{N} is nonsingular.

For notational convenience, the modes will henceforth be designated by one integer instead of two. Thus, the (r, t) mode for specified values of r and t are referred to as the L^{th} mode where L is an integer that, in effect, orders the modes.

Before proceeding, recall that the elements of matrix \mathcal{A} , A^{pm} , correspond to the amplitudes of the incident energy (p, m) modes. In terms of the new notation, these are referred to as elements A^L . Matrix \mathcal{A} is therefore a column vector of incident modes. The elements of matrix \mathcal{D} , D^{pm} (or D^k where k is an integer index) correspond to the amplitudes of reflected energy (p, m) modes. It is a column vector of reflected modes. In Section 4.2, it was presumed that the source condition gave the amplitudes of $A^{\text{pm}}(A^L)$. For this case, Equation 35 may be used to directly solve for the reflected, $D^{\text{pm}}(D^k)$ coefficients. A more general source condition provides an independent relationship between incident A^{pm} and reflected D^{pm} coefficients (for example, $(\mathcal{A} + \mathcal{D})$ may be known). This additional relationship plus Equation 35 then permits one to solve for both the incident and reflected coefficients.

It is again presumed that singular matrices do not result. Once the A and D matrices have been evaluated, the matrix of transmitted energy modes, B , may be determined from matrix Equation 33 or 34.

The preceding paragraph indicated the situation with one junction. (With multiple junctions, it also holds for the junction closest to the source.) In the cascade approximation, it is desired to compute the ratios, R_{nm}^{rt} , defined by

$$R_{nm}^{rt} \equiv \frac{d_{nm}^{rt}}{A_{nm}} \quad (4.4-37)$$

where integers ("r" and "t") and ("n" and "m") refer to the (r, t) and (n, m) modes, respectively, and d_{nm}^{rt} is the reflected (r, t) mode amplitude due to an incident (n, m) mode. Assuming that superposition of modes holds, it follows from the definition that

$$D^{rt} = \sum_{n,m} d_{nm}^{rt} = \sum_{n,m} R_{nm}^{rt} A^{nm} \quad (4.4-38)$$

The similarity between this ratio and the definition of the Γ_{nn}^{rt} ratio in Equation 11 should be apparent. In fact, when the R ratios are "transferred" to the next junction closest to the input, it serves as the Γ ratios in this

junction analysis. The method for transferring these ratios will be considered subsequently. In terms of the new notation, Equation 38 becomes

$$D^k = \sum_L d_L^k = \sum_L R_L^k A^L \quad (4.4-38A)$$

where L is also an integer index and from Equation 37

$$R_L^k = \frac{d_L^k}{A^L} \quad (4.4-37A)$$

Refer now to Equation 35 and decompose matrix vector \mathbf{A} into a set of N matrix vectors \mathbf{A}^k for $k = 1, 2, \dots, N$ such that \mathbf{A}^k is obtained from \mathbf{A} by setting all but the k^{th} element equal to zero. From this definition it follows that

$$\mathbf{A} = \sum_{k=1}^N \mathbf{A}^k \quad (4.4-39)$$

Furthermore, let \mathbf{D}^k be defined by

$$\mathbf{D}^k = \mathbf{A}^{-1} \mathbf{A}^k \quad (4.4-40)$$

The L^{th} element of column vector \mathbf{D}^k , d_L^k , are used in the definition of R_L^k given by Equation 37A and therefore R_L^k may be determined.

The procedure for transferring the "R" ratios to a new location in region "b" and thereby determine the " Γ " ratios for the next junction will now be indicated. From Equations 1 and 38 it follows that

$$\pi_{eb} = \sum_{p=1} \sum_{m=0} \left\{ \left[A^{pm} H_{\frac{p\pi}{\theta_0}}^{(2)}(k_r r) + \sum_{i=1} \sum_{j=0} R_{ij}^{pm} A^{ij} H_{\frac{p\pi}{\theta_0}}^{(1)}(k_r r) \right] \sin \frac{p\pi\theta}{\theta_0} \cos \frac{m\pi y}{b} \right\}$$

(4.4-41)

When the value of r at the next junction to be analyzed is put into this equation, it is seen that Equation 41 replaces Equation 9 for this new junction analysis. One also sees that the "R's" are now the " Γ 's" for this junction analysis.

4.5 Summary and Conclusions

This chapter studied the junction between nonuniform waveguides and suggested that some nonuniform waveguides that cannot be conveniently analyzed by the methods of Chapter 3 can be approximated by a cascade of nonuniform waveguides such that each waveguide section satisfies the necessary constraints. The propagation behavior of the entire nonuniform waveguide can be comprehended by

joining the individual waveguide sections. This cascaded nonuniform waveguide approximation allows large and rapid boundary variations to be considered. In this approximation the study of the junction between nonuniform waveguides is important because the nature of the coupling between the various waveguide modes lies in an understanding of the waveguide junction analysis. A junction, as defined in this dissertation, is the joining of two different coordinate systems. It may (or may not) have an associated edge in the waveguide wall.

The major complication in using the Hertz vector potential to analyze the junction between nonuniform waveguides is that to be consistent with the formulation of Chapter 3, the Hertz vector potential is usually chosen to be in a different orientation on both sides of the nonuniform waveguide junction. This direction change is a consequence of the different coordinates that are used on both sides of the junction in order to facilitate satisfying the waveguide wall boundary considerations. Furthermore, the general multi-mode nonuniform waveguide junction is complicated by cross coupling between E-modes and H-modes. For the cascaded nonuniform waveguide situation being considered, however, the waveguide walls are either smooth or almost smooth and therefore the effects of edge discontinuities at the junction are assumed to be small.

It is therefore assumed that the electric and magnetic field intensities expressed on both sides of the junction can be equated in the junction region. This condition further assumes that in the junction region the modal expansions of the fields on both sides of the junction either form a complete set in the junction region or that the missing terms are negligibly small. In addition, it has been assumed that the coordinate transformation relating the coordinates on the right side of the junction to the coordinates on the left side of the junction is one-to-one and continuous.

The procedure for analyzing a junction of the type being considered is to express the fields in terms of the modes and coordinates on both sides of the junction. The modes on the right side of the junction are then presumed to be expressible in terms of the coordinates and modes on the left side of the junction. These results should be equal to the expansion on the left side of the junction. As a convenient artifice, the modes on the right side of the junction were subdivided into a constituent that is related to the totality of E-modes on the left side of the junction and a constituent that is related to the totality of H-modes on the left side of the junction. The resulting complicated equations hold in the junction region. On the junction aperture surface these equations and outward going

directional derivatives of these equations can, in principal, be used to solve the junction problem. By solving for ratios, it is usually possible to characterize the junction independent of the source and load conditions.

From a practical point of view, engineers usually are interested in the effect that the junction has on propagating modes rather than the fields in the vicinity of the aperture surface. Thus, they usually consider two surfaces, one sufficiently to the right of the junction and one sufficiently to the left of the junction such that nonpropagating modes to have attenuated to negligible amplitudes. By using the transmission line equation for each region for each of the propagating input and output modes, the scatter parameters for the region involved may be determined. For M input propagating modes and N output propagating modes, an $(M + N)$ order scatter parameter matrix results. One advantage of introducing scatter parameters is that these parameters can often be determined experimentally.

For the special case in which one can choose the Hertz vector potentials to be in the same direction on both sides of the junction and there is no cross coupling between E-modes and H-modes, the more complicated junction aperture process yields equations that reduce to

$$\pi_{ea} = \pi_{eb} \quad (4.5-1)$$

$$\frac{\partial \pi_{ea}}{\partial u_a^3} = \frac{\partial \pi_{eb}}{\partial u_a^3} \quad (4.5-2)$$

$$\pi_{ha} = \pi_{hb} \quad (4.5-3)$$

$$\frac{\partial \pi_{ha}}{\partial u_a^3} = \frac{\partial \pi_{hb}}{\partial u_a^3} \quad (4.5-4)$$

This specialization can usually be achieved for the broad class of cases in which one of the coordinate surfaces are sufficiently smooth across the waveguide junction by choosing the Hertz vector to be normal to this surface. The junction between uniform waveguides and sectorial wedges are illustrative of the above specialization. The sectorial wedge to uniform waveguide junction was used to illustrate the details of "transferring" model constants across the junction.

CHAPTER 5

CONCLUSIONS

A nonuniform waveguide is initially analyzed in terms of non-orthogonal generalized coordinates utilizing the Hertz vector potentials and the Riemann metric tensor. When the Hertz potential is expressible as a function of the propagation coordinate, u^3 , times a function of the transverse (u^1, u^2) coordinates (partial separation), then the nonuniform waveguide can be represented by transverse equations and a set of uncoupled nonuniform transmission lines. Propagation is studied along the u^3 coordinate by means of the resulting uncoupled nonuniform transmission lines.¹ The desired partial separation is achieved with coordinates that facilitate satisfying the boundary conditions when the conditions summarized in Table 5-1² are satisfied. It was demonstrated that these constraints provide guidelines for deducing a useful coordinate system to describe the nonuniform waveguide. In terms of the resulting coordinate system the nonuniform waveguide may be described by transverse equations and a set of uncoupled

¹Appendix A reviews the current nonuniform transmission line theory.

²This table is identical to Table 3.4-1.

Table 5-1

Sufficient Conditions to Factor

Out the u^3 Dependence $\left[\bar{\pi}(u^1, u^2, u^3) = \psi(u^1, u^2) I(u^3) \right]$

1. u^1 or u^2 are constants on the waveguide walls.
2. Propagation coordinate, u^3 , is orthogonal to both transverse coordinates (the transverse coordinates need not be orthogonal to each other).
3. The g^{33} metric coefficient is independent of u^1 and u^2 .
For convenience, one usually tries to select $g^{33} = 1$.
4. The logarithmic derivative of the determinant of the metric coefficients depends only upon the propagation coordinate.
It is equal to the logarithmic derivative of the transverse surface area when $g^{33} = 1$.
5. The coordinate surfaces are one-to-one continuous differentiable functions of cartesian coordinates.
6. The transverse Laplacian, ∇_{ξ}^2 , may be expressed in one of two general forms.

A. $\nabla_{\xi}^2 = f_1(u^3) \mathcal{L}_1$ where \mathcal{L}_1 is an operator that is independent of u^3 . In this case $\psi_n(u^1, u^2)$ must satisfy the eigenvalue equation $\mathcal{L}_1 \psi_n + \gamma_{1n}^2 \psi_n = 0$ where $(-\gamma_{1n}^2)$ are the eigenvalues to be determined. The corresponding u^3 equation for $I_n(u^3)$ is

$$I_n'' + \frac{f_3(u^3)}{f_2(u^3)} I_n' + K_0^2 - \xi_1(u^3) \gamma_{1n}^2 I_n = 0$$

Table 5-1 (continued)

6. B. $\nabla_t^2 = \xi_1(u^3) \mathcal{L}_1 + \xi_2(u^3) \mathcal{L}_2$ where \mathcal{L}_1 and \mathcal{L}_2 are operators that are independent of u^3 . In this case, $\psi_n(u^1, u^2)$ must simultaneously satisfy eigenvalue equations

$$\mathcal{L}_1 \psi_n + \gamma_{1n}^2 \psi_n = 0$$

$$\mathcal{L}_2 \psi_n + \gamma_{2n}^2 \psi_n = 0$$

where $(-\gamma_{1n}^2)$ and $(-\gamma_{2n}^2)$ are the eigenvalues to be determined. When this is achieved, the corresponding u^3 equation for $I_n(u^3)$ is

$$I_n'' + \frac{f_3(u^3)}{f_2(u^3)} I_n' + K_0^2 - \xi_1(u^3) \gamma_{1n}^2 - \xi_2(u^3) \gamma_{2n}^2 I_n = 0$$

nonuniform transmission lines and thereby enables nonuniform transmission line theory to be applied to the study of nonuniform waveguides. These guidelines are also significant because, in general, one does not know what coordinates to choose. Furthermore, when the g^{33} component of the metric tensor is unity, terms in the nonuniform transmission line differential equation and nonuniform transmission line parameters such as characteristic impedance, and the per length admittance and impedance are related to the logarithmic derivative of the transverse surface area. All results reduce to those of the uniform waveguide as a special case.

When the above constraints cannot be satisfied it is often possible to approximate the overall nonuniform waveguide by a cascade of nonuniform waveguides such that each waveguide section satisfies the required constraints. This led to a study of the junction between nonuniform waveguides. The general junction analysis is valid for both multimode and single mode situations. In addition, the theory allows cross-coupling between E-modes and H-modes to occur at the junction. The specialization of the general junction theory to the analysis of junctions which can be solved by choosing the Hertz vector potential to be in the same direction on both sides of the junction, was also considered and illus-

strated. It was also noted that the appropriate waveguide wall boundary conditions depend upon the direction of the Hertz vector potential.

CHAPTER 6

SUGGESTIONS FOR FURTHER INVESTIGATION

Areas for future investigation follow directly from removing or relaxing constraints and assumptions that have been imposed. Thus, for future investigation one may also consider the presence of inhomogeneous dielectrics, media losses, and/or waveguide wall losses. One can also attempt to extend the results to open structured nonuniform waveguides, dielectric nonuniform waveguides, slow wave nonuniform waveguide structures and/or leaky wave structures. In addition, the case in which the waveguide boundary is described by more than two sets of surfaces can be considered.¹

Another promising area is to investigate the effect on the solution of small perturbations in the constraints. Such results may justify using the results of Chapter 3 even when the required conditions are only approximately true.

As far as junctions are concerned, the theory presented in this dissertation may be viewed as a stepping stone towards the analysis of more complicated junctions. This

¹The author has initiated further work in this area and initial results are encouraging.

theory would benefit greatly from a further study of the case in which the modes on both sides of the junction do not have overlapping or tangential domains of definition. A study of conditions at the edge and with larger discontinuities would also be helpful. Furthermore, in the engineering analysis of junctions, the infinite sets of equations and variables are truncated to finite sets. In general, however, the specific finite selection is not clearly apparent and further investigation of the methods for choosing the truncated set is in order. This latter problem is already of current interest [22, 30, 54].

It would also be useful to obtain greater insight about which specific geometries are solvable by the techniques proposed in this dissertation. Towards this end, it will be useful to apply the theory to many examples.¹ The examples presented in this dissertation used a g^{33} metric coefficient of unity. These examples should also investigate non-unity values of this metric coefficient.¹ Insight may also be gained by investigating the analytic properties of the solutions by function theoretic methods and by experimental measurements on various nonuniform waveguides and junctions. These studies may form the basis of nonuniform waveguide synthesis procedures.

APPENDIX

APPENDIX A

ANALYSIS OF NONUNIFORM TRANSMISSION LINES

A1. Introduction

One of the goals of Chapter 3 is to represent the non-uniform waveguide by a set of uncoupled nonuniform transmission lines. This appendix reviews the techniques for analyzing the nonuniform transmission lines that result.¹

Nonuniform transmission lines have many significant practical applications. T.E.M. wave nonuniform transmission lines finds application as a broadband matching device [13], directional coupler [51], and specialized filters [13] (especially the all-pass variety [58]). These devices find a great deal of application in microwave radar and communication systems. Waveguide types were discussed in Chapter 1.

The analysis techniques to be discussed are broadly classified as exact solution techniques and approximate solution techniques.

A2. Exact Solution Techniques

Exact solutions to the non-uniform transmission line are obtained either by direct solution (when the problem

¹Additional bibliography is indicated in reference [19].

is simple enough) or by means of transformations. This section will discuss these approaches. Only sinusoidal excitation is considered.

The problem is to solve

$$\frac{\partial I}{\partial x} = -y(x)V \quad (A-1)$$

and

$$\frac{\partial V}{\partial x} = -z(x)I \quad (A-2)$$

where $V = V(x)$ and $I = I(x)$ are the steady state sinusoidal phasor voltage and current, respectively, along the transmission line; $z(x)$ and $y(x)$ are the series impedance per length and shunt admittance per length, respectively, along the transmission line, and x is the distance measured along the line. Equations 1 and 2 can be written in terms of current or voltage alone by differentiating one equation with respect to x and substituting the value of the first derivative from the other equation. When this is done, it results that

$$V'' = \frac{z'}{z} V' + yzV \quad (A-3)$$

and

$$I'' = \frac{y'}{y} I' + yzI \quad (A-4)$$

where primes denote differentiation with respect to position, x . These equations are often rewritten as

$$V = (\ln z)' V' + yzV \quad (\text{A-5})$$

$$I = (\ln y)' I' + yzI \quad (\text{A-6})$$

One observes that for a lossless transmission line, the admittance per length becomes the capacity per length and that the impedance per length becomes the inductance per length.

With this as background, consider the exponential line [13, 57] defined such that the impedance and admittance per length are given by

$$z(x) = z_1 e^{ax} \quad (\text{A-7})$$

$$y(x) = y_1 e^{-ax} \quad (\text{A-8})$$

where the constant, a , (or its negative) is called the "flare" constant of the line and z_1 and y_1 are constants. One observes that for this specific variation, Equation 3 (or 5) and Equation 4 (or 6) become

$$V'' = aV' + z_1 y_1 V \quad (\text{A-9})$$

and

$$I'' = -aI' + z_1 y_1 I \quad (\text{A-10})$$

respectively. Since these are constant coefficient equations, the problem is readily solvable.

If Equations 7 and 8 are substituted into Equations 1 and 2, one obtains

$$\frac{\partial I}{\partial x} = -y_1 e^{-ax} V \quad (\text{A-11})$$

$$\frac{\partial V}{\partial x} = -z_1 e^{ax} I \quad (\text{A-12})$$

These equations are often used as an alternate definition of the exponential line. Also note that the characteristic impedance (and admittance) also varies exponentially since

$$Z_o(x) \equiv \sqrt{\frac{z(x)}{y(x)}} = \sqrt{\frac{z_1 e^{ax}}{y_1 e^{-ax}}} = \sqrt{\frac{z_1}{y_1}} = \frac{1}{Y_o(x)} \quad (\text{A-13})$$

In a similar manner, some other types of variations are observed to yield differential equations that are directly solvable. One such nonuniform transmission line is the Bessel line defined by

$$z(x) = z_1 x^{\alpha} \quad (A-14)$$

$$y(x) = y_1 x^{\beta} \quad (A-15)$$

where z_1 , y_1 , α and β are constants.

Recently, Berger [5] succeeded in extending any of the solved problems into a whole set of solved problems by means of transformation of variables. He observed that if a nonuniform transmission line that is characterized by

$$z = A(x) \quad y = B(x) \quad (A-16)$$

has a solution

$$V(x) = K_1 V_1(x) + K_2 V_2(x) \quad (A-17)$$

where $V_1(x)$ and $V_2(x)$ are linearly independent functions and K_1 and K_2 are constants, then the problem

$$z = f'(x) A[f(x)] \quad y = f'(x) B[f(x)] \quad (A-18)$$

where $f(x)$ is an arbitrary differentiable function, has a solution

$$V(x) = K_1 V_1[f(x)] + K_2 V_2[f(x)] \quad (A-19)$$

For example the uniform transmission line

$$V' = -z_1 I \quad ; \quad I' = -y_1 V \quad (A-20)$$

has a solution

$$V(x) = K_1 e^{\sqrt{z_1 y_1} x} + K_2 e^{-\sqrt{z_1 y_1} x} \quad (A-21)$$

The solution to the more general problem

$$V' = -I z_2 f'(x) \quad ; \quad I' = -V y_2 f'(x) \quad (A-22)$$

(where $f(x)$ is relatively arbitrary and z_2 and y_2 are constants) is seen by Equations 19 and 21 to be

$$V(x) = K_1 e^{\sqrt{z_2 y_2 f(x)} x} + K_2 e^{-\sqrt{z_2 y_2 f(x)} x} \quad (A-23)$$

In a similar manner, Berger extends the solutions to the exponential and Bessel line to encompass a broader class of problems.

The idea of transforming to a new set of variables can also be used to transform Equations 3 and 4 into a Riccattian type of Equation [4] which, because of its non-linearity, is often solved either by the numerical or by the

approximation techniques that will be discussed subsequently. In order to obtain this Riccatian type equation, define a new variable, $z(x)$, by

$$z(x) = -\frac{1}{y(x)} \frac{I'(x)}{I(x)} \quad \text{or} \quad I' = -y z I \quad (\text{A-24})$$

Then

$$I'' = (y z)^2 I - y' z I - y z' I \quad (\text{A-25})$$

By substituting Equations 24 and 25 into Equation 4 one obtains

$$z'(x) = -[z(x) - y(x) z^2(x)] \quad (\text{A-26})$$

This is in the desired form. If l is the length of the nonuniform line and d is the distance from its end, then $d = l - x$. At a specified point on the line $z'(d) = -z'(l - x)$ by virtue of the different direction being considered positive. Furthermore, one should observe that Equation 26 is satisfied by an initial value problem. From Equation 1, Equation 24 can be rewritten as

$$z(x) = \frac{V}{I} \quad (\text{A-27})$$

One observes that $z(x)$ is the impedance seen looking towards the load at any point on the nonuniform transmission line. Thus, $z(l) = Z_L = \text{load impedance}$. (In terms of variable "d" this is $z(0) = Z_L = \text{load impedance}$.)

Once one has solved for $z(x)$ (more precisely if one can solve for $z(x)$), $I(x)$ is obtained from Equation 24 and then $V(x)$ can be obtained from Equation 2.

In passing, it should be noted that Bellman derived the equivalent of Equation 26 in terms of distances from the load by a slightly different procedure than the one presented above. He stratifies the problem in the x direction and uses the principle of invariant imbedding to derive his result. He considers the impedance looking toward the load at an arbitrary point and also at a second point that is a differential stratum distance away. By assuming smooth variations and expanding the impedance at the second point in a Taylor series about the first point and neglecting higher order terms, the desired non-linear Riccattian type differential equation is derived.

By working with accumulated inductance and accumulated capacitance (notice that this is also an invariant imbedding) the L-C transmission line has been transformed into Sturm-Liouville equations [40]. A similar technique has also

been used on the R-C transmission line [39].

A3. Approximate Solution Techniques

Approximate solution techniques can be broadly subdivided into techniques requiring stratification of the medium and techniques that do not require stratification of the medium. The techniques that do not require stratification of the medium can be classified as perturbation, iteration, and variational techniques. Techniques requiring stratification of the medium include the WKB approximation, the Bremmer series solution, and infinite cascade of two port box techniques. Numerical analysis can be applied to both of these classifications.

The most common approximate solution techniques that have found application in the analysis of nonuniform transmission lines use the principle of stratification. The remainder of this appendix discusses stratification techniques.

The basic idea behind stratification is to assume that the parameters describing the situation remain constant over a sufficiently small interval. These parameters vary from interval to interval. The problem can be thought of as being "layered" in the direction of propagation with

respect to the parameters involved. (In its most common sense, one usually reserves this term for medium variations. When this is done the medium is called a "layered Medium").

The WKB approximation [4] (which is sometimes referred to as the Liouville approximation) is obtained by only considering the transmitted wave and ignoring all reflections. (This, in effect, assumes a slowly varying geometry). Let K_1 , K_2 and K_n be the propagation constants in the first, second and nth stratum, respectively. Then the forward wave (neglecting multiple reflection) in the second stratum (assuming that the wave in the first stratum is e^{jK_1x}) is

$$a_2 = \frac{2K_1}{K_1+K_2} e^{jK_2x} \quad \text{for } x_1 < x < x_2 \quad (\text{A-28})$$

In the third stratum

$$a_3 = \left(\frac{2K_1}{K_1+K_2} \right) e^{jK_2 \Delta x_2} \left(\frac{2K_2}{K_2+K_3} \right) e^{jK_3(x-x_2)} \\ \text{for } x_2 < x < x_3 \quad (\text{A-29})$$

By continuing this process and taking the limit as the interval, Δx_1 , approaches zero (as the number of inter-

vals, n , approaches infinity) in such a manner that $\sum \Delta x_1 = x$, it follows that the approximate solution, U_0 , to the equation

$$U'' + k^2(x)U = 0 \quad (\text{A-30})$$

is

$$U_0(x) = \left(\frac{k_1}{k(x)} \right)^{1/2} e^{j \int_0^x k(s) ds} ; j = \sqrt{-1} \quad (\text{A-31})$$

This is the WKB approximation.

The physical model of the WKB approximation that has just been presented can be refined by considering the effects of successive reflections. Let $U_1(x)$ be the contribution of those waves which are the result of exactly one reflection (and neglecting higher reflections as was done in the WKB approximation). Similarly, let $U_n(x)$ be the contribution of those waves which are the result of exactly n reflections. The general solution, $U(x)$, is seen to be the infinite sum of the sequence of functions generated by the above procedure.

$$U(x) = \sum_{i=0}^{\infty} U_i(x) \quad (\text{A-32})$$

This series is called the Bremmer series. In practical problems this series often converges fast enough to use a few terms. The general term of the Bremmer series can be shown to be given by

$$U_k(x) = (-1)^k \cdot \frac{1}{2\sqrt{k(x)}} \int_0^{\infty} \frac{k'(s)}{\sqrt{k(s)}} U_{k-1}(s) e^{j \int_k(t) dt} ds$$

(A-33)

Another class of techniques that uses stratification describes each stratum by a set of "black box" parameters and then cascades these "boxes" in order to determine the "black box" parameters of the overall nonuniform transmission line. For example, the ABCD matrix parameters of a differential stratum may be used to determine the ABCD matrix parameters of the overall nonuniform transmission line by matrix multiplication [40]. By using this technique in the limiting process some properties of the ABCD parameters have been determined. The scatter parameters and the z-parameters [21] have also been used for this purpose.

When two T.E.M. nonuniform transmission lines are coupled, it is possible to extend the matrix multiplication technique to 4 x 4 matrices instead of 2 x 2 matrices.

However, it can often be "bi-sected" into two two-port problems by using the bisection theorem with even and odd mode excitation [51]. Each of these problems are then handled by the methods discussed previously. The cited reference applies this technique to analyze directional couplers and all-pass networks with nonuniform T.E.M. coupled transmission lines.

REFERENCES

REFERENCES

1. Bahar, E., "Wave Scattering in Nonuniform Waveguides with Large Flare Angles and Near Cutoff", I.E.E.E. Transactions on Microwave Theory and Techniques, Volume MTT-16, Number 8, August 1968, pp. 503-510.
2. Baher, E. and J. R. Wait, "Propagation in a Model Terrestrial Waveguide of Nonuniform Height: Theory and Experiment", Journal Research NBS (Radio Propagation), Volume 69D, 1965, pp. 1445-1463.
3. Barrow, W. L. and L. J. Chu, "Theory of the Electromagnetic Horn", Proceedings of the I.R.E., January 1939, pp. 51-64.
4. Bellman, R. and R. Kalaba, "Functional Equations, Wave Propagations and Invariant Imbedding", Journal of Mathematics and Mechanics, Volume 8, Number 5, 1959, pp. 683-704.
5. Berger, H., "Generalized Nonuniform Transmission Lines", I.E.E.E. Transactions on Circuit Theory, Volume CT-13, Number 1, March 1966, pp. 92-3.
6. Bolinder, F., "Fourier Transforms in the Theory of Inhomogeneous Transmission Lines", Transactions Roy Institute Tech., (Stockholm, Sweden), Number 48, 1951.
7. Booker, H. G., and W. Walkinshaw, "The Mode Theory of Tropospheric Refraction and Its Relation to Waveguides and Diffraction in Meteorological Factors in Radio Wave Propagation", The Physical Society, London, 1946, pp. 80-127.
8. Brillouin, Leon, Tensors in Mechanics and Elasticity, Academic Arts Press, 1964.
9. Chin, J. I., "Trapped Waves in Varying Dielectric Media", I.R.E. Institute Convention Record Part I, pp. 99-105.
10. Collin, R. E., "The Optimum Tapered Transmission Line Matching Section," Proceedings I.R.E., Volume 44, Jan. 1956, pp. 31-35.
11. Collin, R. E., Field Theory of Guided Waves, McGraw Hill, 1960.

12. Frank, N. H., "Reflections from Sections of Tapered Transmission Lines and Waveguides", M.I.T. Radiation Laboratory Report, Jan. 6, 1943, pp. 43-47.
13. Ghose, N. R., "Exponential Transmission Lines as Resonators and Transformers", I.R.E. Transactions on Microwave Theory and Techniques, Volume MTT-5, Number 3, July, 1957, pp. 213-217.
14. Harrington, Time Harmonic Fields, McGraw-Hill, 1961.
15. Harrington, R. E., Field Computation by Moment Methods, MacMillan; 1968.
16. Hildebrand, Methods of Applied Mathematics, Prentice-Hall.
17. Johnson, C. C., Field and Wave Electrodynamics, McGraw-Hill: 1965.
18. Johnson, R. C., "Design of Linear Double Tapers in Rectangular Waveguides", I.R.E. Transactions on Microwave Theory and Techniques, July 1959, pp. 374-378.
19. Kaufman, H., "Bibliography of Nonuniform Transmission Lines", I.R.E. Transactions on Antennas and Propagation, Vol. AP-3, October 1955, pp. 218-20.
20. Jones, D. S., The Theory of Electromagnetism, New York Pergamon, 1967.
21. Kirstrom, J., "The Z-Matrix Parameters of Tapered Transmission Lines", I.R.E. Transactions on Circuit Theory, Volume CT-9, June 1962, pp. 132-5.
22. Lee, S. W., W. R. Jones, and J. J. Campbell; "Convergence of Numerical Solutions of Iris-type Discontinuity Problems", I.E.E.E. Transactions on Microwave Theory and Techniques; Volume MTT-19, Number 6, pp. 528-536, June 1971.
23. Lewin, L, "On the Inadequacy of Discrete Mode-Matching Techniques in Some Waveguide Discontinuity Problems" (followed by Nielsen and Lewin commentaries); I.E.E.E. Transactions on Microwave Theory and Techniques, Volume MTT-18, Number 7, pp. 364-372, July 1970.

24. Lewin, L., "On the Restricted Validity of Point-Matching Techniques", I.E.E.E. Transactions on Microwave Theory and Techniques, Volume MTT-18, Number 12, pp. 1041-8, December, 1970.
25. Louisell, W. H., "Analysis of a Single Tapered Mode Coupler", Bell System Technical Journal, Volume 34, 1955, pp. 853-870.
26. Louisell, W. H., Coupled Mode and Parametric Electronics, Wiley, 1960.
27. Marcuitz, N., Waveguide Handbook, M.I.T. Radiation Laboratory Series, Volume 10, McGraw Hill, 1951.
28. McConnell, A. J., Applications of Tensor Analysis, Dover, 1957.
29. Millar, R. F. and R. H. T. Bates, "On the Legitimacy of an Assumption Underlying the Point-Matching Method", I.E.E.E. Transactions on Microwave Theory and Techniques, Volume MTT-18, Number 6, pp. 325-6, June 1970.
30. Mittra, R., T. Itoh, and T. S. Li, "Analytical and Numerical Studies of the Relative Convergence Phenomenon Arising in the Solution of an Integral Equation by the Moment Method", I.E.E.E. Transactions on Microwave Theory and Techniques, Volume MTT-20, Number 2, pp. 96-104, February, 1972.
31. Montgomery, Dicke and Purcell, Principles of Microwave Circuits, Volume 8, Radiation Laboratory Series, McGraw Hill, 1948.
32. Moon, Parry and Domina E. Spencer, "Separability in a Class of Coordinate Systems", Journal of the Franklin Institute, Volume 254, 1952, pp. 227-242.
33. Moon, Parry and Domina E. Spencer, "Separability Conditions for the Laplace and Helmholtz Equations", Journal of the Franklin Institute, Volume 252, 1952, pp. 585-600.
34. Moon and Spencer, Field Theory for Engineers, Van Nostrand.
35. Moorse and Fishbach, Methods of Theoretical Physics, McGraw-Hill, 1953.
36. Panofsky and Phillips, Classical Electricity and Magnetism, Addison Wesley, 1962.

37. Piefke, G., "Die Ausbreitung elektromagnetischer Wellen in einem Phramidentrichter", Z. Angew. Phy. 6 (1954) pp. 499-507.
- 38-39. Protonotarios, E. N. and O. Wing; Part I: "Analytic Properties and Realizability Conditions in the Frequency Domain". Part II: "Analytic Properties in the Time Domain". I.E.E.E. Transactions on Circuit Theory, Volume CT-14, Number 1, March 1967, pp. 2-20.
40. Protonotarios, E. N. and O. Wing, "Analysis and Intrinsic Properties of the General Nonuniform Transmission Line", I.E.E.E. Transactions on Microwave Theory and Techniques, Volume MTT-15, Number 3, March 1967, pp. 142-50.
41. Ramo, Whinnery, Van Duzer; Fields and Waves in Communication Electronics, Wiley, 1965.
42. Share, I. and G. Ching, "Optimum Coordinates for Nonuniform Waveguides", Fall USNC/URSI Meeting and International IEEE/G-AP Symposium; Paper #U-VI-28, September, 1971.
43. Schelkunoff, S. A., "Conversion of Maxwell's Equations into Generalized Telegraphist's Equations", The Bell System Technical Journal, September, 1955, pp. 995-1043.
44. Schelkunoff, S. A., "Generalized Telegraphist's Equations for Waveguides", The Bell System Technical Journal, July, 1952, pp. 784-801.
45. Snyder, H. H., "Propagation in Periodically Deformed Circular and Rectangular Waveguides", Electrical Communications, Volume 42, Number 3, 1967, pp. 415-438.
46. Solymar, L., "Spurious Mode Generation in Nonuniform Waveguides", I.R.E. Transactions on MTT, July, 1959, pp. 379-383.
47. Stevenson, A. F., "General Theory of Electromagnetic Horns", Journal of Applied Physics, Volume 22, Number 12, December 1951, pp. 1447-1462.
48. Tang, C. H., "Delay Equalization by Tapered Cutoff Waveguides", I.E.E.E. Transactions on MTT, Volume MTT-12, Number 6, November 19, pp. 608-615.

49. Tang, C. H., "Nonuniform Waveguide High-Pass Filters With Extremely Steep Cutoff", I.E.E.E. Transactions on Microwave Theory and Techniques, pp. 300-309, May, 1964.
50. Tang, C. H., "Optimization of Waveguide Tapers Capable of Multimode Propagation", I.R.E. Transactions on MTT, September 1961, pp. 442-452.
51. Tresselt, C. P., "The Design and Construction of Broad-band High Directivity, 90-degree Couplers using Nonuniform Line Techniques", (paper presented at the Eleventh International G-MTT Symposium), Palo Alto, California.
52. Ungers, H. G., "Wave Propagation in Horns and Through Horn Junctions", A.E.U. Band 19 (1965), Heft 9.
53. Weeks, Electromagnetic Theory for Engineering Applications, Wiley, 1964.
54. Wexler, A., "Solution of Waveguide Discontinuities by Modal Analysis", I.E.E.E. Transactions on Microwave Theory and Techniques, Volume MTT-15, Number 9, pp. 508-517, September, 1967.
55. Whinnery, J. R., H. W. Jamieson, and T. E. Robins, "Coaxial Line Discontinuities", Proceedings at the I.R.E. November, 1944.
56. Whinnery, J. R., and D. C. Stinson, "Radial Line Discontinuities", Proceedings of the I.R.E., 43, Number 1, Jan. 1955, pp. 46-51.
57. Womack, C. P., "The Use of Exponential Transmission Lines in Microwave Components", I.R.E. Transactions on Microwave Theory and Techniques, Volume MTT-10, Number 2, March, pp. 124-32.
58. Yamamoto, S., T. Azakami, and K. Itakura, "Coupled Nonuniform Transmission Line and Its Applications", I.E.E.E. Transactions on Microwave Theory and Techniques, Volume MTT-15, Number 4, April 1967.

